UNIVERSITY OF CALGARY

Arabidopsis thaliana D group MPKs interactions with RLPH2 and PP1

by

Ryan Brendan Toth

A THESIS

SUBMITTED TO THE FACULTY OF GRADUATE STUDIES

IN PARTIAL FULFILMENT OF THE REQUIREMENTS FOR THE

DEGREE OF MASTER OF SCIENCE

GRADUATE PROGRAM IN BIOLOGICAL SCIENCES

CALGARY, ALBERTA

JANUARY 2021

ABSTRACT

Mitogen activated protein kinases (MPK) are key members of the MPK cascade, a pathway that results in an immediate response from (external) stimuli such as infection, cold, or drought. The activation of an MPK relies its activation loop being phosphorylated on a threonine and tyrosine residue. A unique bacteria-like phosphatase *Rhizobiales*-like phosphatase 2 (RLPH2), which we bioinformatically characterized as a serine/threonine phosphatase, has been discovered to act as a tyrosine phosphatase. In this thesis, data monitoring RLPH2s dephosphorylation of different peptides derived from MPK activation loops would reveal a preference for the dephosphorylation of D group MPKs over non-D group MPKs, and indicate that the central residue in the TXY motif plays a key role in RLPH2 substrate determination. Additionally, RLPH2 would show a preference for the *in vitro* dephosphorylation of MPK9 (a D group MPK) over MPK3 (a non-D group MPK). An engaging observation is that right next to the TxY motif in D group MPKs is a putative Protein Phosphatase 1 (PP1) regulatory protein binding RVxF motif. This motif is not present in any other characterized MPK, suggesting an interaction between PP1 and D group MPKs. In this thesis, PP1 protein binding assays with MPK9 WT and an MPK9 RASA mutant would show binding occurs between MPK9 and PP1 through the RVXF motif *in vitro*. Peptide and protein substrate dephosphorylation assays with PP1 would show threonine dephosphorylation on MPK9 and the effect the RVXF motif plays on this interaction. In summary, the specificity of RLPH2 as a D group MPK regulator was examined along with the interaction between PP1 and the D group MPKs via the RVXF motif, with mention of a potential relationship between these three interactions.

ACKNOWLEDGEMENTS

This MSc thesis would not have been possible without the support, mentorship, and in some cases friendship, of people I wish to acknowledge.

I wish to first and foremost, with the highest appreciation thank Dr. Gregory Moorhead. While the internal debate continues whether I could be considered a “good” or “bad” researcher, I have no doubts about my love of research and could not imagine living my life directed towards any other cause. Greg has mentored and guided me on how to think like a scientist, given me the opportunity to be included on papers, and has given me every possible chance to succeed in research as so many great scientists have before under his guidance. It is therefore worth noting that without the initial backing of Greg, it is unlikely I would have ever been given the chance to research, as an unpromising undergraduate prospect. He has stuck his neck out for me more times than I can count, and I am eternally grateful for the chance he offered. I hope that beyond the consistently terrible jokes and that time I presented a video of him dancing, he has not regretted the opportunity he gave me.

I also wish to thank Dr. Anne Marie Labandera, who became one of my closest friends and is still one of my greatest mentors. From day one in the Moorhead lab she helped me beyond the call of mentorship, not only offering her time and experience to support our project, but to encourage my future in science. I will always regard her as the highest model of a scientist, someone who is intensely passionate about her research, who works with an extraordinary dedication, and who truly understands that the key to success is making sure everyone succeeds. Without her I would not have gotten close to where I am today.

I would like to thank my committee members Dr. Kenneth Ng and Dr. Marcus Samuel. Dr. Ng and his graduate student Samuel Carr were both kind and patient enough to give me a chance

at delving into the complex art of protein crystallography, and Dr. Ng has offered his countless biochemical wisdom that can only come from years of delicate crystal work that has deepened my understanding of protein biochemistry. Dr. Samuel has offered tons of insightful plant guidance, MPK knowledge, and a few constructs that have aided this project's goal of unravelling a strand in the MPK pathway. On a personal level, Dr. Samuel was also the professor who in his second-year biology course convinced me to direct myself towards plant research.

I wish to thank Dr. Amr Kataya, for all the interesting conversations we had on science in terms of both proteomics and genetics, his advice with his years of experience in the field of plant genetics, and his friendly personality. If it was not for the fact that every time I come back to the lab he ends up leaving and vice-versa, I'm sure I would have laughed more.

I wish to thank the past and present Moorhead lab members, Chris White-Gloria, Jayde Johnson, Jordan Mattice, and Sibapriya Chaudhuri who kept every day interesting and welcoming. I specifically would like to thank Kaitlin Chan who was an undergraduate researcher that worked on this project, generating the anti-MPK9 antibodies and working on the immunoprecipitations. I'd also like to thank Sierra Mitchell who did a short summer project on RLPH2, but more for listening to my long-winded science rants and laughing at the worst of my jokes. I'm happy to know she will be keeping the project going after I am gone.

DEDICATION

To my parents,

For their truly endless support

TABLE OF CONTENTS

LIST OF TABLES

LIST OF FIGURES AND ILLUSTRATIVES

LIST OF SYMBOLS, ABBREVIATIONS, AND NOMENCLATURE

ABBREVIATION	DEFINITION
ABS	Absorbance
ATP	Adenosine-5'-triphosphate
BETA-ME	2-Mercaptoethanol
BSA	Bovine serum albumin
BSL1	Bri1 suppressor-like 1
BSL2	Bri1 suppressor-like 2
BSL3	Bri1 suppressor-like 3
BSU1	Bri1 suppressor
CAMKK4	Constitutively active mutant of MKK4
CD DOMAIN	Common docking domain
COL-0	Columbia-0
CV	Column volumes
DMP	Dimethylpimelimidate dihydrochloride
DMSO	Dimethyl sulphoxide.
DNA	Deoxyribonucleic acid
DTT	Dithiothreitol
ECL	Enhanced chemiluminescence
ERK1/2	Extracellular signal-regulated kinase 1/2
GEM	GL2 expression modulator
GFP	Green fluorescent protein
GST	Glutathione S-transferase
GTP	Guanosine-5'-triphosphate
I2	Inhibitor-2
IGG	Immunoglobulin G
IP	Immunoprecipitation
IPTG	Isopropyl β-D-1-thiogalactopyranoside
KDA	Kilodalton
KLH	Keyhole limpet hemocyanin
KO	Knock out
MC-LR	Microcystin-LR
MKK	Mitogen Activation Protein Kinase Kinase
MKKK	Mitogen Activation Protein Kinase Kinase Kinase
MPK	Mitogen Activation Protein Kinase
MS	Mass spectrometry
NA_3VO_4	Sodium orthovanadate
NAPPI	Sodium pyrophosphate
NI-NTA	Nickel nitrilotriacetic acid
NIPP1	Nuclear inhibitor of protein phosphatase 1
OD	Optical density
PAGE	Polyacrylamide gel electrophoresis
PBS	Phosphate buffered saline
PDB	Protein data bank
PIS	Pre-immune serum

PMSF	Phenylmethylsulfonyl fluoride
PNUTS	Protein phosphatase-1 nuclear targeting subunit
PP1	Protein phosphatase 1
PPKL	Protein phosphatase kelch-like
PPM	Metallo-dependent phosphatase
PPP	Phospho-protein phosphatase
PSER	Phosphorylated serine
PTHR	Phosphorylated threonine
PTK	Protein tyrosine kinase
PTP	Protein-tyrosine phosphatase
PTYR	Phosphorylated tyrosine
RLK	Receptor-like kinases
RLPH	*Rhizobiales*-like phosphatase
RNA	Ribonucleic acid
RT	Room temperature
SDS	Sodium dodecyl sulfate
SLP	Shewanella-like phosphatase
SPINO	Spinophilin
TBS	Tris-buffered saline
TFA	Trifluoracetic acid
TIO_2	Titanium dioxide
TMM	Too many mouths
TOPP	Type One Protein Phosphatase
WT	Wild type

EPIGRAPH

"*Success is going from failure to failure,*
without losing your enthusiasm"

-Winston Churchill

INTRODUCTION

1.1 Protein Phosphorylation – The Most Common Post-Translational Modification

Eukaryotic organisms utilize a wide array of tools and mechanisms to control and regulate the functions of life. One of the most crucial of these tools is reversible protein phosphorylation, the most common form of a post-translational modification. This mechanism establishes an additional layer of complexity to proteins that goes beyond what the genome or transcriptome can already accomplish, with the additional benefit of this modification being reversible (Prabakaran *et al.*, 2012). In most Eukaryotic organisms, 2-4% of the protein-encoding genome are enzymes that directly add or remove the phosphate groups on substrate proteins, and it has been estimated that 70% of both the *Arabidopsis thaliana* and *Homo sapiens* proteome is phosphorylated, with potential for phosphorylation on more than one site on a single protein (Olsen *et al.*, 2006; Kerk, Templeton and Moorhead, 2008; Hunter and Pawson, 2012).

The process of protein phosphorylation occurs when a protein kinase transfers the gamma phosphoryl group of ATP/GTP onto a substrate's serine, threonine, or tyrosine hydroxyl group forming a phosphomonoester **(Figure 1A)** (Nigg *et al.*, 2010). This presence of a phosphoryl group on a protein can result in a wide array of outcomes, such as a conformational shift in tertiary structure, resulting in activation or inactivation of protein function, blocking of binding sites, revealing new binding sites, or a change in the subcellular localization of the protein (Seo and Lee, 2004). The reversibility of phosphorylation is due to the function of protein phosphatases, enzymes which can hydrolyze the phosphoryl group, releasing phosphate from the protein and reverting the substrate to its original pre-phosphorylated state (Shi, 2009).

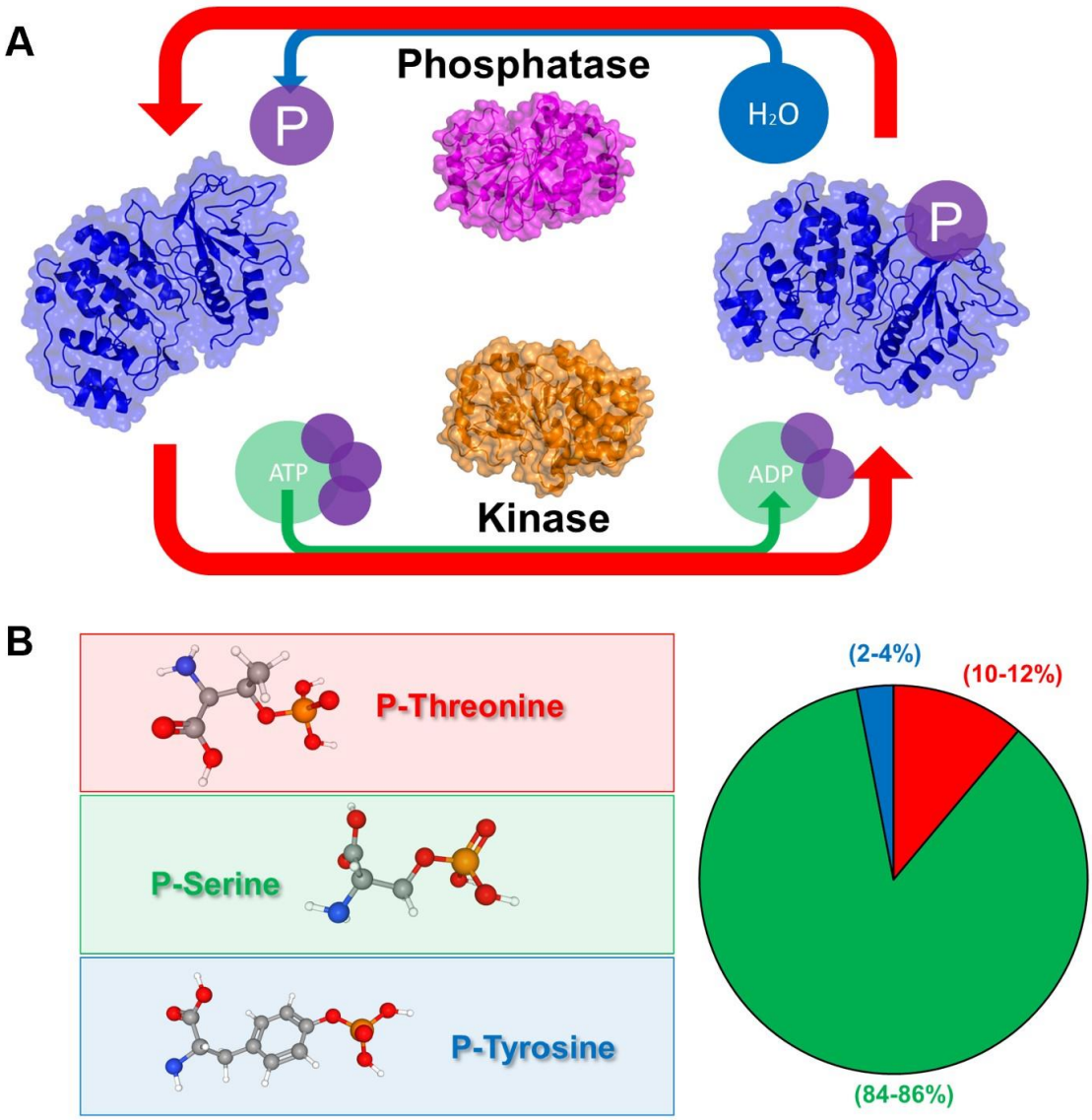

Figure 1. The mechanism of reversible protein phosphorylation with the phosphorylated amino acids and associated phosphorylation percentages. **A)** Shows a summary of the reversible protein phosphorylation mechanism. Purple sphere represents phosphoryl group, blue arrow shows the hydrolysis of phosphoryl group by phosphatase, green arrow represents the transfer of a phosphoryl group from ATP to the substrate protein by the protein kinase, resulting in ADP. Blue protein structures represent substrate protein, purple protein structure represents protein phosphatase, orange protein represents protein kinase. **B)** In red is the structure of phosphothreonine, in green is the structure of phosphoserine, and in blue is the structure of phosphotyrosine. On the right is a pie chart representing what percent of total proteome phosphorylation occurs on each different amino acid in both *Arabidopsis thaliana* and in *Homo sapiens* (Olsen *et al.*, 2006; Sugiyama *et al.*, 2008; Nakagami *et al.*, 2010).

Phosphorylation was discovered first by Kennedy in 1954 who found a protein that was capable of phosphorylating casein (Burnett and Kennedy, 1954; Cohen, 2002b). Following this Fischer and Krebs would characterize the well-known example of glycogen phosphorylase *b* being phosphorylated by phosphorylase kinase which results in its alteration into its active glycogen phosphorylase *a* conformation (Cohen, 2002b). After the impact that phosphorylation had on a protein was recognized, there was a surge of interest in the topic leading to a research crusade to further study the process of reversible protein phosphorylation. Today, phosphorylation is seen as an essential mechanism of all life, playing key roles in cellular development and differentiation, the repairing of DNA, metabolic pathways, apoptosis, and diseases including cancer which has made kinases and phosphatases a promising focus for pharmaceutical companies as drug targets (Cohen, 2002a).

In the plant model organism *Arabidopsis thaliana*, serine phosphorylation accounts for 84-86% of phosphorylated sites, with threonine and tyrosine accounting for the other 10-12% and 2-4% respectively, an intriguing composition as it is nearly identical to the *Homo sapiens* phosphorylation percentages **(Figure 1B)** (Olsen *et al.*, 2006; Sugiyama *et al.*, 2008; Nakagami *et al.*, 2010). Today it has been determined that protein phosphorylation plays a key role in numerous plant functions such as signalling cascades in biotic or abiotic stresses, reacting to hormones, and plant development (Rodriguez, Petersen and Mundy, 2010). Further cementing its importance in plant biology, the presence of protein phosphorylation has been determined in the plant cellular compartments mitochondria, chloroplasts, cytosol, peroxisome, nuclei, and in extra-cellular environments, implying its impact in essentially all plant operations (Olsen *et al.*, 2006; Ito *et al.*, 2009; Reiland *et al.*, 2009; Tagliabracci *et al.*, 2013; Kataya, Muench and Moorhead, 2019).

From a broad perspective, the phosphorylation of both the mammalian and the plant proteome gives the impression of them being almost identical, however, once the underlying protein mechanisms are uncovered, key differences are observed. For one, plants lack the classic receptor tyrosine kinases that mammalian organisms use as transmembrane proteins which act as receptors that respond to external ligands. To fill the gap left by the lack of receptor tyrosine kinases, plants instead have numerous receptor-like kinases (RLKs) but all are thought to be serine/threonine specific (Shiu and Bleecker, 2001). Furthermore, a curious difference observed between mammalian and plant phosphorylation is that through bioinformatic analysis of the *Arabidopsis* genome only two protein tyrosine kinases (PTK) were revealed (Robinson, Wu and Lin, 2000). Moreover, these two potential protein tyrosine kinases in *Arabidopsis* seem to be lacking key catalytic residues which theoretically would leave these kinases inactive (Ghelis, 2011). When comparing the two most likely inactive PTKs to the 90 *Homo sapiens* PTKs, this would indicate a potential for less prevalence of tyrosine phosphorylation in plants (Robinson, Wu and Lin, 2000). This was challenged when phosphoproteomic data showed the same 2-4% of phosphorylation occurring on tyrosine residues in *Arabidopsis*, similar to what is observed in *Homo sapiens* phosphorylation, which could indicate hidden novel tyrosine kinases not yet determined (Olsen *et al.*, 2006).

1.2.1 Protein Kinases – Drivers of Protein Phosphorylation

The process of protein phosphorylation is propelled forward by protein kinases, which transfer the gamma phosphoryl group of ATP or GTP onto their substrate's serine, threonine, and tyrosine residues (Hanks, 2003). The protein kinases all belong to one super family, which all share the same approximate 260 catalytic amino acids called the catalytic kinase domain, creating a list of 941 protein kinases in *Arabidopsis thaliana* (Zulawski *et al.*, 2014). Some further separation of

kinases can be classified based on substrate specificity. This creates the serine/threonine specific kinases, the tyrosine specific kinases, and the dual-specific kinases which are able to phosphorylate both types of substrates (Ghelis, 2011).

The key structural features of a protein kinase include the glycine rich repeat that plays a role in the binding of ATP, the xRDxKxxN motif, and the activation loop (T-loop) designated between the DFG and APE residues (Hemmer *et al.*, 1997; Cargnello and Roux, 2011; Taylor and Kornev, 2013). The activation loop gets its name from the amino acid sequence, between the DFG and APE flanks, containing a site that when phosphorylated causes a change in conformation of the kinase from inactive to active and allows the active site to phosphorylate substrates (Kyosseva, 2003). The xRDxKxxN motif is also found within the catalytic loop and plays a key role in the catalytic function of a kinase. The aspartic acid residue within this motif acts as the proton acceptor for the substrate's hydroxyl group allowing the substrate phospho-receiving amino acid to be phosphorylated (Kornev, Taylor and Ten Eyck, 2008).

1.2.2 Mitogen Activated Protein Kinases – The MPK Signal Cascade

Mitogen Activated Protein Kinases (MPKs) are the final protein component of the prominent MPK cascade, a signaling mechanism used to transmit external signals internally, leading towards a cellular response (Kyosseva, 2003). The MPK cascade is the signaling pathway that is composed of MPKK Kinases (MKKK), MPK Kinases (MKK), and MP Kinases (MPK) (Kyosseva, 2003). Commonly the activation of the MPK cascade begins with a ligand interacting with the external domain of a receptor such as a receptor-like kinase, which results in an internal protein complex being able to phosphorylate a MPKKK, thereby activating it (Cristina, Petersen and Mundy, 2010). An active MPKKK is now capable of phosphorylating its MPKK substrate at the activation loop converting the MPKK into an active state allowing it to phosphorylate the TXY

motif in the activation loop of its designated MPK substrate (Cristina, Petersen and Mundy, 2010). As each layer of kinase phosphorylates the next layer within the MPK signalling cascade, the strength of the signal is multiplied, allowing for a strong signal response based on the initial ligand binding.

In MPKs the site within the activation loop that when phosphorylated converts the MPK into its active state is the TXY motif and requires phosphorylation on both the threonine and tyrosine residues, sometimes referred to as dual phosphorylation, for MPK activation **(Figure 2)** (Cristina, Petersen and Mundy, 2010). Once phosphorylated and activated, the MPK is capable of either remaining in the cytosol or in some cases translocating to the nucleus to phosphorylate its substrates (Cardinale *et al.*, 2002).

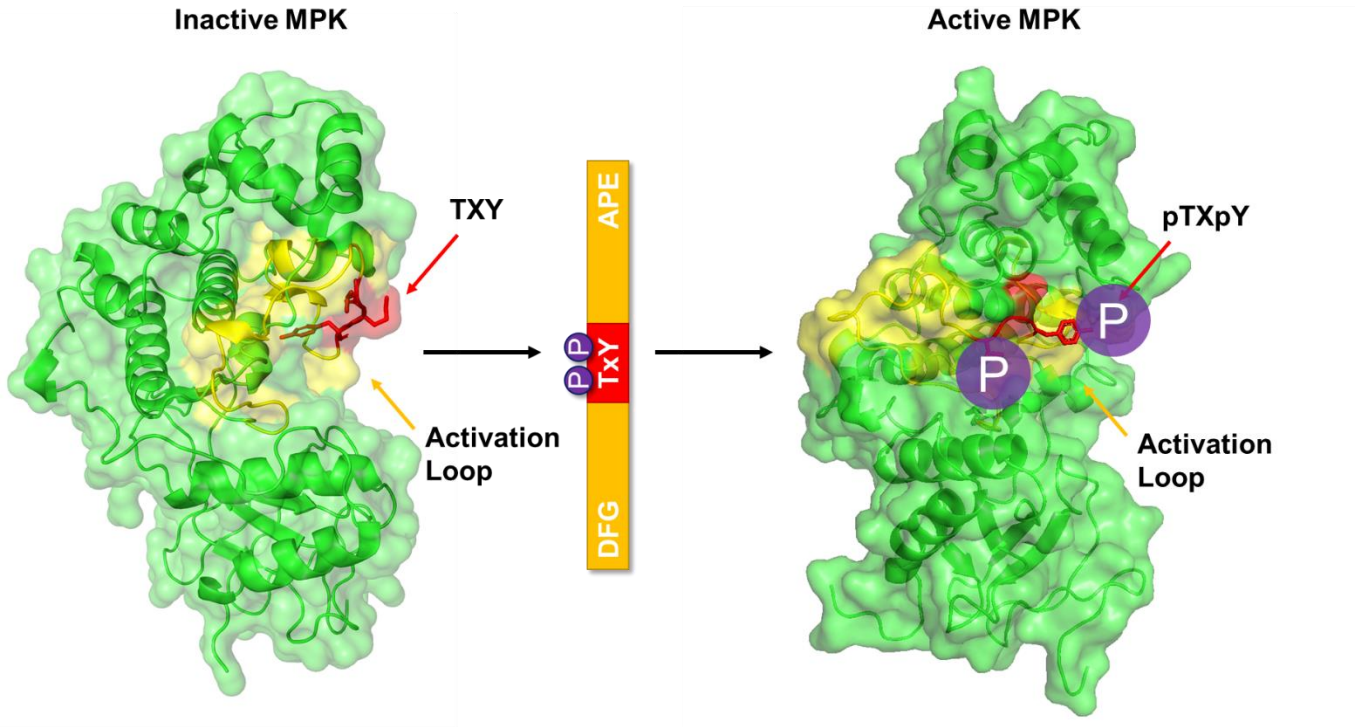

Figure 2. Model of a Mitogen Activated Protein Kinase. Structure for an inactive MPK (PDB: 4ERK) and structure for an active MPK (PDB: 2ERK). The activation loop highlighted in yellow and the TXY motif highlighted in red. Structures were generated using PyMOL.

In *Arabidopsis thaliana,* there are 60 MKKKs, 10 MKKs, and 20 MPKs. The 20 MPKs are grouped based on bioinformatic analysis of their sequences into either groups A, B, C, or D **(Figure 3)** (Ichimura *et al.*, 2002). The largest ordering of the MPKs bioinformatically is based on 12 MPKs containing a glutamic acid within their TXY motif (TEY) while 8 MPKs contain an aspartic acid (TDY). These TDY containing MPKs are designated as the D group of the MPKs, while the other 12 are further separated into groups A, B, and C. The A and B group MPKs both contain the conserved CD domain which has been characterized extensively in other MPKs as a docking site for MKKs, protein substrates, and regulatory phosphatases via a [LH][LHY]Dxx[DE]xx[DE]EPxC sequence (Ichimura *et al.*, 2002). A modified version of the CD domain is also present in the C group MPKs while it is completely missing in any recognizable form within the D group MPKs (Ichimura *et al.*, 2002). Another feature that makes the D group of the MPKs unique is their extended C terminus of 60-80 amino acids when compared to the C terminus of the other groups. These regions are noted to be rich in serine and glutamic acid within two of the D group MPK members, MPK8 and MPK9 (Ichimura *et al.*, 2002).

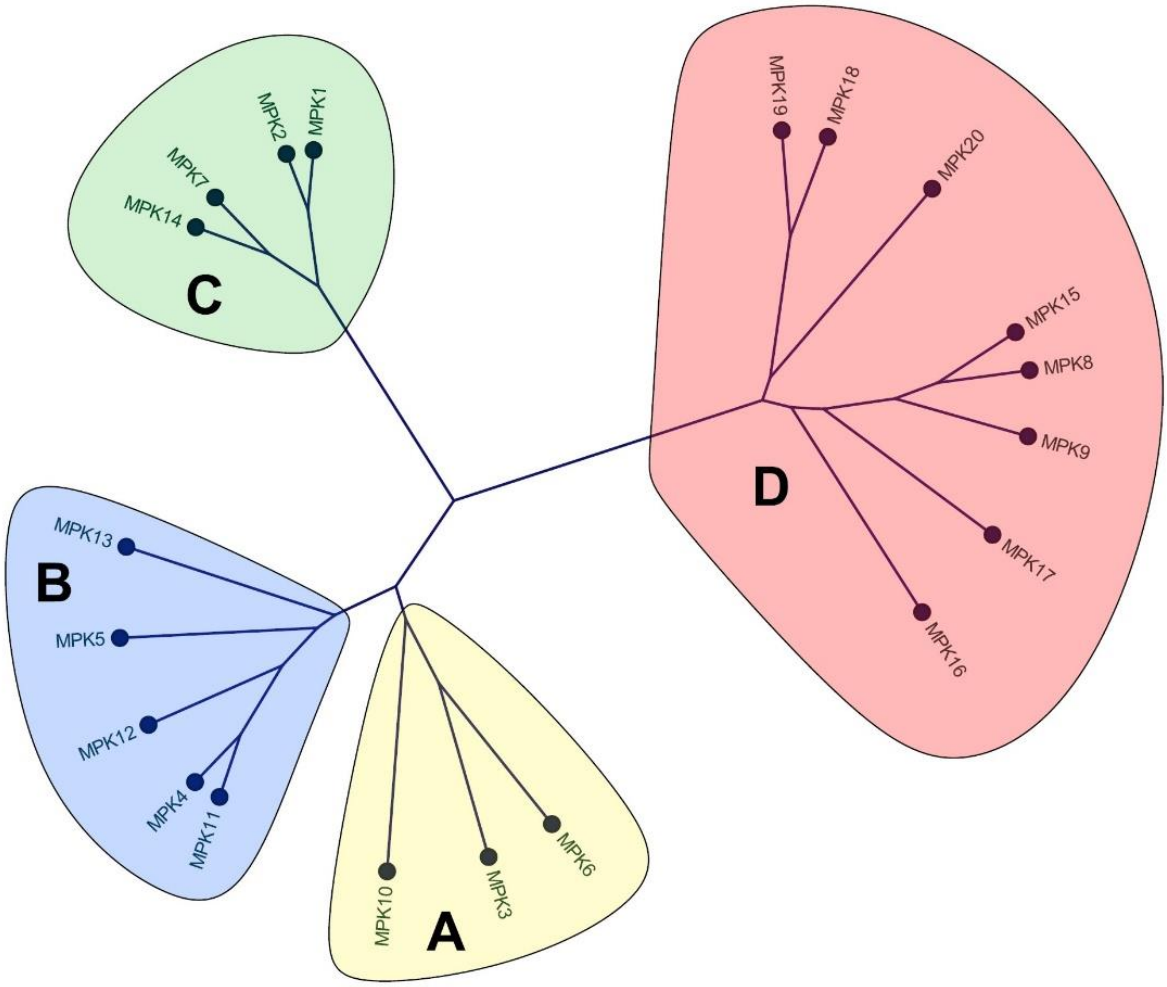

Figure 3. Phylogenetic tree of the 20 MPKs found in *Arabidopsis thaliana.* Each of the 20 MPKs are separated into their respective groups A, B, C, or D. CLC Sequence Viewer 8.0 was used to align the sequences and generate the phylogenetic tree.

MPK's have been characterized to play important roles in plants such as cellular development and differentiation, as part of the plant's immunity pathways, and interacting with the plant's external environment (Xu and Zhang, 2015). The A and B group MPK3, MPK4, and MPK6 have been widely researched based on their roles in plant immune response, salt and cold stress tolerance (Cristina, Petersen and Mundy, 2010). Unfortunately, the D group of the MPK's have been researched less and little is known about their function beyond MPK9s role in stomatal

closure and MPK17s role in peroxisome proliferation (Khokon *et al.*, 2017; Frick and Strader, 2018).

An additional distinctive feature of the D group MPKs compared to the other groups is that in all eight D group MPK members there is an RVXF motif nine amino acids upstream from their TXY motif **(Figure 4)**. This is a well characterized putative protein phosphatase 1 (PP1) binding motif that regulatory subunits utilize to interact with PP1 and regulate its substrate specificity or localization. A recent study has revealed a previously unknown extension of the RVXF motif in the *Homo sapiens* PP1 regulatory subunits PNUTS (Protein phosphatase-1 nuclear targeting subunit), SPINO (Spinophilin), and NIPP1 (Nuclear inhibitor of protein phosphatase 1) (Choy *et al.*, 2014). This extension involves two hydrophobic amino acids residues 7-9 amino acids C-terminal of the RVXF motif and an arginine residue 9-10 amino acids C-terminal from that, which the D group MPKs have a similar version of, and provides more evidence for the D group MPKs potential interaction with PP1 (Choy *et al.*, 2014).

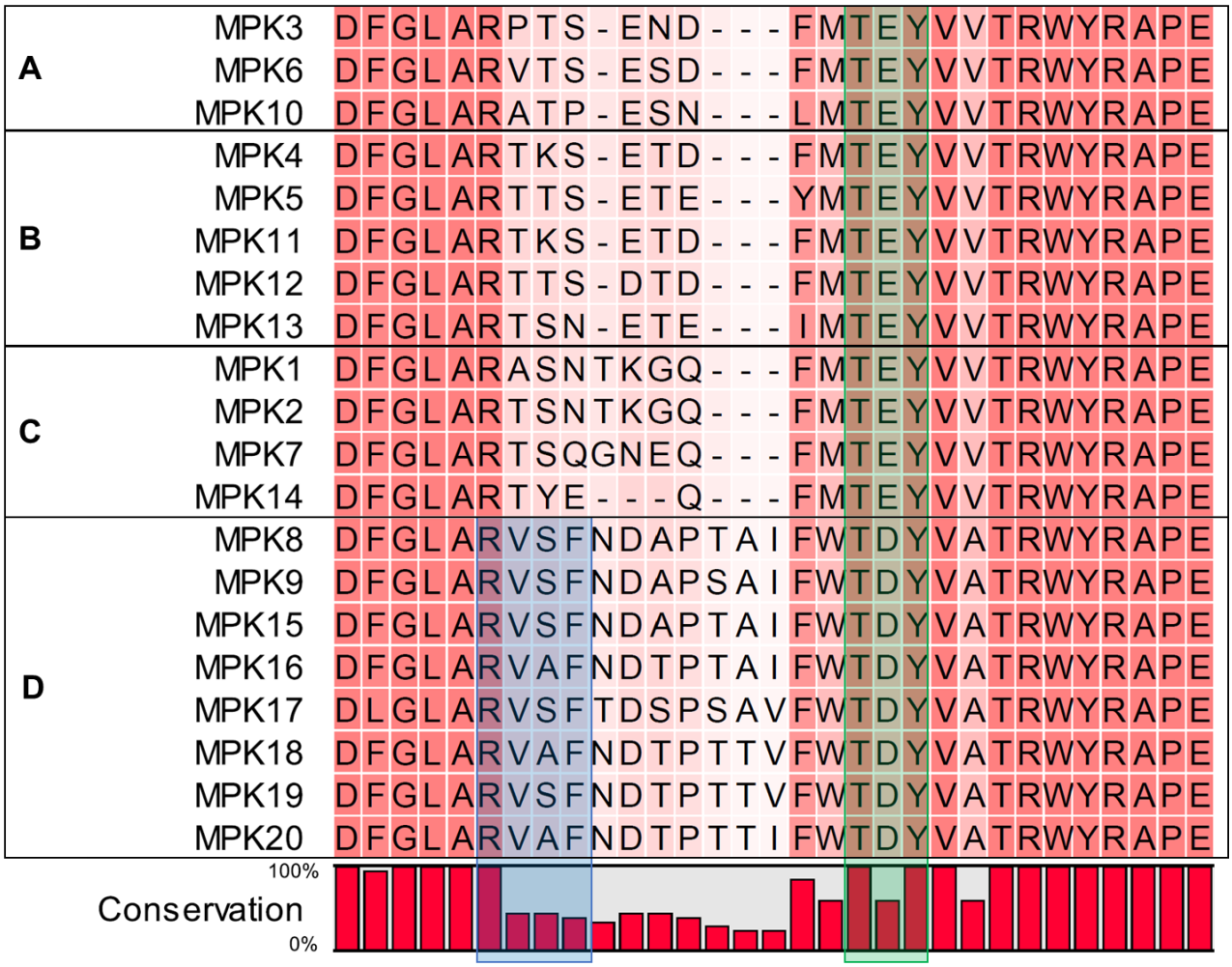

Figure 4. Bioinformatic alignment of the activation loops from all 20 MPKs in *Arabidopsis thaliana*. Green highlighted region representing the TXY motif. Aligned sequences are presented in their respective MPK groups (A, B, C, and D) **(Table 1)**. The blue highlighted region is the RVXF motif for group D only. CLC Sequence Viewer 8.0 was used to align the sequences.

Table 1. Protein name, gene identifier, and the corresponding activation loop sequence for the 20 MPKs found in *Arabidopsis thaliana.* Sequences found in this table were used to generate the MPK activation loop sequence alignment seen in Figure 4.

Name	Gene Identifier	Activation Loop Sequence
MPK1	At1g10210	DFGLARASNTKGQFMTEYVVTRWYRAPE
MPK2	At1g59580	DFGLARTSNTKGQFMTEYVVTRWYRAPE
MPK3	At3g45640	DFGLARTSNTKGQFMTEYVVTRWYRAPE
MPK4	At4g01370	DFGLARTKSETDFMTEYVVTRWYRAPE
MPK5	At4g11330	DFGLARTTSETEYMTEYVVTRWYRAPE
MPK6	At2g43790	DFGLARVTSESDFMTEYVVTRWYRAPE
MPK7	At2g18170	DFGLARTSQGNEQFMTEYVVTRWYRAPE
MPK8	At1g18150	DFGLARVSFNDAPTAIFWTDYVATRWYRAPE
MPK9	At3g18040	DFGLARVSFNDAPSAIFWTDYVATRWYRAPE
MPK10	At3g59790	DFGLARATPESNLMTEYVVTRWYRAPE
MPK11	At1g01560	DFGLARTKSETDFMTEYVVTRWYRAPE
MPK12	At2g46070	DFGLARTTSDTDFMTEYVVTRWYRAPE
MPK13	At1g07880	DFGLARTSNETEIMTEYVVTRWYRAPE
MPK14	At4g36450	DFGLARTYEQFMTEYVVTRWYRAPE
MPK15	At1g73670	DFGLARVSFNDAPTAIFWTDYVATRWYRAPE
MPK16	At5g19010	DFGLARVAFNDTPTAIFWTDYVATRWYRAPE
MPK17	At2g01450	DLGLARVSFTDSPSAVFWTDYVATRWYRAPE
MPK18	At1g53510	DFGLARVAFNDTPTTVFWTDYVATRWYRAPE
MPK19	At3g14720	DFGLARVSFNDTPTTVFWTDYVATRWYRAPE
MPK20	At2g42880	DFGLARVAFNDTPTTIFWTDYVATRWYRAPE

1.3 Protein Phosphatases – The Four Families of Protein Phosphatases

The enzymes responsible for the reversibility of protein phosphorylation is the protein phosphatases. Originally thought of as "housekeeper" enzymes whose sole function was to remove and maintain the phosphorylation status of the proteome, it was later realized that these enzymes played many essential roles in cell function. While there are 942 different kinases within *Arabidopsis thaliana*, there are only ~150 protein phosphatases (Gribskov, 2001; Manning *et al.*, 2002; Uhrig, Labandera and Moorhead, 2013; Zulawski *et al.*, 2014). This seems to be a significant difference in quantity which, based on their antagonistic relationship, we would expect to be similar. This difference in quantity of protein kinases and phosphatases is based on protein phosphatases commonly having multiple regulatory subunits that designate substrate specificity to

a common catalytic subunit, while one kinase often only has a few targets based on its built-in specificity (Uhrig, Labandera and Moorhead, 2013).

There are four families of protein phosphatases which are separated based on their sequence similarity in catalytic motifs, which substrate a protein phosphatase preferably dephosphorylates, dependency on divalent metal ions, and vulnerability towards different inhibitors (Hanks, 2003; Uhrig, Labandera and Moorhead, 2013).

The phospho-protein phosphatase (PPP) family is serine and threonine phosphatases grouped based on their sequence similarity in the catalytic residues that are involved in their dephosphorylation mechanism (Uhrig, Labandera and Moorhead, 2013). The PPP family use a catalytic mechanism utilizing two metal ions (commonly Mg^{2+}/Mn^{2+}) and are characterized to dephosphorylate phosphoserine and phosphothreonine residues (Uhrig, Labandera and Moorhead, 2013). The catalytic motifs that define a member of the PPP family are GDxHG, DGxVDRG, GNHE, and HGG (Uhrig, Labandera and Moorhead, 2013). The PPP family is an immensely versatile group of proteins because alone they are simple catalytic subunits but can often interact with a wide array of regulatory subunits that direct the localization and substrate specificity of these phosphatases (Moorhead *et al.*, 2009). In *Arabidopsis thaliana,* the 11 members identified within the PPP family of phosphatases are PP1 (PP1), PP2A, PP4, PP5, PP6, PP7, SLP1, SLP2, RLPH1, RLPH2, and PPKL **(Figure 5)** (Uhrig, Labandera and Moorhead, 2013). It should be noted that there is no identified homologue of the PPP member PP2B found in plants.

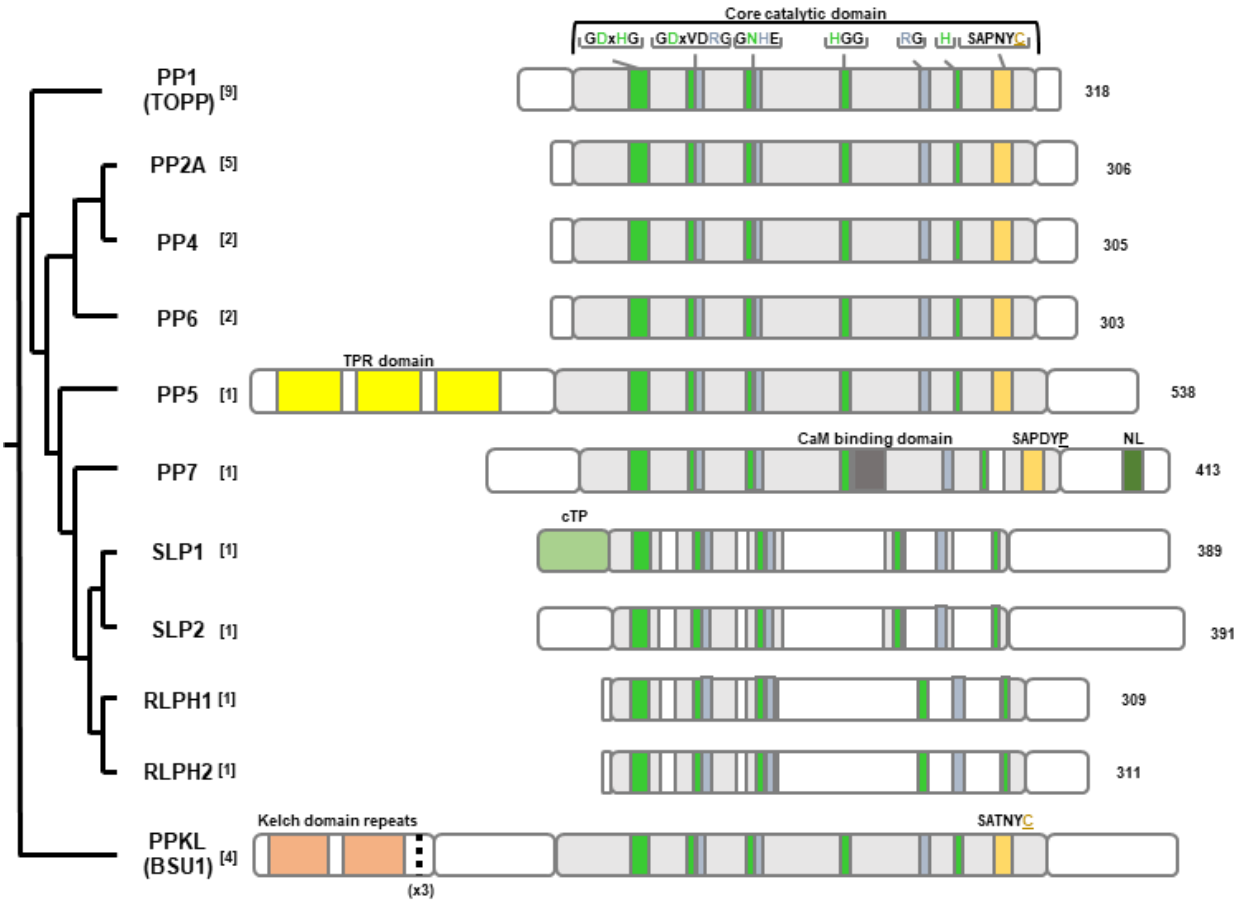

Figure 5. Sequence similarity between known members of the PPP subfamily of phosphatases. Green regions represent the conserved catalytic motifs in all PPPs. The purple regions represent the SAPNYC domain where inhibitors such as microcystin bind (Uhrig, Labandera and Moorhead, 2013).

The phospho-tyrosine phosphatase (PTP) family is grouped based on a common (V/H)CX$_5$R motif acting as the catalytic dephosphorylation mechanism and having primarily tyrosine phosphorylated substrates (Jia *et al.*, 1995). Some members of the PTP family are capable of dephosphorylating both phosphorylated tyrosine and threonine residues, hence being classified as dual specific phosphatases (DSPs) (Kerk, Templeton and Moorhead, 2008; Stanford and Bottini, 2017). The PTP family also contains some members that have been characterized to

dephosphorylate molecular substrates that are not proteins (Kerk, Templeton and Moorhead, 2008; Shi, 2009).

The metallo-dependent protein phosphatase (PPM) family are grouped based on their need for divalent Mg^{2+}/Mn^{2+} ions to function, similar to the PPP family, yet the PPM family utilize RxxxD, DGxxG, DG, and GxxDN motifs to make up their catalytic mechanism which differs from the motifs utilized by the PPP family (Shi, 2009; Fuchs *et al.*, 2013). Another difference between these two groups of phosphatases is the PPM members use of built-in motifs that control the subcellular localization and substrate specificity, unlike the PPP family which use interactions with regularity subunits (Ubersax and Ferrell, 2007; Shi, 2009). PPM family members have been characterized to participate in MPK signaling pathways in biotic and abiotic stress pathways (Meskiene *et al.*, 2003; Leung *et al.*, 2006; Schweighofer *et al.*, 2007; Ma *et al.*, 2009). This is by far the largest of the phosphatase families in *Arabidopsis* containing over 70 members, approximately four times the number found in mammalian proteomes (Schweighofer, Hirt and Meskiene, 2004).

The aspartate-based protein phosphatase family is grouped together based on their utilization of aspartic acid residues to dephosphorylate substrates. The aspartic acid residue found within their unique DxDxT/V motif acts in the catalytic mechanism that interacts with and coordinates with Mg^{2+} to dephosphorylate substrates (Szöör, 2010). The aspartate-based protein phosphatases are poorly characterized, with their only identified members being an RNA polymerase II protein phosphatase and a few members of the haloacid dehalogenase (HAD) family (Kerk, Templeton and Moorhead, 2008; Seifried, Schultz and Gohla, 2013).

1.4.1 Novel Bacteria-like Protein Phosphatases

In a bioinformatic study of *Arabidopsis thaliana* and other plant species, a group of novel phosphatases were first brought into the light, unique in their presence in only higher plants and some eukaryotes, but not mammals **(Table 2)** (Andreeva and Kutuzov, 2004; Uhrig, Kerk and Moorhead, 2013). Bioinformatically characterized as members of the PPP family, these new phosphatases were named Protein Phosphatase Kelch-like (PPKL), *Shewanella*-like phosphatase (SLP) and *Rhizobiales*-like phosphatase (RLPH). PPKL was named based on the presence of its N-terminal kelch repeats which are known to play a role in protein-protein interaction. SLP and RLPH were named based on their relation to the two bacterial species *Rhizobiales* and *Shewanella* (Andreeva and Kutuzov, 2004; Uhrig, Kerk and Moorhead, 2013). *Arabidopsis thaliana* has four PPKLs, two SLPs, and two RLPHs. The four PPKLs are Bri1 suppressor 1 (BSU1), Bri1 suppressor-like 1 (BSL1), Bri1 suppressor-like 2 (BSL2), and Bri1 suppressor-like 3 (BSL3).

Table 2. Phospho-Protein Phosphatase family members. Number of PPP family genes for each subclass in both *Arabidopsis thaliana* and *Homo sapiens.*

PPP Sub-Family	*Arabidopsis* Genes	*Homo sapiens* Genes
PP1	9	3
PP2A	5	2
PP2B	0	3
PP4	2	1
PP5	1	1
PP6	2	1
PP7	1	2
PPKL	4	0
SLP	2	0
RLPH	2	0
Total	28	13

1.4.2 *Shewanella*-like phosphatase (SLP)

There are two SLP genes in *Arabidopsis,* AtSLP1 which is localized to chloroplasts and AtSLP2 which is localized to mitochondria (Uhrig, Kerk and Moorhead, 2013; Uhrig *et al.*, 2017). Dephosphorylation assays conducted *in-vitro* shows SLP1 has no preference towards a certain phosphorylated serine, threonine, or tyrosine substrate and SLP2 has been characterized to have a preference towards phospho-serine and threonine substrates (Uhrig *et al.*, 2017). While members of the PPP family, the SLPs do not contain the SAPNYC motif which common PPP inhibitors such as okadaic acid and microcystin bind to. It has been experimentally shown that these two inhibitors have no impact on these phosphatases (Uhrig, Kerk and Moorhead, 2013).

1.4.3 *Rhizobiales*-like Phosphatase 2 (RLPH2) – A Bacterial Like Protein Phosphatase

The RLPHs, designated a novel bacteria-like protein phosphatase, is mostly found in higher plants, with some cases in other photosynthetic organisms such as green algae, and even a few cases of non-photosynthetic organisms such as the excavate *Naegleria gruberi* and the opisthokont *Salpingoeca rosetta* (Uhrig, Kerk and Moorhead, 2013).

There are two RLPH genes which share an 85% amino acid sequence identity but while RLPH1 only has high levels of transcription in the roots of *Arabidopsis thaliana*, RLPH2 has a much higher transcription level throughout the entire plant with the highest found in pollen **(Figure 6)**. Based on the low transcription levels of RLPH1, more research focus has been directed towards RLPH2 and today not much is known about RLPH1.

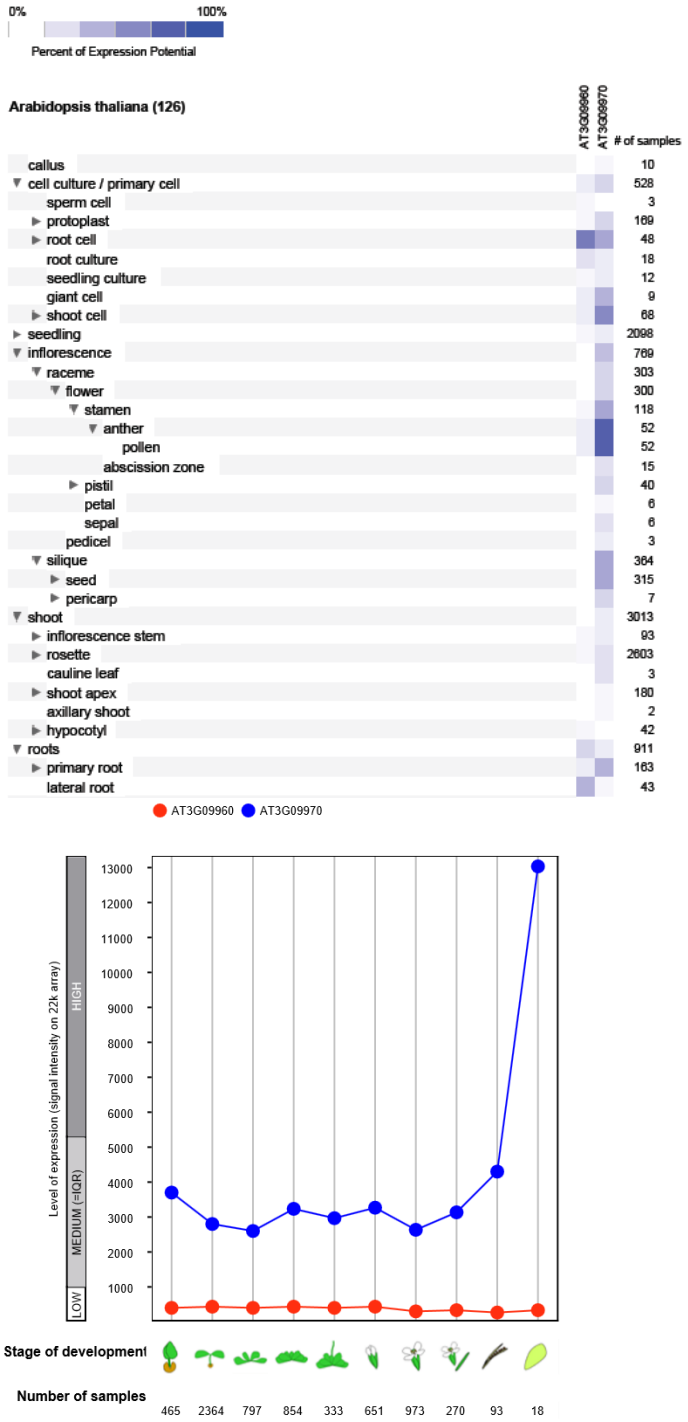

Figure 6. Transcription of RLPH1 and RLPH2 across tissues and developmental stages. (Left) tissue specific transcriptional data for RLPH1 (At3g09960) and RLPH2 (At3g09970) in different tissues. Dark blue indicates a higher transcription, white indicates a lower transcription, and the # of samples indicates the number of microarrays used to determine the transcription levels. (Right) transcriptional data of RLPH1 (At3g09960) in red and RLPH2 (At3g09970) in blue at different developmental stages of *Arabidopsis thaliana.* Number of samples represents the number of microarrays used to determine the transcription levels (Labandera, 2017).

While bioinformatically placed in the PPP family based on its presence of the shared catalytic motifs involved in the PPP dephosphorylation mechanism, it was shown through peptide dephosphorylation assays that RLPH2 prefers phosphotyrosine residues instead of the phosphoserine and phosphothreonine residues preferably dephosphorylated by members in the PPP family (Uhrig, Kerk and Moorhead, 2013; Labandera *et al.*, 2018). It was also shown that because it does not have the SAPNYC motif, the motif that PPP inhibitors such as microcystin or okadaic acid bind to, RLPH2s activity is not diminished in the presence of these inhibitors **(Figure 7A, 7B)**. Another intriguing detail was that the presence of the phosphotyrosine phosphatase inhibitor orthovanadate showed a significant decrease in RLPH2 activity **(Figure 7C)**. It has also been shown that there does not seem to be a dependency on metal ions, which the dependency of is one of the key features of the PPP family, as the presence of different metal cations caused no change in RLPH2 activity **(Figure 7D)**. In the presence of Zn^{2+} there is a slight inhibitory effect on RLPH2, which is a common PTP family member characteristic. These characteristics show that while on a bioinformatic level RLPH2 is observed as a member of the PPP family, it has characteristics on an enzymatic level that are PTP-like.

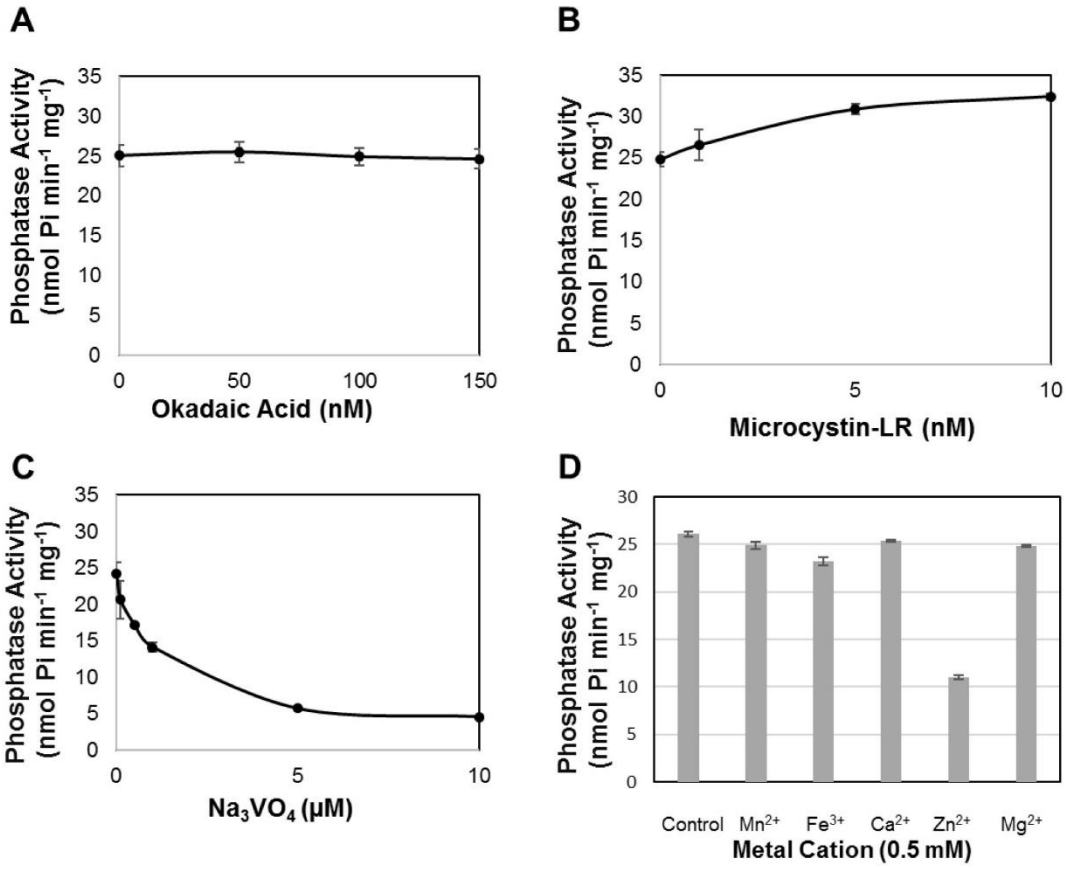

Figure 7. RLPH2 pNPP dephosphorylation assays in the presence of PPP and PTP inhibitors, and different divalent metal cations. 150ng of recombinant purified RLPH2 incubated with *p*NPP and different concentrations of Okadaic acid (a PPP inhibitor), Microcystin-LR (a PPP inhibitor), Sodium Orthovanadate (a PTP inhibitor), and different divalent metal cations Mn^{2+}, Fe^{2+}, Ca^{2+}, Zn^{2+}, and Mg^{2+} (Uhrig and Moorhead, 2011a; Labandera, 2017).

Recently, the structure of RLPH2 was solved using protein crystallography revealing a deep active site, too deep to accommodate a phosphoserine or phosphothreonine residue, but perfect for a phosphotyrosine residue providing a possible explanation for its phosphotyrosine directed activity **(Figure 8)** (Labandera *et al.*, 2018). Another interesting observation that was made from the crystal structure was the presence of a basic pocket directly next to the active site.

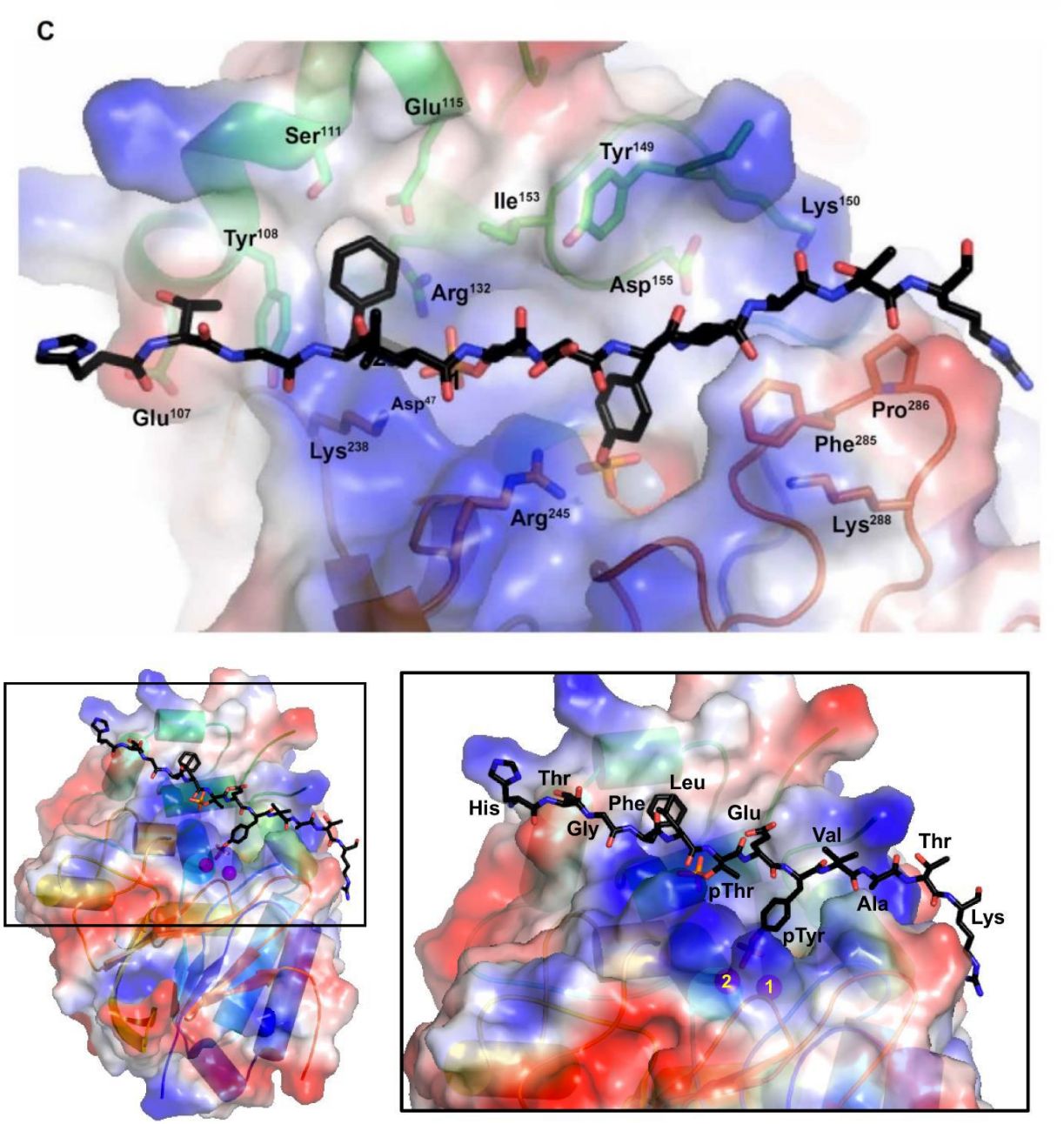

Figure 8. Active site of RLPH2. Close up view of the RLPH2 crystal structure active site with the adjacent basic binding pocket. Peptide modeled into the structure is HTGFLpTEpYVATR, derived from human ERK1/2. Red shaded regions represent areas with a negative charge, while blue shaded regions represent areas with a positive charge (Labandera *et al.*, 2018).

The potential purpose for the basic pocket would be revealed through phosphoproteomic mass spectrometry conducted by Dr. Glen Uhrig at the University of Alberta. Comparing the

phosphorylation status of phosphotyrosine peptides in WT and RLPH2 KO lines (*atrlph2-1*, *atrlph2-2*) revealed the biological substrates of RLPH2 to be the D group mitogen activated protein kinases (MPK) with the site of dephosphorylation being the tyrosine of the activation loops TXY motif **(Table 3)** (Labandera, 2017). As the TXY motif is known to be dual phosphorylated, the phosphothreonine creates the perfect ligand to bind into the basic pocket next to the active site. This addition of a phosphorylated threonine residue in the TXY motif has been shown through Michaelis-Menten enzyme kinetics to increase the binding affinity of RLPH2 to the substrate **(Figure 9)** (Labandera *et al.*, 2018).

Table 3. RLPH2 phosphoproteomic results. Comparison of the phosphorylation status of pTyr in proteins within WT and RLPH2 KO *Arabidopsis* lines (*atrlph2-1*, *atrlph2-2)*. Samples were enriched for phospho-peptides using TiO_2 followed by tyrosine phosphorylated peptide immunoprecipitation to enrich phosphotyrosine peptides. Blank cells represent no identified peptides from MS. Table contains AGI gene identifier, protein description, and then the confidence number of the phosphorylated peptide being observed. Pink cells represent protein peptides found to be dephosphorylated in WT but not RLPH2 KO mutant lines. Grey cells represent protein peptides that contained one experiment where the WT line showed dephosphorylated protein. Yellow cells represent proteins phosphorylated in both lines (Labandera, 2017).

AGI	Description	Experiment 1			Experiment 2		
		WT	*atrlph2-1*	*atrlph2-2*	WT	*atrlph2-1*	*atrlph2-2*
AT3G18040	ATMPK9_mitogen-activated protein kinase 9		99% (1)	99% (1)			99% (1)
AT1G53510	ATMPK18_mitogen-activated protein kinase 18			99% (1)			100% (1)
AT2G42880	ATMPK20_mitogen-activated protein kinase 20		99% (1)	99% (1)			99% (1)
AT4G00720	ATSK32, ASKTHETA, SK32 | shaggy-like protein kinase 32	88% (0)	98% (1)	99% (1)	95% (0)	99% (1)	99% (1)
AT3G15730	PLDALPHA1, PLD | phospholipase D alpha 1	99% (0)		53% (0)	99% (0)	98% (1)	100% (1)
AT3G61160	Protein kinase superfamily protein	44% (0)	99% (1)	64% (0)	94% (0)	99% (1)	99% (1)
AT1G06410	ATTPS7, trehalose-phosphatase/synthase 7		99% (1)	99% (1)	99% (1)	99% (1)	99% (1)
AT5G19010	ATMPK16_mitogen-activated protein kinase 16		99% (1)	99% (1)	99% (1)	99% (1)	99% (1)
AT2G43790	ATMPK6_mitogen-activated protein kinase 6	99% (1)	99% (1)	99% (1)	99% (1)	100% (1)	100% (1)
AT3G45640	ATMPK3_mitogen-activated protein kinase 3	100% (2)	99% (1)	99% (1)	100% (1)		100% (2)
AT1G10210	ATMPK1_mitogen-activated protein kinase 1	99% (1)		99% (1)	99% (1)	90% (0)	99% (1)
AT1G09840	ATSK41| shaggy-like protein kinase 41	99% (1)	99% (1)	99% (1)	99% (1)	99% (1)	99% (1)
AT1G73460	Protein kinase superfamily protein	99% (1)	99% (1)	99% (1)	100% (1)	94% (0)	100% (1)
AT2G39730	RCA | rubisco activase	100% (1)	100% (1)	100% (1)	100% (1)	100% (0)	100% (1)
AT2G40120	Protein kinase superfamily protein	99% (1)	99% (1)	99% (1)	95% (0)	98% (1)	
AT3G25840	Protein kinase superfamily protein	99% (1)	99% (1)	99% (1)	100% (1)	100% (1)	99% (1)
AT3G45140	Lipoxygenase 2	99% (1)	93% (0)	99% (1)	100% (1)	100% (1)	100% (1)
AT4G18710	BIN2, ATSK21	99% (1)	99% (1)	99% (1)	99% (1)	98% (0)	100% (1)
AT5G04140	Glutamate synthase 1	100% (1)	99% (1)	100% (1)	100% (1)	100% (1)	100% (1)

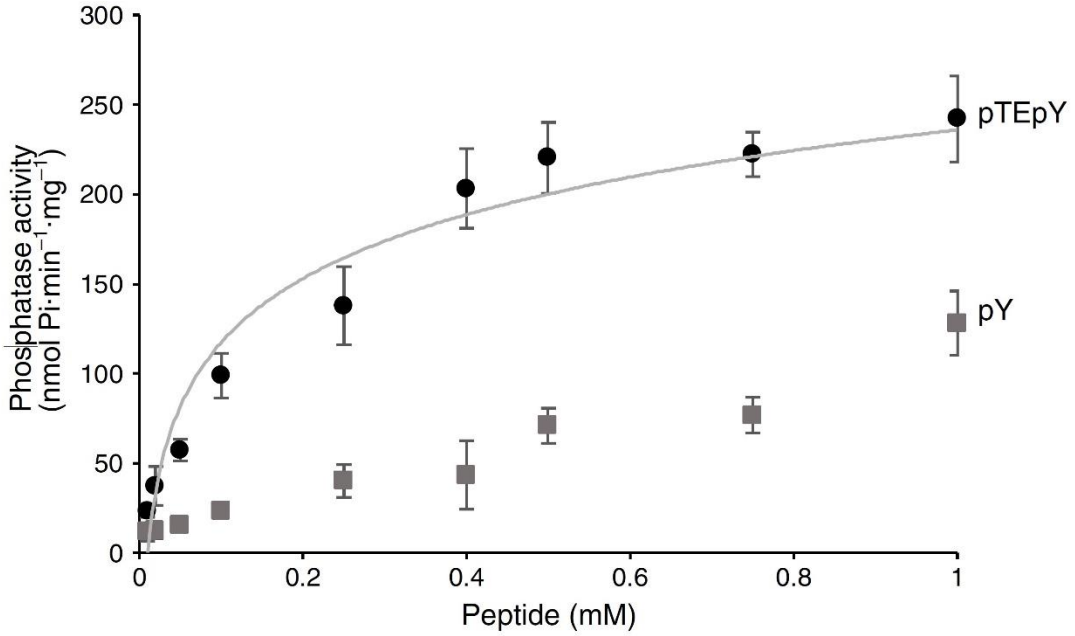

Figure 9. Bacterially-expressed RLPH2 Michaelis-Menton plot showing substrate preference. Activity was determined using a malachite green dephosphorylation. Substrate peptides were ERK1/2 (pTEpY, black) and ERK1/2 (TEpY, grey) (Labandera, 2017).

1.5 Protein Phosphatase 1 (PP1) – A Phosphatase with many Regulatory Subunits

Protein Phosphatase 1 (PP1), sometimes referred to as Type One Protein Phosphatase 1 (TOPP), is a classic member of the PPP family containing the key catalytic motifs and with activity directed towards phosphoserine and phosphothreonine substrates. It is also undoubtably one of the most significant signalling proteins in all eukaryotic organisms and is the paragon of protein-protein interaction mechanisms as it has been characterized to interact with 220 regulatory subunits in *Homo sapiens,* but has been hypothesized to interact with potentially up to 600 different regulatory subunits (Templeton *et al.*, 2011). This massive interactome of PP1 is strong supporting evidence of PP1's importance, and while many of its interactors in *Homo sapiens* have been unraveled, only nine PP1 regulatory subunits in *Arabidopsis thaliana* have been characterized, including proteins such as the nuclear inhibitor of protein phosphatase 1 (NIPP1), GL2 expression modulator (GEM), and inhibitor-2 (I2) **(Figure 10)** (Templeton *et al.*, 2011). Nonetheless, with

the plant proteome containing more proteins than the mammalian proteome, the number of unrevealed PP1 regulatory subunits that have yet to be determined can only be hypothesized as enormous.

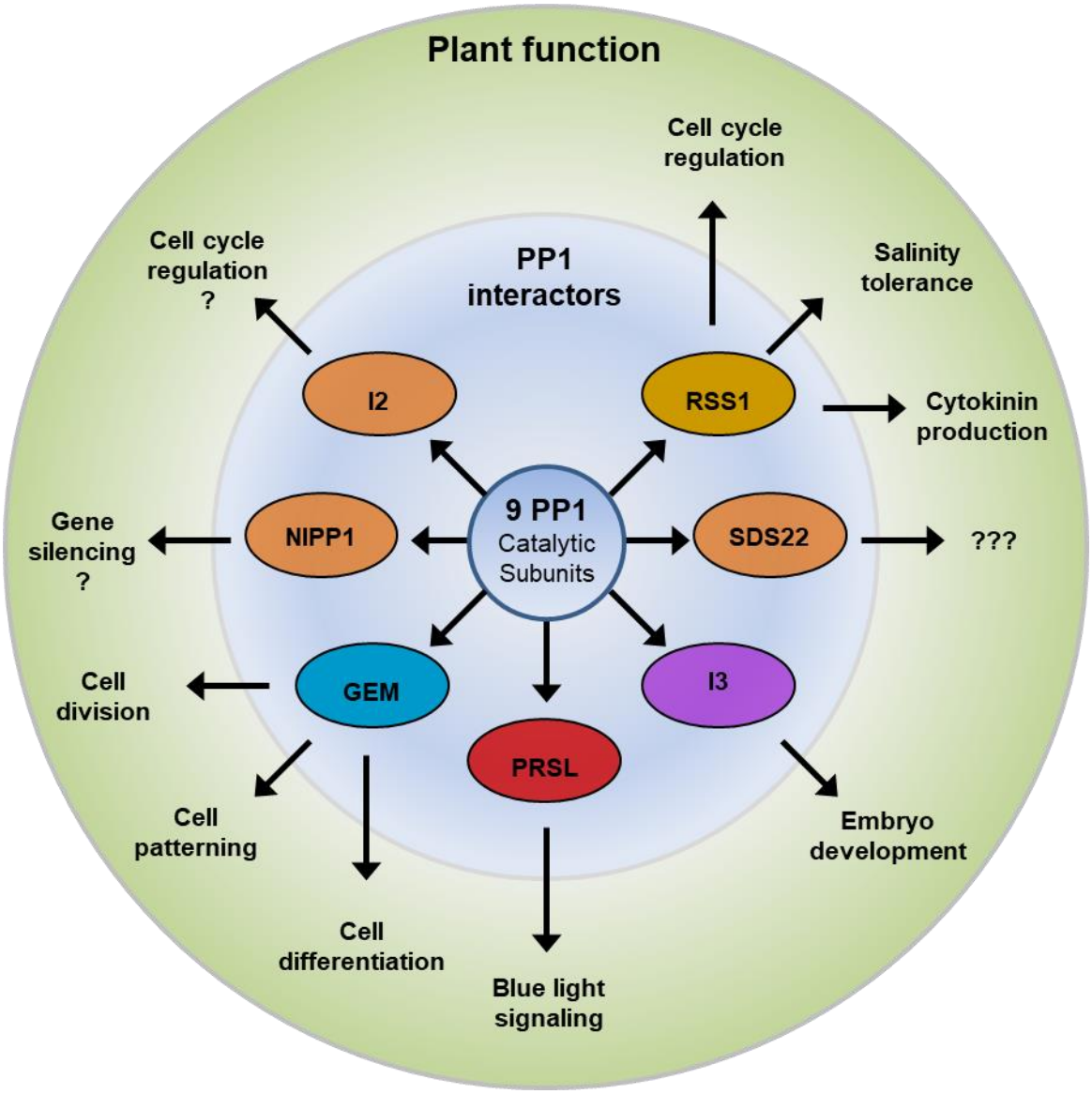

Figure 10. Regulatory proteins effect on PP1 in *Arabidopsis thaliana*. Shown are regulatory proteins to PP1 and their downstream pathways. Question marks represent unknown functions, or in the case where a pathway is given, the known homologous pathway in *Homo sapiens* (Uhrig, Labandera and Moorhead, 2013).

The discovery of PP1 occurred in the early history of protein phosphorylation as a protein that was classically purified from rabbit skeletal muscle for its dephosphorylation activity on glycogen phosphorylase *a* converting it to its dephosphorylated state named phosphorylase *b* (Alemany *et al.*, 1986). Later it was realized that the simple ~35kDa protein phosphatase was more complex than the original impression gave, as it was being purified with other interacting proteins that were in complexes with PP1, and these interacting proteins had an impact on the activity of PP1 in a regulatory capacity.

This interaction between regulatory proteins and PP1 occurs through the strongly characterized RVXF motif that is found on proteins that regulate the function of PP1 **(Figure 11)** (Wakula *et al.*, 2003). This interaction is based on the RVXF motif utilizing the valine and phenylalanine residues to interact with a hydrophobic binding pocket on the surface of PP1 **(Figure 12)** (O'Connell *et al.*, 2012; Choy *et al.*, 2014). The valine and phenylalanine residues are tremendously vital to the binding interaction between a regulatory subunit and PP1, as a result, a single mutation in only one of these amino acids to alanine has been characterized to nullify the binding affinity for the motif to PP1 (Trinkle-Mulcahy *et al.*, 2006). Over time it was realized that the RVXF motif can have extended additions, or secondary interactions which aid in the binding interaction between the motif carrying regulatory protein onto the PP1 catalytic subunit. A few examples of these are the SILK, MyPhoNE, the RVXF-ΦΦ, and the RVXF-ΦΦ-R motif **(Figure 13)** (Hendrickx *et al.*, 2009; Choy *et al.*, 2014). While the characterization of the RVXF motif has led to an advancement in the determination of PP1 regulatory subunits, because of the potential flexibility of this motif, the presence of this motif alone is not enough to conclusively determine a PP1 regulatory subunit **(Figure 11)**.

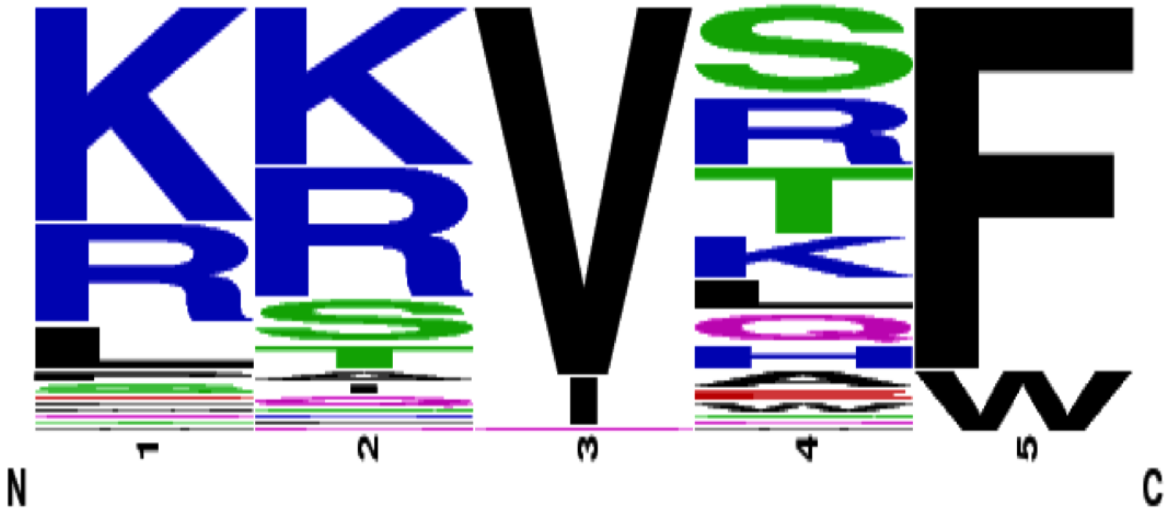

Figure 11. Amino acid frequency of the RVXF motif. Representation of the prevalence of amino acids that are found in *Homo sapiens* PP1 confirmed regulatory binding proteins RVXF motif (Nasa, 2018).

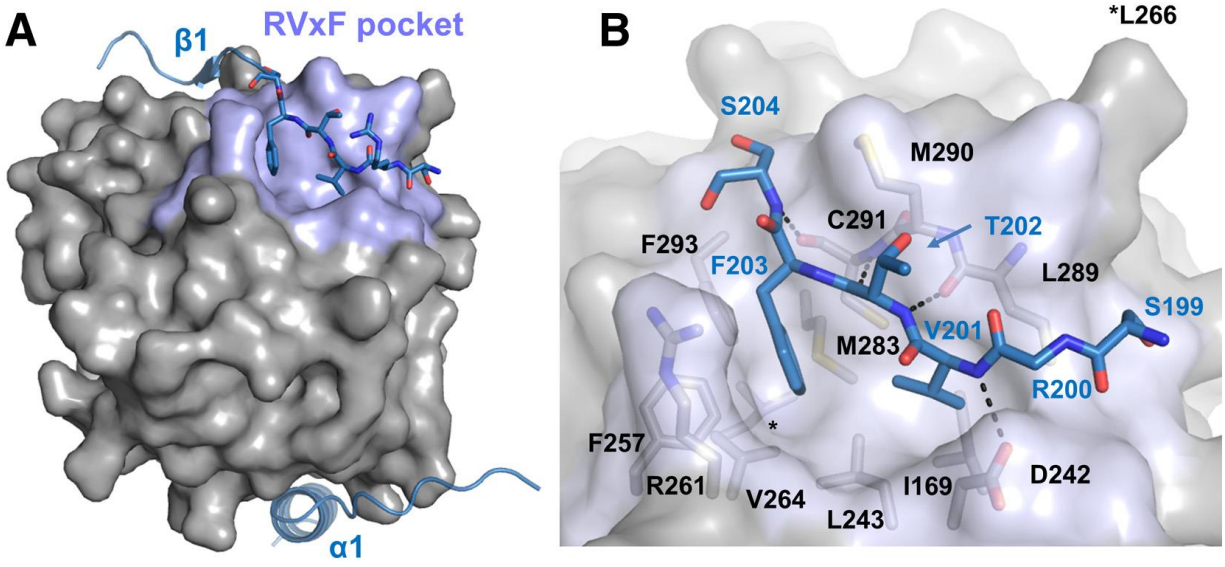

Figure 12. Binding between PP1 and the RVXF motif. A. Interaction shown is between PP1 and the NIPP1 sequence containing the RVXF motif. PP1 structure is in grey with the hydrophobic pocket (RVXF pocket) highlighted light blue. **B.** An enlarged view of the interaction between the RVXF motif and the pocket. Blue chain is the NIPP1 sequence containing the RVXF motif (O'Connell *et al.*, 2012).

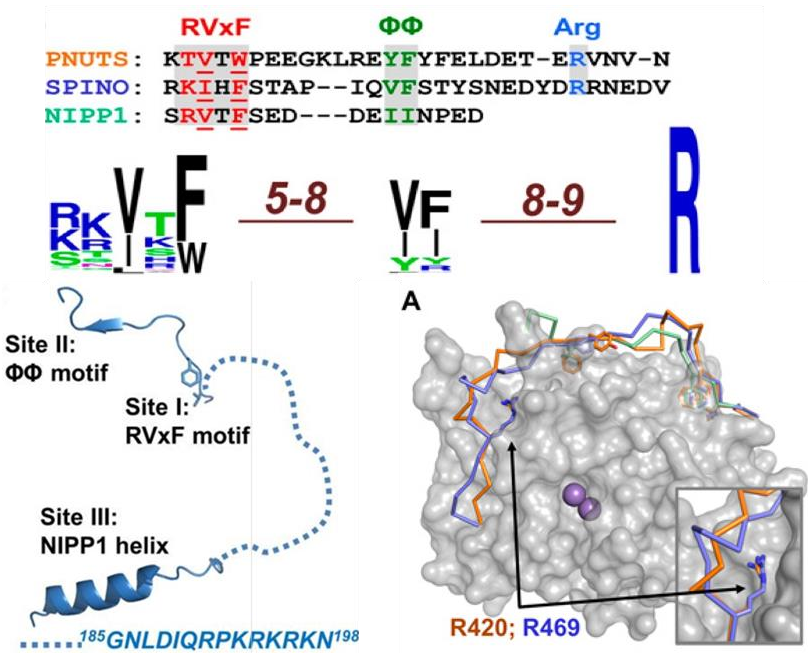

Figure 13. RVXF-ΦΦ-R, an Extended RVXF motif. (Top) shows the extended RVXF motif was present in NIPP1, SPINO, and PNUTS and utilizes two hydrophobic residues five to eight amino acids downstream of the RVXF motif, then an additional arginine residue eight to nine amino acids further down stream (Choy *et al.*, 2014). (Bottom) shows the structural binding of NIPP1 to PP1 and where the extended key residues interact (O'Connell *et al.*, 2012).

The nine isoforms of PP1 in *Arabidopsis* beyond most of them localizing to the nucleus (Takemiya, Ariyoshi and Shimazaki, 2009). The nine isoforms of *Arabidopsis* PP1 share at least a 64% sequence similarity with some isoforms sharing a 90% sequence similarity, which is interesting in the fact that the four PP1 isoforms in *Homo sapiens* all have at least a 90% sequence similar identity. This indicates the potential for the nine isoforms of *Arabidopsis* PP1 to have a wider variety in functions and mechanisms, with a key example being PP1-6 being a PPP member that does not contain the SAPNYC motif which famously interacts with potent PPP inhibitors such as microcystin (Uhrig, Kerk and Moorhead, 2013)

1.6 Hypothesis and Objectives

The novel and unique protein phosphatase RLPH2 fills a gap in the *Arabidopsis* phospho-proteome when it comes to the unique differences in plant tyrosine phosphorylation kinases and phosphatases compared to mammalian. With phosphoproteomic data indicating that the D group of MPKs are substrates of RLPH2, the hypothesis is that RLPH2 is directly responsible for dephosphorylating the tyrosine of the TXY motif in the D group MPK activation loop. This would indicate RLPH2 plays a key role in the deactivation in 8 of the 20 MPKs in *Arabidopsis thaliana,* as it is commonly required for both sites in the TXY motif to be phosphorylated for the activation of MPKs. Based on bioinformatic analysis of the D group MPKs sequence which is distinctively separate from the A, B, or C groups, the regulatory mechanism for substrate specificity of RLPH2 towards the D group may rest in the unique activation loop sequences. One of the objectives of this thesis is to provide further evidence of RLPHs interaction with the D group MPKs, and to determine the mechanism by which RLPH2 interacts with the D group and not the A, B, or C group.

Additionally, the D group MPKs also contain the well characterized RVXF motif, the motif that recruits regulatory subunits to protein phosphatase 1, which formulates the hypothesis that the D group MPKs interact with nine isoforms of PP1 in a possible regulatory capacity. An objective of this thesis is to confirm that the D group MPKs can interact with PP1, that this interaction occurs through the RVXF motif, and possibly deciphers the purpose of this interaction.

Finally, it is predicted that the interaction between RLPH2 and PP1 with the D group of the MPKs occurs within proximity of each other. Another objective of this thesis, if possible, is to determine if these two interactions are dependent on one another resulting in a mechanism that involves cross-talk with both RLPH2 and PP1 towards the D group MPKs.

METHODS

2.1 Bradford concentration determination assay

Protein concentrations were determined using the Bradford protein concentration determination assay. 10 µL of protein sample was added to 990 µL Bradford reagent (0.05% (w/v) Coomassie brilliant blue G250, 25% ethanol, 50% phosphoric acid) and left at RT for 10 min before using a spectrophotometer to measure the absorbance of the sample at 595 nm. Absorbance obtained was converted to protein concentration by comparison with a standard curve generated against BSA.

2.2 SDS-PAGE and western blotting

SDS-PAGE and western blots were conducted using the following methodology. All 12% gels were run at 120 V for 30 min followed by 180 V until the dye front runs off the gel. For gels that were to be colloidal stained, gels were excised from the gel apparatus and placed in a tray. Destain solution (10% acetic acid, 25% methanol) was added and the gel was left shaking for 20 min, before being washed four times for 5 min each with distilled water, then left in colloidal dye for 18 hr or until bands developed.

For gels that were to be used for immunoblotting, gels were excised from the gel apparatus and placed in a transfer apparatus for the protein bands to be transferred onto a nitrocellulose membrane. Transfer was run for 2 hr at 100 V. Transferred nitrocellulose membrane was then left in a milk blocking solution (5% evaporated milk (w/v)) for 1 hr at RT. Milk solution was washed off using TBS buffer (12.5 mM Tris-HCl pH 7.5, 500 mM NaCl) four times for 5 min each. After washing off the milk solution, the primary antibody was added for the recommended time. After primary antibody incubation was complete, membrane was washed with TBS 0.2% (TBS buffer plus 0.2% Tween-20) four times for 5 min each. Following the washing of the primary, secondary

antibody was added (1:5000, either anti-rabbit or anti-mouse antibodies) in 5% milk (w/v) in TBS 0.1% (TBS buffer plus 0.1% Tween-20). After washing off the secondary antibody, membrane was incubated for 3 min with ECL (GE Healthcare).

2.3 Cloning, expression, and purification of the *Arabidopsis thaliana Rhizobiales*-like Phosphatase 2 (RLPH2)

The RLPH2 gene At3g09970 was cloned by Dr. R Glen Uhrig (Uhrig, 2013). Gene was obtained from the Arabidopsis Information Resource (http://www.arabidopsis.org/) which was cloned into the pDNR221 gateway donor vector (Invitrogen) using gateway terminal specific primers that through a BP reaction (Invitrogen) the gene was transported into the expression vector via gene recombination. Utilizing the LR reaction of gateway vectors, the RLPH2 gene was recombinantly transported into a pDEST42 gateway expression vector (Invitrogen) which genetically engineered a C-terminus His6 and V5 tag (a unique epitope "GKPIPNPLLGLDST" for protein detection via immunoblotting experiment with anti-V5 antibodies) onto RLPH2 to be utilized for His6 specific protein purification.

The RLPH2-V5-His6 pDEST42 construct was transformed in a BL21 (DE3) CodonPlus-RIL *E. coli* strain and grown until an OD_{600} of 0.4-0.6 ABS was reached, at which point 0.1 mM IPTG was added to induce gene expression for 18 hr at 22 °C. Afterwards, induced cells were centrifuged at 3300 xg for 20 min and the resulting pellet was resuspended in Resuspension Buffer (50 mM Hepes-NaOH pH 7.5, 150 mM NaCl, 5% (v/v) glycerol) with the addition of 10 mM imidazole, 1 mM benzamidine and 1 mM PMSF before cells were lysed. Resuspended cells were lysed by French press (three passes at 1000 psi), then centrifuged at 50,000 xg for 45 min. Supernatant containing the soluble fraction was collected and filtered through miracloth before being incubated with 1 mL Ni-NTA matrix (Qiagen) that was equilibrated in 50 mM HEPES pH

7.5, 150 mM NaCl, for 1 hr at 4 °C. Following the matrix-protein incubation, the matrix was washed with 300 mL of Wash Buffer A (50 mM Hepes-NaOH pH 7.5, 1 M NaCl, 5% (v/v) glycerol, 1% (v/v) Tween-20 and 10 mM imidazole). The salt conditions were normalized with an additional wash of 100 mL of Wash Buffer B (50 mM HEPES pH 7.5, 150 mM NaCl, 5% glycerol, 10 mM imidazole) before proteins were eluted in 15 mL of Elution Buffer (50 mM HEPES pH 7.5, 150 mM NaCl, 400 mM imidazole, 5% glycerol).

Eluted protein was concentrated in a 30 kDa centricon (Amicon), and then using the same centricon, the buffer was exchanged for Wash Buffer B. Protein concentration was determined using Bradford protein concentration assay. Protein was stored at -80 °C until use.

2.4 RLPH2 specific antibody generation and affinity purification

RLPH2 antibody was generated by Dr. R Glen Uhrig (Uhrig, 2013). RLPH2-V5-His6 was purified following methodology found in section 2.3 and dialyzed over 18 hr in distilled water before being injected into a New Zealand rabbit for antibody generation against RLPH2. Anti-RLPH2-V5-His6 IgG was purified from the serum using a strip membrane purification method. Briefly, 1 mg of purified RLPH2-V5-His6 was loaded into ten wells of a 12% SDS-PAGE and then subsequently transferred onto a nitrocellulose membrane. RLPH2-V5-His6 bands were visualized using Ponceau S staining, and the corresponding bands representing RLPH2-V5-His6 was cut out and blocked with 5% (w/v) skim milk powder in TBS for 1 hr at RT. Membrane strip was washed using four 5 min washes with TBS. The strip membrane was then incubated with the serum for 1 hr at RT. The membrane was then washed with TBST 0.1% four times for 5 min each, before being incubated with 4.5 mL of 100 mM glycine pH 2.0 for 2 min to elute off the bound RLPH2-V5-His6 IgG. Eluted IgG was immediately neutralized with 0.5 mL of 1 M Tris pH 8.8.

Affinity purified antibodies were then dialyzed overnight at 4 °C in 1X PBS, following which they were concentrated in a 10 kDa centricon (Amicon), and stored at -80 °C.

2.5 RLPH2 malachite green dephosphorylation assays against peptides derived from the activation loops of MPKs

Affinity purified RLPH2-V5-His6 (1 µg) was incubated for 30 min at 200 rpm at 30 °C in 160 µL of Assay Buffer (50 mM HEPES-NaOH pH 7.5, 150 mM NaCl) containing 0.5 mM of peptide substrates **(Table 4)**. Control assays were performed in parallel with identical conditions except without RLPH2-V5-His6 enzyme. The reaction was stopped with the addition of 40 µL malachite green solution and O.D. measured at 630 nm. The activity of RLPH2 was measured by comparing absorbance at 630 nm with the standard curve of free Pi prepared in parallel.

2.6 Bacterial expression profile of MPK9-V5-His6 at 37 °C over hourly time points between 2 to 9 hours

MPK9-V5-His6 was grown in *E. coli* BL21 (DE3) CodonPlus-RIL at 37 °C until an OD_{600} of 0.4-0.6 ABS was reached, followed by expression via induction by 0.1 mM IPTG. After 2 hr, a 50 mL sample of the expressed cell culture was removed and centrifuged at 3300 xg for 20 min. The resulting cell pellet was resuspended in 15 mL of Resuspension Buffer (50 mM HEPES pH 7.5, 150 mM NaCl, 5% (v/v) glycerol, 10 mM imidazole, 1 mM benzamidine and 1 mM of fresh PMSF). Resuspended cells were lysed by French press (three times at 1000 psi), followed by centrifugation at 50,000 xg for 45 min. Protein concentration of the supernatant was determined by Bradford protein concentration determination assay, and boiled in 5X SDS loading buffer before being run on a 12% SDS-PAGE.

2.7 Cloning, expression, and purification of the *Arabidopsis thaliana* Mitogen Activated Protein Kinase 9 (MPK9) and its derived mutants

MPK9 gene At3g18040 was codon optimized (GenScript) to be expressed in a BL21 (DE3) CodonPlus-RIL *E. coli* strain. The gene was extracted from the pUC57 vector using PCR primers with gateway terminals and using a BP reaction (Invitrogen) which utilized gene recombination to transport the gene into the pDNR221 gateway donor vector (Invitrogen). Following which, the MPK9 gene was recombinantly transformed into the destination pDEST42 expression vector (Invitrogen) to be expressed as MPK9-V5-His6 for Ni-NTA column chromatography.

MPK9-V5-His6 was grown in *E. coli* BL21 (DE3) CodonPlus-RIL at 37 °C until an OD_{600} of 0.4-0.6 ABS was reached. This was followed by expression via induction with 0.1 mM IPTG for 7 hr at 37 °C, a condition which was determined through a expression profile to optimize expression at 37 °C. Induced cells were centrifuged at 3300 xg for 20 min, and the resulting cellular pellet was resuspended in 15 mL of Resuspension Buffer (50 mM HEPES pH 7.5, 150 mM NaCl, 5% v/v glycerol, 10 mM imidazole, 1 mM benzamidine and 1 mM of fresh PMSF). Resuspended cells were lysed by French press (three times at 1000 psi), followed by centrifugation at 50,000 xg for 45 min. The supernatant was collected and filtered through miracloth before a 1 hr incubation with 1 mL of Ni-NTA matrix (Qiagen). Matrix was washed with 300 CV of Wash Buffer A (50 mM HEPES pH 7.5, 1 M NaCl, 5% glycerol, 10 mM imidazole, 0.5% Tween-20) followed by an additional 100 mL of Wash Buffer B (50 mM HEPES pH 7.5, 150 mM NaCl, 5% glycerol, 10 mM imidazole) before being eluted in 15 mL of Elution Buffer (50 mM HEPES pH 7.5, 150 mM NaCl, 400 mM imidazole, 5% glycerol).

Elution was concentrated in a 30 kDa centricon (Amicon), and then using the same centricon, the buffer was exchanged for Wash Buffer B. Protein concentration was determined by Bradford protein concentration determination assay. Protein was stored at -80C until use.

2.8 Generating single amino acid changed mutants using site directed mutagenesis

Using the QuikChange Lightning Site-Directed Mutagenesis Kit (Agilent Technologies) mutants of MPK9 and MPK3 were generated by point mutations in their respective activation loops. The MPK9 RASA mutant construct had the two hydrophobic valine and phenylalanine amino acids in the MPK9 RVSF motif switched for two alanines. The MPK9 TEY mutant construct had the aspartic acid within MPK9s TDY motif switched for a glutamic acid. The MPK9 TDF mutant construct had its tyrosine residue switched out for a phenylalanine, resulting in a similar amino acid structure that cannot be phosphorylated. The MPK3 TDY mutant construct had its glutamic acid in TEY motif switched out for an aspartic acid. Primers utilized were computationally generated using PrimerX.

2.9 Coupling MPK9 Peptide to Keyhole Limpet Hemocyanin (KLH) for Anti-MPK9 antibody generation

An MPK9 peptide (16 mg) (KPRNKSEYGE) derived from a unique portion of the MPK9 C-terminus was dissolved in 500 µL 1X PBS buffer and 0.5 mL of 10 mg/mL KLH was added to the dissolved peptide followed by 370 µL of 0.2 M NaPPi pH 7.5. Next, 2.5% glutaraldehyde was added into the solution, and incubated end-over-end for 4 hr at RT. Reaction was stopped and blocked with the addition of 150 µL of 1 M Tris pH 7.5 and incubated for 1 hr at RT. The BSA-MPK9 and KLH-MPK9 coupled peptide was then dialyzed in 1X PBS overnight at 4 °C.

2.10 MPK9 antibody generation and purification

An MPK9 peptide (KPRNKSEYGE) derived from the C-terminus of MPK9 coupled to KLH/BSA following section 2.5 was injected into a New Zealand rabbit for antibody generation. Anti-MPK9-V5-His6 IgG was purified from serum using a protein column purification method. CNBr-activated Sepharose (0.5 g) (GE Healthcare) was hydrated in 1 mM ice cold HCl for 15 min, before being washed with coupling buffer (0.1 M $NaHCO_3$ pH 8.0, 0.5 M NaCl). 3 mg of MPK9-V5-His6 affinity purified following the methodology found in section 2.6 was incubated with the swelled CNBr-activated Sepharose (GE Healthcare) for 4 hr at RT end-over-end. Matrix was then blocked with 0.1M Tris-HCl pH 8.0 for 1 hr at RT end-over-end before being left to block for 18 hr at 4 °C end-over-end.

Rabbit serum was dialyzed for 18 hr at 4 °C in 1 L of 1X PBS. Dialyzed serum was diluted 10-fold with 10 mM Tris pH 7.5 before being incubated with the MPK9 protein Sepharose column for 4 hr at 4 °C. Column was washed with 20 CV of Wash A (10 mM Tris pH 7.5, 500 mM NaCl) followed by 20 CV of Wash B (10 mM Tris pH 7.5). Purified antibodies were eluted with 4.5 mL of glycine pH 2.0 which was directly neutralized by 0.5 mL of Tris pH 8.8. Affinity purified antibodies were dialyzed in 1 L of 1X PBS buffer for 18 hr at 4 °C before being concentrated in a 10 kDa centricon. Purified antibody concentration was determined by Bradford protein concentration assay.

2.11 Determining effectiveness of anti-MPK9 antibody generation and affinity purification by immunoblotting

Dot blotted membranes containing either BSA, KLH, BSA or KLH coupled with the MPK9 antigen peptide (100 ng, 10 ng, 1 ng) aftering being blocked in milk 5% (w/v) was incubated with either rabbit pre-immune serum, first bleed, second bleed, final bleed, or affinity purified

antibodies from the final bleed. Primary antibodies (1 µg/mL) were incubated with the membrane for 2 hr at RT, followed by washing four times with TBST 0.1% (TBS + 0.1% Tween-20). Secondary anti-rabbit antibody (1:5000, TBST 0.1%) was then incubated for 1 hr, followed by a second round of washing four times with TBST 0.1%. After washing off the secondary antibody, membrane was incubated for 3 min with ECL (GE Healthcare).

2.12 Autophosphorylation of MPK9 and MPK9 derived mutants (RASA, TEY, TDF, ADY)

Immediately following the purification of MPK9 or an MPK9 derived mutants, the concentrated protein was diluted to 15 mL in Autophosphorylation Buffer (25 mM Hepes pH 7.5, 10 mM NaCl, 15 mM $MgCl_2$, 5 mM ATP). The protein sample was then incubated at 35 °C for 2 hr shaking at 150 rpm to induce autophosphorylation. Following the autophosphorylation of MPK9 or MPK9 derived mutants, the samples were concentrated in a 30 kDa centricon. The centricon was then used to exchange the buffer with Storage Buffer (50 mM HEPES pH 7.5, 150 mM NaCl, 5% glycerol) a minimum of 5 times to ensure that there is no longer ATP in the solution. Concentration of phosphorylated protein was determined by Bradford assay. Protein sample was then stored at -80 °C until day of use.

2.13 Cloning, expression, and purification of the *Arabidopsis thaliana* Mitogen Activated Protein Kinase 3 (MPK3) and its derived mutants (MPK3 TDY)

An MPK3 gene (At3g45640) pDEST42 gateway expression vector (Invitrogen) construct was obtained from Dr. Marcus Samuel, University of Calgary, Canada, to be expressed in *E. coli* as MPK3-V5-His6 for His6 tag affinity purification. MPK3-V5-His6 pDEST42 construct was expressed in BL21 (DE3) CodonPlus-RIL *E. coli* strain. MPK3-V5-His6 was grown in *E. coli* BL21 (DE3) CodonPlus-RIL at 37 °C until an OD_{600} of 0.4-0.6 ABS was reached, followed by expression via induction with 0.1 mM IPTG for 4 hr at 37 °C. Cells were then centrifuged at 3300

xg for 20 min. Cell pellet was resuspended in 15 mL of Resuspension Buffer (50 mM HEPES pH 7.5, 150 mM NaCl, 5% v/v glycerol, 10 mM imidazole, 1 mM benzamidine and 1 mM of fresh PMSF). Resuspended cells were lysed by French press (three times at 1000 psi), followed up centrifugation at 50,000 xg for 45 min. The supernatant was collected and filtered through miracloth before a 1 hr incubation with 1 mL of Ni-NTA matrix (Qiagen). Matrix was washed with 300 CV of Wash Buffer A (50 mM HEPES pH 7.5, 1 M NaCl, 5% glycerol, 10 mM imidazole, 0.5% Tween-20) followed by an additional 100 mL of Wash Buffer B (50 mM HEPES pH 7.5, 150 mM NaCl, 5% glycerol, 10 mM imidazole) before being eluted in 15 mL of Elution Buffer (50 mM HEPES pH 7.5, 150 mM NaCl, 400 mM imidazole, 5% glycerol).

Eluted protein was concentrated in a 30 kDa centricon, and then using the same centricon, the buffer was exchanged for Wash Buffer B (50 mM HEPES pH 7.5, 150 mM NaCl, 5% glycerol, 10 mM imidazole). Concentration of protein was determined by a Bradford assay. Protein was stored at -80 °C until use.

2.14 Cloning, expression, and purification of constitutively active Mitogen Activated Protein Kinase-Kinase 4 (CAMKK4)

CAMKK4-GST construct was obtained from Dr. Marcus Samuel, University of Calgary, Canada. CAMKK4-GST construct was expressed in a BL21 (DE3) CodonPlus-RIL *E. coli* strain. Cells were grown until an OD_{600} of 0.4-0.6 ABS was reached, at which point 0.1 mM IPTG was added to induce expression for 6 hr at 30 °C. After expression, cells were centrifuged at 3300 xg for 20 min at 4 °C, after which the pellet was resuspended in 15 mL of Resuspension Buffer (50 mM HEPES pH 7.5, 150 mM NaCl, 3 mM DTT, 0.05% NP-40, 2 µg/mL leupeptin, 5 µg/mL pepstatin). Resuspended cells were lysed by French press (three times at 1000 psi), followed up centrifugation at 50,000 xg for 45 min. The supernatant was collected and filtered through

miracloth before a 1 hr incubation with 1 mL of glutathione-Sepharose 4B matrix (GE Healthcare). Matrix was washed with 300 CV of Wash Buffer A (50 mM HEPES pH 7.5, 750 mM NaCl, 1 mM DTT, 0.1% NP-40) followed by an additional 100 mL of Wash Buffer B (50 mM HEPES pH 7.5, 150 mM NaCl, 1 mM DTT) before being eluted in 15 mL of Elution Buffer (50 mM HEPES pH 7.5, 150 mM NaCl, 20 mM reduced glutathione, 1 mM DTT).

Elution was concentrated in a 30 kDa centricon, and then using the same centricon, the buffer was exchanged for Wash Buffer B (50 mM HEPES pH 7.5, 150 mM NaCl, 1 mM DTT). Concentration of protein was determined by a Bradford assay. Protein was stored at -80 °C until use.

2.15 Phosphorylation of MPK3 and MPK3 derived mutants by CAMKK4

Following the purification of MPK3 or one of its derived mutants, the concentrated protein was diluted to 15 mL in Phosphorylation Buffer (25 mM Hepes pH 7.5, 10 mM NaCl, 15 mM $MgCl_2$, 5 mM ATP) in the presence of 100 ng of affinity purified AtCAMKK4 following the methodology in section 2.14. The combined sample was incubated at 30 °C for 2 hr shaking at 150 rpm. After the phosphorylation of MPK3 has been completed, the protein sample was concentrated in a 30 kDa centricon. The centricon was then used to exchange the buffer with Storage Buffer (50 mM HEPES pH 7.5, 150 mM NaCl, 5% glycerol) a minimum of 5 times to ensure that there is no longer ATP in the solution. Concentration of protein was determined by a Bradford assay. Protein sample was then stored at -80 °C until day of use.

2.16 MPK9 and MPK3 dephosphorylation assay with RLPH2

Either 5 µg of MPK9-V5-His6 or MPK3-V5-His6 was incubated with 1 µg of RLPH2-V5-His6 in 80 µL assay buffer (20 mM Hepes-NaOH pH 7.5, 10 mM NaCl, 5 mM $MgCl_2$, 0.1 mM DTT). Proteins were incubated together for 1 hr at 30 °C while shaking at 200 rpm before the

reaction was stopped by the addition of 20 µL 5X SDS Loading Buffer followed by heating the samples at 95 °C for 10 min. Samples were run on a 12% SDS-PAGE and then visualized by immunoblotting for anti-V5 (Immunology Consultants Laboratory, RV5-45A-Z, 1 µg/mL), anti-pT (Cell Signaling Technologies, 42H4, 1 µg/mL), and anti-pY (Cell Signaling Technologies, P-Tyr-100, 1 µg/mL).

2.17 Generation of the MC-Sepharose Matrix for PP1 affinity purification

Microcystin Sepharose matrix was generated by coupling Microcystin-LR, Cysteamine Hydrochloride, and CNBr-activated Sepharose (Moorhead *et al.*, 1994). Initially, 1 mg of Microcystin-LR (Cayman Chemicals) was dissolved in 1 mL of 95% ethanol. Distilled water, DMSO, and 5 M NaOH were separately purged using N_2 gas to remove any possible O_2 in solution. Immediately before use, 1 mg/mL Cysteamine Hydrochloride (Cayman Chemicals) was dissolved in purged distilled water. 1.5 mL of purged distilled water, 1.998 mL DMSO, 0.666 mL 5 M NaOH, and 0.99 mL of dissolved Cysteamine Hydrochloride were added to the 1 mL of MC-LR in ethanol. The resulting solution was then purged with N_2 gas, before being sealed and incubated at 50 °C for 1 hr.

After incubation, sample was cooled on ice and in a fume hood 0.99 mL of 100% acetic acid was added. Solution was then diluted with 19.8 mL of 0.1% (v/v) trifluoracetic acid (TFA), and the pH was lowered to 1.5 by 100% TFA.

Sample was applied to a C18 Sep-Pak cartridge in 0.1% (v/v) TFA after being prewet with methanol. C18 Sep-Pak cartridge was washed with 0.1% (v/v) TFA in 10% (v/v) acetonitrile in water, and then eluted with 10 mL of 0.1% (v/v) TFA in 100% acetonitrile into ten separate 1 mL fractions. Fractions were dried by rotary evaporation and the resulting pellet was resuspended with

20 µL of methanol. Methanol resuspended microcystin with the cysteamine hydrochloride linker were pooled and 0.6 mL of 100 mM $NaHCO_3$ pH 8.2 was added.

To hydrate the matrix, 2 g of CNBr-Activated Sepharose (GE Healthcare) was incubated in water for 15 min, then washed with 500 mL of 1 mM HCL followed by 100 mL of 100 mM $NaHCO_3$ pH 8.2 on a scintered glass funnel. Resuspended microcystin with the cysteamine hydrochloride linker was added to the activated CNBr-activated Sepharose end-over-end at RT for 1.5 hr. Excess ligand was washed with 100 mM $NaCO_3$ pH 8.2. Matrix was blocked with 0.1 M Tris pH 8 for 2 hr. Matrix was then washed with three alternating washes of 50 mM Tris pH 8, 0.5 M NaCl and 50 mM acetate pH 4, 0.5 M NaCl. Matrix was stored in 10% ethanol with 0.02% sodium azide, to prevent bacterial growth, and stored at 4 °C until use. Storage solution was washed off before use.

2.18 Cloning, Expression, and Purification of *Arabidopsis thaliana* Protein Phosphatase 1 (PP1)

Nine isoforms of PP1 (PP1-1: AT2G29400, PP1-2: AT5G59160, PP1-3: AT1G64040, PP1-4: AT2G39840, PP1-5: AT3G46820, PP1-6: AT5G43380, PP1-7: AT4G11240, PP1-8: AT5G27840, PP1-9: AT3G05580) were cloned by Dr. George Templeton (Templeton, 2010) into the pET101 vector (Invitrogen) using gateway extended primers. The genes were genetically engineered with their stop codons intact, resulting in the expressed protein not containing the His6 tag found in the pET101 vector.

PP1 isoforms were grown in a BL21 STAR strain (Invitrogen) until an OD_{600} of 0.4-0.6 ABS was reached, at which point 0.1 mM IPTG was added to induce expression. PP1 isoforms were expressed at 37 °C for 18 hr and then centrifuged at 3300 xg for 20 min. Cell pellet was resuspended in 15 mL of Resuspension Buffer (25 mM Tris-HCl pH 7.5, 100 mM NaCl, 5% v/v

glycerol, 0.1% β-ME, 1 mM benzamidine and 1 mM of fresh PMSF). Resuspended cells were lysed by French press (three times at 1000 psi), followed up centrifugation at 50,000 xg for 45 min. The supernatant was collected and filtered through miracloth before a 1 hr incubation with 0.5 mL of microcystin Sepharose matrix generated following the methodology found in section 2.17. Matrix was washed with 300 CV of Wash Buffer (25 mM Tris-HCl pH7.5, 1 M NaCl, 5% glycerol, 1 mM $MnCl_2$, 0.1% β-ME, 0.1% Brij-35) before being incubated for 20 min in 15 mL of Elution Buffer (25 mM Tris-HCl pH 7.5, 3 M NaSCN, 5% glycerol, 1 mM $MnCl_2$, 0.1% β-ME, 0.1% Brij-35).

Elution was dialyzed for 18 hrs in Dialysis Buffer (25 mM Tris-HCl, 250 mM NaCl, 250 mM KCl, 1 mM $MnCl_2$ and 0.1% β-ME) before being concentrated in a 10kDa centricon. Concentrated PP1 protein was dialyzed for 18 hr in Dialysis Buffer (25 mM Tris-HCl, 250 mM NaCl, 250 mM KCl, 1 mM $MnCl_2$ and 0.1% β-ME) with 50% glycerol and stored at -20 °C.

2.19 PP1 antibody generation and purification

Dr. Templeton (Templeton, 2010) generated a coupled mixture of BSA with peptides (GEFDNAGALLSVDK and GEFDNAGAMLSVDK) taken from the C-terminus of the *Arabidopsis thaliana* PP1 isoforms. This peptide coupled to BSA mixture was then injected into a New Zealand rabbit for antibody generation.

PP1 polyclonal antibody was purified using a strip membrane affinity purification method. One mg total of PP1 isoforms 1-5, 7-9 were loaded onto a 12% SDS-PAGE and transferred onto a nitrocellulose membrane. PP1 bands were visualized using Ponceau S staining, and the corresponding band representing the different PP1 isoforms were cut out and blocked with 5% (w/v) skim milk powder in TBS for 1 hr at RT. Membrane strip was washed using four 5 min washes with TBS. Rabbit serum was dialyzed three-fold with 5% (w/v) skim milk powder in

TBST0.1%. The strip membrane was then incubated with the diluted serum for 1 hr at RT. Strip membrane was then washed with TBST0.1% four times for 5 min each, before being incubated with 2 mL of 100 mM glycine pH 2.0 for 2 min to elute off the bound PP1 IgG. Eluted IgG was immediately neutralized with 0.4 mL of 1 M Tris pH 8.8. Affinity purified antibodies were then dialyzed overnight at 4 °C in PBS, following which they were concentrated in a 10 kDa centricon, and stored at -80 °C. Concentration of affinity purified antibody was determined by Bradford assay.

2.20 *In Vitro* binding assay between MPK9 and PP1

Affinity purified MPK9 WT/RASA (5 µg) and Microcystin Affinity Purified PP1 isoform 5 (1 µg) was incubated together for 1 hr at 37 °C. Simultaneously, 200 µL of Ni-NTA matrix (Qiagen) was incubated with 5 mg/mL BSA for 1 hr at RT. Following a 1 hr incubation, 40 µL of beads were added to the solutions containing either purified MPK9-V5-His6, PP1, or both MPK9 and PP1 isoforms. After a 1 hr incubation at 37 °C the beads were washed 5X using 1 mL Wash Buffer (50 mM Hepes pH 7.5, 300 mM NaCl Buffer, and 0.1% Tween-20), followed by a 1 mL wash using Neutral Buffer (50 mM Hepes pH 7.5 and 150 mM NaCl). Afterwards, 100 µL of 2X SDS loading buffer was added and then boiled for 5 min at 95 °C.

2.21 Growing *Arabidopsis thaliana*

Wild Type *Arabidopsis thaliana* Col-0 seeds were plated on MS agar plates for 14 days until germination. Seedlings were then transplanted into soil. 20-20-20 fertilizer was used once a week, while the pots were left in growth chambers for 5 weeks. After plants reached their adult stage, rosettes were removed and immediately frozen in liquid N_2, then stored at -80^{o}C.

2.22 Extracting Protein from *Arabidopsis thaliana* rosette

Arabidopsis thaliana rosette sample (15 g) was removed from -80 °C freezer and immediately placed into liquid N_2. The mortar and pestle were chilled with liquid N_2, then 20 g of rosette tissue was powderized. Powder was resuspended in 20 mL extraction buffer (50 mM HEPES pH 7.5, 150 mM NaCl, 10% glycerol, 0.1% Tween, 1 mM PMSF, and 1 mM benzamidine). Sample was spun down at 466 xg for 30 min at 4 °C. Supernatant was collected, filtered through Miracloth and used as plant rosette input sample.

2.23 Immunoprecipitation of MPK9

To equilibrate, 100 µL of Protein A Sepharose beads (Pierce) was washed with 50 CV of Wash A (50 mM pH 7.5, 150 mM NaCl) before being incubated in either 20 µg of anti-MPK9 affinity purified antibody or pre-immune serum antibody to act as a control. Total volume was brought to 1 mL with Wash A before being incubated end-over-end at RT for 1.5 hr. The resulting matrix was washed with 20 CV of 0.1 sodium borate pH 9. Afterwards 10.9 mg DMP (Dimethylpimelimidate dihydrochloride) was added in 2 mL of sodium borate and then 1 mL of the DMP/sodium borate mixture was added to the matrix and incubated end-over-end for 1 hr at RT. After an hr, an additional 1 mL of the DMP/sodium borate mixture was added for another 1 hr end-over-end incubation at RT before leaving the matrix to block for 18 hr in 0.2M Tris pH 8 at 4 °C end-over-end.

Arabidopsis thaliana rosette leaves (15 g) were ground up and resuspended following the methodology found in section 2.22. The Anti-MPK9 antibody Sepharose matrix was washed with 50 CV of Wash A before incubation in 1 mL of 100 mM glycine pH 2.0 for 1 min. Matrix was washed again with 50 CV of Wash A. Plant protein input was added to the anti-MPK9 antibody or pre-immune serum matrix and left to incubate end-over-end for 4 hr at 4 °C. Matrix was washed

with 50 CV of Wash A, before being washed with 50 CV of Wash B (50 mM HEPES pH 7.5, 300 mM NaCl, and 0.1% Tween-20). Matrix was washed again with 50 CV of Wash A before being eluted in 100uL of 2X SDS loading buffer and boiled at 95 °C for 10 min.

2.24 PP1 malachite green dephosphorylation assays against peptides derived from the activation loops of MPKs

Affinity purified PP1 isoform 5 (1 µg) was incubated for 30 min at 30 °C shaking at 200 rpm in 160 uL of Assay Buffer (50 mM HEPES-NaOH pH 7.5, 150 mM NaCl) containing 0.5 mM peptide substrate **(Table 5)**. Control assays were performed without PP1 enzyme. The reaction was stopped with the addition of 40 µL malachite green solution and solution was measured at 630 nm. The activity of PP1 was measured by comparing absorbance at 630 nm with a Pi standard curve prepared in parallel with the assay.

2.25 MPK9 dephosphorylation assay with PP1

For the PP1 protein dephosphorylation assays, 5 µg of MPK9-V5-His6 was incubated with 1 µg of PP1 isoform 2 in 80 µL assay buffer (50 mM Hepes-NaOH pH 7.5, 150 mM NaCl). Proteins were incubated together for 1 hr at 30 °C before the reaction was stopped by the addition of 20 µL 5X SDS Loading Buffer followed by heating the samples at 95 °C for 10 min. Samples were run on a 12% SDS-PAGE and then visualized by immunoblotting for anti-V5 (Immunology Consultants Laboratory, RV5-45A-Z, 1 µg/mL), anti-pT (Cell Signaling Technologies, 42H4, 1 µg/mL), and anti-pY (Cell Signaling Technologies, P-Tyr-100, 1 µg/mL).

2.26 Bioinformatics

The sequences for the 20 *Arabidopsis thaliana* MPKs were obtained from UniProt based on their specific gene identifier **(Table 1)**. An alignment of the 20 MPKs activation loop regions designated between sites DFG and APE was conducted using CLC sequence viewer 8.0.

RESULTS

3.1 Ni-NTA column chromatography of RLPH2 results in a pure protein with one major contaminant band.

The RLPH2-V5-His6 purified via Ni-NTA column chromatography resulted in a semi-pure protein sample containing only two major bands, one just below the 45 kDa marker and one just below the 35 kDa marker **(Figure 14)**. The anti-V5 immunoblotting experiment would indicate that the band just below the 45 kDa corresponds with RLPH2. This is similar to the 38 kDa calculated size of RLPH2.

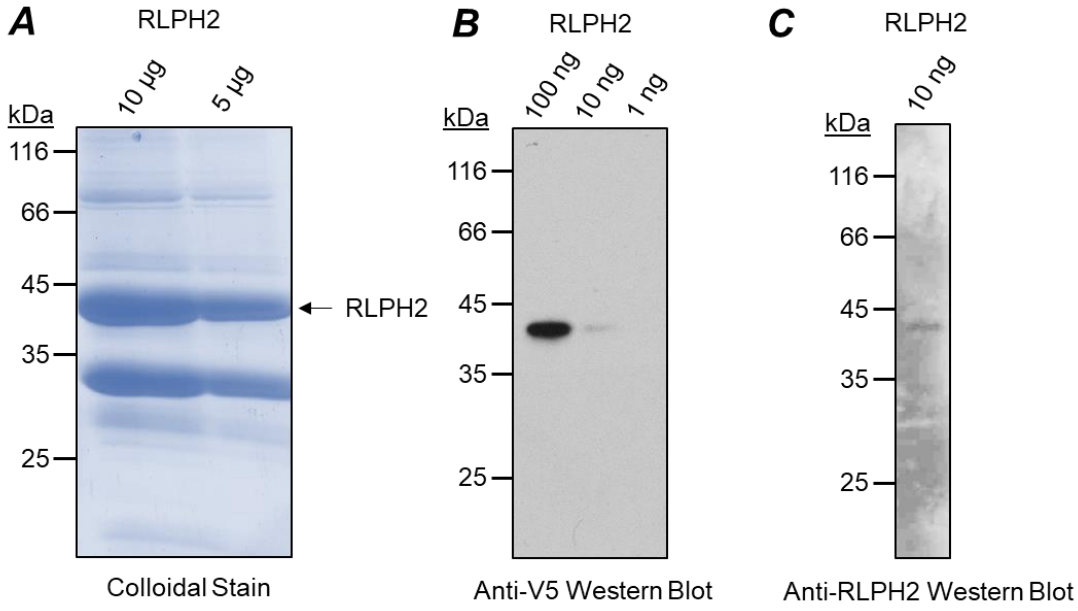

Figure 14. RLPH2-V5-His6 affinity purified protein. A) Colloidal stained 12% SDS-PAGE visualizing the affinity purified RLPH2-V5-His6 at 10 µg and 5 µg of total protein with an arrow indicating which of the major migrating bands was determined to correspond with RLPH2-V5-His6. **B)** Anti-V5 (Immunology Consultants Laboratory, RV5-45A-Z, 1 µg/mL) western blot of 100 ng, 10 ng, and 1 ng of affinity purified RLPH2-V5-His6 separated on 12% SDS-PAGE for detection of the V5 tag. **C)** Anti-RLPH2 (50 ng/mL) western blot of 10 ng recombinant purified RLPH2-V5-His6. Immunoblotting for anti-V5 (Immunology Consultants Laboratory, RV5-45A-Z, 1 µg/mL) primary incubation was for 2 hr, followed by washing four times for 5 min in TBST 0.1%, before incubation with secondary anti-rabbit antibody (1:5000) for 1 hr. Anti-rabbit secondary antibody was washed off with TBST0.1% four times for 5 min before blot was incubated with ECL (GE Healthcare) for 3 min and developed. Low molecular weight ladder is shown to the left of the blot.

3.2 The TXY motif of *Arabidopsis thaliana* MPKs plays a role in the substrate specificity of RLPH2

Phosphoproteomic data conducted by Dr. R Glen Uhrig (Labandera, 2017) comparing the phospho-status of endogenous proteins between two *atrlph2* knockout lines and a wild type *Arabidopsis thaliana* line suggested that potential substrates of RLPH2 were the D group of the MPKs. Previous peptide dephosphorylation assays and structural data of RLPH2 conducted by Dr. Anne Marie Labandera (Labandera *et al.*, 2018) have also shown that there is a preference towards MPK substrates containing a dual phosphorylated TXY motif.

To further examine RLPH2s substrate specificity, a malachite green dephosphorylation assay was conducted to determine affinity purified RLPH2-V5-His6 activity against dual phosphorylated peptide substrates derived from the activation loop of *Arabidopsis thaliana* MPKs. The widely studied MPK9 (Khokon *et al.*, 2017; Frick and Strader, 2018) was chosen as a representative for the D group MPKs as it was determined through the phosphoproteomic data to be a potential substrate of RLPH2. MPK3 is a well characterized member of the A group MPKs (Cristina, Petersen and Mundy, 2010), and therefore was chosen to represent the non-D group MPKs.

The malachite green dephosphorylation assay showed that the MPK9 peptide had a 21-fold increase in dephosphorylation activity by RLPH2 compared to the MPK3 peptide **(Figure 15)**. This significant change in substrate dephosphorylation via RLPH2 shows a clear preference for the D group MPK peptide over the non-D group MPK peptide, supporting the results obtained from the phosphoproteomic data that RLPH2s substrate specificity is directed towards the D group MPKs.

The substrate specificity of RLPH2 is clearly present in the peptide dephosphorylation assay with a 21-fold increase in dephosphorylation by RLPH2 against D group MPKs. The MPK peptide substrates only contain sequences from the activation loop of MPK9 and MPK3, and therefore indicate that the substrate specificity of RLPH2 is being directed in some capacity by the sequence of the activation loop. When aligning the activation loops of the 20 *Arabidopsis thaliana* MPKs **(Figure 4)** two key differences were observed, the presence of an insert in the D group MPKs, named the APSAI insert, and the difference between the central amino acid within the MPK activation loops TXY motif, specifically the aspartic acid within the D group MPKs and the glutamic acid in the non-D group MPKs.

To investigate if the APSAI insert had an impact in the RLPH2 substrate specificity towards D group MPKs, the APSAI insert was added into the MPK3 peptide in relation to its location in the D group MPKs. This MPK3 peptide containing the APSAI insert resulted in no significant change in dephosphorylation via RLPH2 when compared to the unchanged wild type MPK3 peptide. This indicates that the APSAI insert does not play a clear role in the regulation of RLPH2 substrate specificity.

To investigate whether the TXYs central amino acid (aspartic acid or glutamic acid) played a key role in the substrate specificity of RLPH2, the aspartic acid in the MPK9 peptide was switched out for a non-D group MPK-like glutamic acid. This MPK9 TEY peptide resulted in a significant 14-fold decrease in the activity that RLPH2 exerted on this peptide substrate. This indicates that the central amino acid of the TXY motif plays a significant role in regulating RLPH2s substrate specificity.

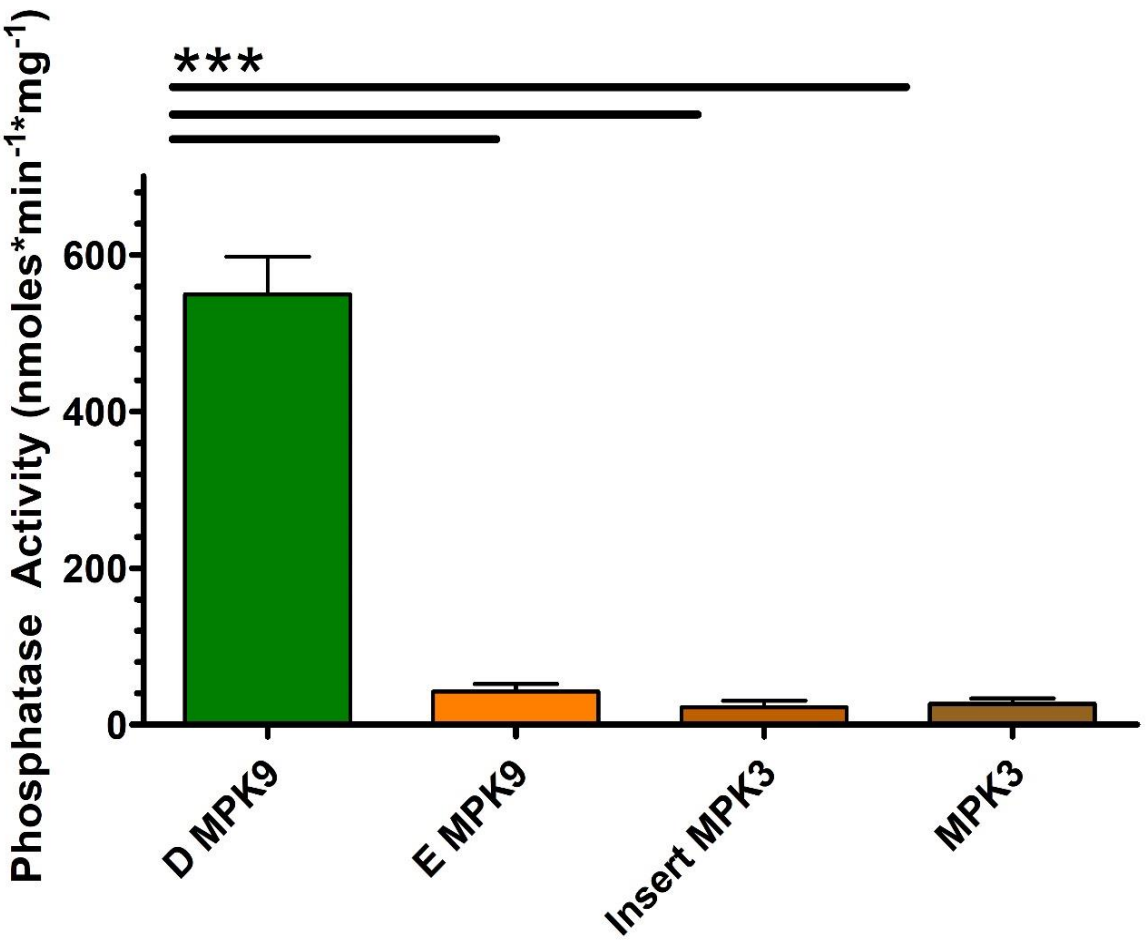

Figure 15. RLPH2 malachite green dephosphorylation assays against peptides derived from the activation loop of MPK9 and MPK3. Observed RLPH2 dephosphorylation activity using the malachite green assay and different peptide substrates derived from the activation loop of AtMPK9 and AtMPK3 each with modified variants **(Table 4)**. Assays were performed at 30 °C for 30 min using 0.5 mM peptide D MPK9 (GLARVSFND**APSAI**FW**pTDpY**VATR), E MPK9 (GLARVSFND**APSAI**FW**pTEpY**VATR), Insert MPK3 (GLARPTSEND**APSAI**FM**pTEpY**VVTR), and MPK3 (ICDFGLARPTSENDFM**pTEpY**VVTR). Malachite green solution was added and a 96 well plate spectrophotometer measured absorbance at 630 nm. Comparison of D MPK9 to E MPK9, Insert MPK9, and MPK3 using a statistical one-way ANOVA test was conducted and showed a significant difference between D MPK9 and the other three points. *** represents that the P value for the difference was <0.0001. For D MPK9 n = 15, for E MPK9, Insert MPK3, and MPK3 peptides n = 8. This data was obtained through technical replicates.

Table 4. Peptides derived from the activation loops of MPK9 and MPK3 for RLPH2 malachite green dephosphorylation assay. Single letter amino acid code is shown, with "p" indicating a phosphorylated amino acid.

Peptide Name	Peptide Sequence
D MPK9	GLARVSFNDAPSAIFWpTDpYVATR
E MPK9	GLARVSFNDAPSAIFWpTEpYVATR
Insert MPK3	GLARPTSENDAPSAIFMpTEpYVVTR
MPK3	ICDFGLARPTSENDFMpTEpYVVTR

3.3 MPK9 expression profile shows best expresses at 37 °C for 7 hours

The expression profile of MPK9 at 37 °C shows that the best expression conditions for MPK9 is a 7 hr induction with 0.1 mM IPTG after cells were grown to an OD_{600} of 0.4-0.6 ABS **(Figure 16)**. The expression profile, monitored hourly by an anti-V5 immunoblotting experiment from 2 to 9 hours after induction, revealed the highest detection of MPK9 at the 7 hr time point. Expression of MPK9 steadily increases from the 2 to 4 hr time point where it peaks around the 5 to 7 hr time point before falling again from the 8 to 9 hr time point.

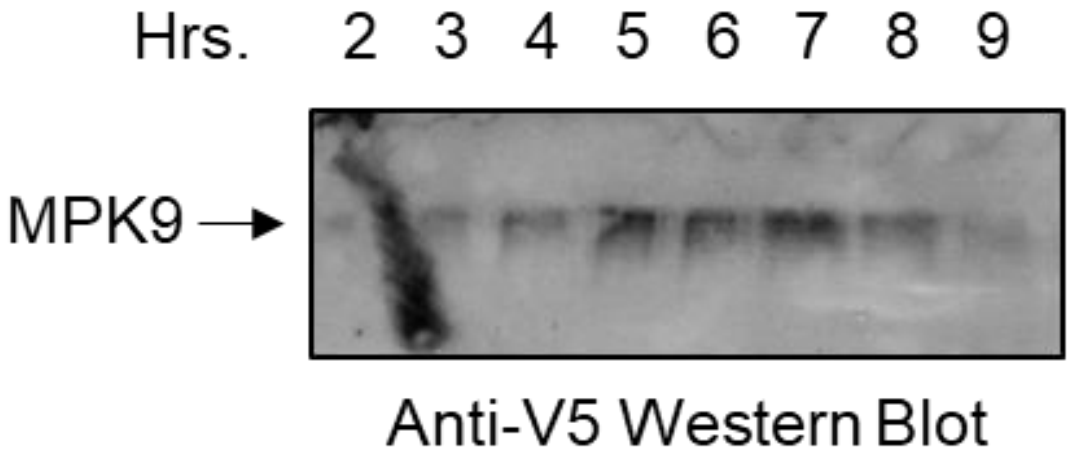

Figure 16. Expression profile of MPK9-V5-His6. Anti-V5 western blot monitoring the expression of MPK9-V5-His6 in a pDEST42 construct in BL21 (DE3) CodonPlus-RIL *E. coli* strain (GenScript) at hourly time points from two to nine hours after induction with 0.1mM IPTG. Sample was lysed by French press (three passes at 1000 psi) and centrifuged at 50,000 xg.

Immunoblotting for anti-V5 (Immunology Consultants Laboratory, RV5-45A-Z, 1 μg/mL) primary incubation was for 2 hr, followed by washing four times for 5 min in TBST 0.1%, before incubation with secondary anti-rabbit antibody (1:5000) for 1 hr. Anti-rabbit secondary antibody was washed off with TBST0.1% four times for 5 min before blot was incubated with ECL (GE Healthcare) for 3 min and developed.

3.4 Ni-NTA column chromatography of MPK9 results in a semi-pure protein.

The purified MPK9-V5-His6 via Ni-NTA column chromatography resulted in a semi-pure protein, present enough to be run in assays. Purified protein sample consists of three major bands, one just below, one on, and one just above the 66 kDa low molecular weight marker **(Figure 17)**. Examining the anti-V5 immunoblotting experiment of MPK9 shows that the top band just above the 66 kDa marker is the band corresponding with purified MPK9. This slightly higher than the theoretical MPK9-V5-His6 size of 63 kDa but could be the result of phosphorylation sites causing a decrease in MPK9 migration through the gel.

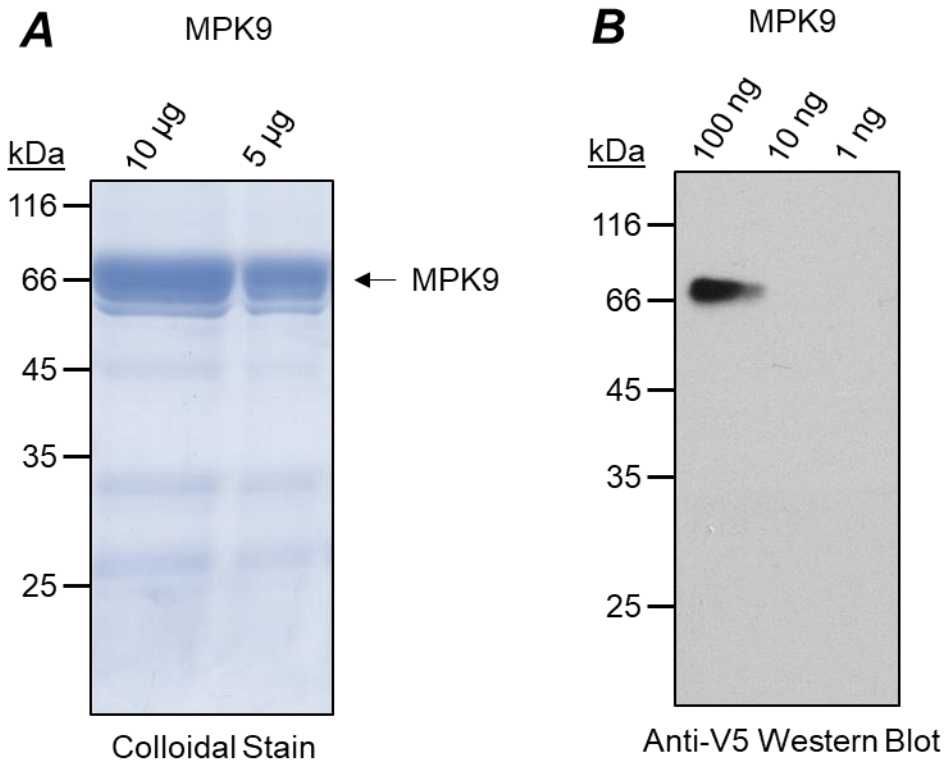

Figure 17. MPK9-V5-His6 affinity purified protein. A) Colloidal stained 12% SDS-PAGE visualizing affinity purified MPK9-V5-His6 at 10 µg and 5 µg of protein with an arrow indicating which of the major bands was determined to correspond with MPK9-V5-His6. **B)** Anti-V5 western blot of 100 ng, 10 ng, and 1 ng of affinity purified RLPH2-V5-His6 separated on a 12% SDS-PAGE for detection of MPK9-V5-His6. Immunoblotting for anti-V5 (Immunology Consultants Laboratory, RV5-45A-Z, 1 µg/mL) primary incubation was for 2 hr, followed by washing four times for 5 min in TBST 0.1%, before incubation with secondary anti-rabbit antibody (1:5000) for 1 hr. Anti-rabbit secondary antibody was washed off with TBST0.1% four times for 5 min before blot was incubated with ECL (GE Healthcare) for 3 min and developed. Low molecular weight ladder is shown to the left of the blot.

3.5 Autophosphorylation of recombinant affinity purified MPK9

The evidence obtained from the RLPH2 malachite green peptide dephosphorylation data indicated a potential mechanism for the substrate specificity of RLPH2. To further confirm and validate the directed activity of RLPH2 against the D group MPKs over the non-D group MPKs, protein dephosphorylation data was pursued. In order to obtain protein dephosphorylation data,

the recombinant full-length MPK9 and MPK3 proteins were expressed in bacteria, affinity purified and then subsequently phosphorylated.

In order to phosphorylate MPK9, research has shown that there is no clear upstream MPK kinase that phosphorylates the TXY motif of MPK9, but it has also shown that MPK9 has the capabilities to autophosphorylate its own TXY motif (Nagy *et al.*, 2015). After affinity purification of MPK9 there was detection of phosphotyrosine in an anti-pY immunoblotting experiment, indicating MPK9 autophosphorylation during expression in a bacterial environment. Not knowing the degree of phosphorylation of the bacterially purified enzyme, MPK9 autophosphorylation was induced via an autophosphorylation assay to enhance the phospho-status of MPK9. The results from the autophosphorylation show an increase in the phosphorylation status of MPK9 through an observed increase in detection of phosphotyrosine via immunoblotting with anti-pY antibodies. Over the 4 hours of autophosphorylation monitoring, it was observed that a large portion of the increase in phospho-status occurred within the first ten minutes (time point 0 – time point 10 min) **(Figure 18 B)**. Based on the observed detection of phosphotyrosine at the one hour to four hour time points, the phosphorylation of MPK9 reached its peak phospho-status that can be obtained through an autophosphorylation assay at the one hour time point, as there was no further increase in the phosphorylation status of MPK9 in further time points **(Figure 18 A)**.

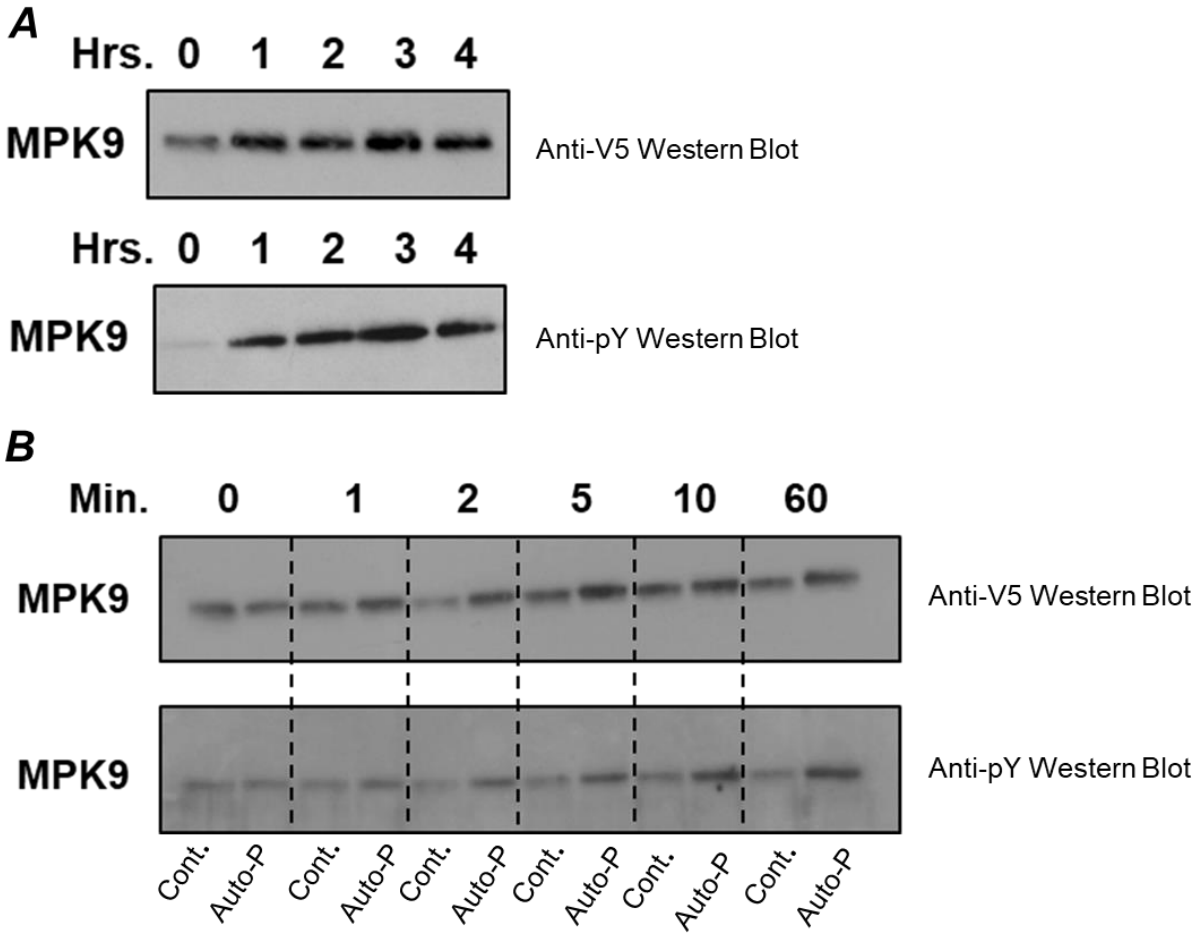

Figure 18. Autophosphorylation of MPK9. A) Anti-V5 and anti-pY western blots monitoring the autophosphorylation of 50 ng MPK9-V5-His6 during an autophosphorylation assay (in the presence of 20 mM HEPES pH 7.5, 15 mM $MgCl_2$, 5 mM ATP, 1 mM DTT shaking at 150 rpm at 35 °C). Samples were taken at hourly time points to monitor change in phosphorylation status of MPK9-V5-His6. **B)** Anti-V5 and anti-pY western blots monitoring the autophosphorylation status of 50 ng MPK9-V5-His6 with samples taken at short time points (0, 1, 2, 5, 10, 60 min). Immunoblotting for anti-V5 (Immunology Consultants Laboratory, RV5-45A-Z, 1 μg/mL) and anti-pY (Cell Signaling Technologies P-Tyr-100) primary incubation was for 2 hr, followed by washing four times for 5 min in TBST 0.1%, before incubation with either secondary anti-rabbit or anti-mouse antibody (1:5000) for 1 hr. Anti-rabbit secondary antibody was washed off with TBST0.1% four times for 5 min before blot was incubated with ECL (GE Healthcare) for 3 min and developed. Low molecular weight ladder is shown to the left of the blot.

3.6 Ni-NTA column chromatography of MPK3 results in a semi-pure protein.

Purified MPK3-V5-His6 via Ni-NTA column chromatography resulted in a protein sample containing two major bands, one being MPK3 and the other being a major contaminant **(Figure 19)**. The immunoblotting experiment utilizing anti-V5 antibodies would indicate the band just below the 45 kDa molecular weight marker is the MPK3 corresponding band. This is similar to MPK3s theoretical size of 45 kDa. This would indicate that the band at approximately 55 kDa is a major contaminant band.

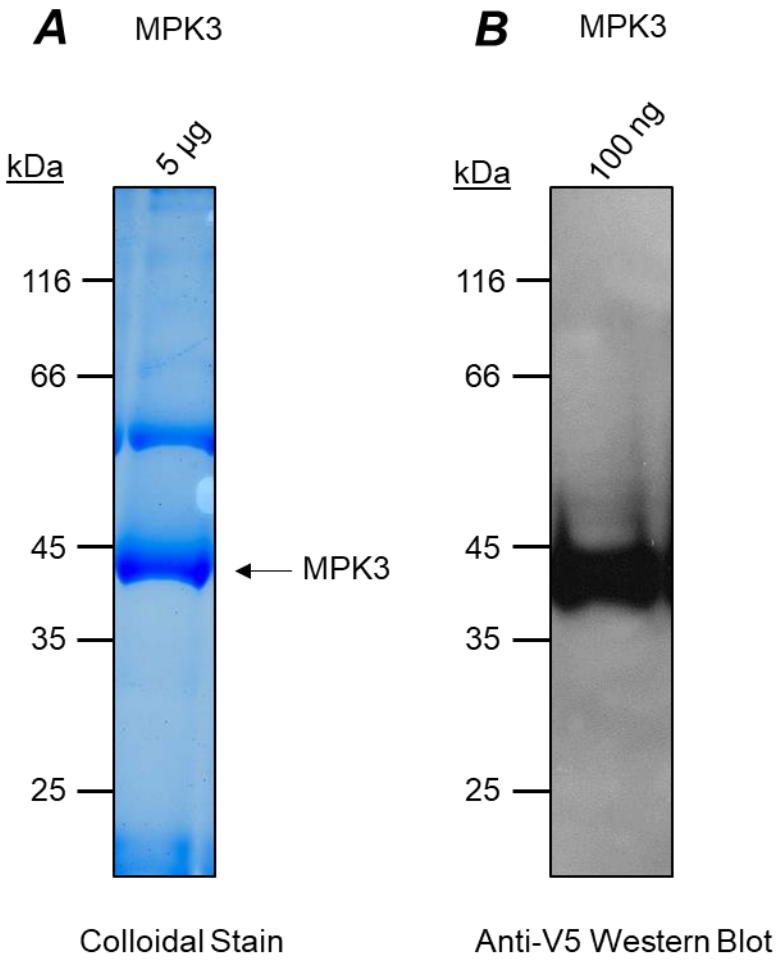

Figure 19. MPK3-V5-His6 Affinity Purified Protein. A) Colloidal stained 12% SDS-PAGE visualizing affinity purified of MPK3-V5-His6 at 5 µg of total protein with an arrow indicating which of the major bands was determined to correspond with the MPK3-V5-His6. **B)** Anti-V5 western blot of 100 ng of affinity purified MPK3-V5-His6 separated on a 12% SDS-PAGE for

detection of MPK3-V5-His6. Immunoblotting for anti-V5 (Immunology Consultants Laboratory, RV5-45A-Z, 1 μg/mL) primary incubation was for 2 hr, followed by washing four times for 5 min in TBST 0.1%, before incubation with secondary anti-rabbit antibody (1:5000) for 1 hr. Anti-rabbit secondary antibody was washed off with TBST0.1% four times for 5 min before blot was incubated with ECL (GE Healthcare) for 3 min and developed. Low molecular weight ladder is shown to the left of the blot.

3.7 GST column chromatography of CAMKK4 results in an impure protein.

The constitutively active MKK4-GST mutant purified via GST column chromatography resulted in a highly impure protein sample, that did contain CAMKK4. The anti-GST immunoblotting experiment indicates that the minor band above the 66 kDa molecular weight marker is the corresponding band for CAMKK4, similar to its theoretical 66 kDa size **(Figure 20)**. The anti-GST immunoblotting experiment also reveals that there are many bands hovering around the 35 kDa molecular weight marker that are potentially degraded products of GST. While the purity of this sample is low, it has been shown through phosphorylation assays to phosphorylate MPK3 protein substrates.

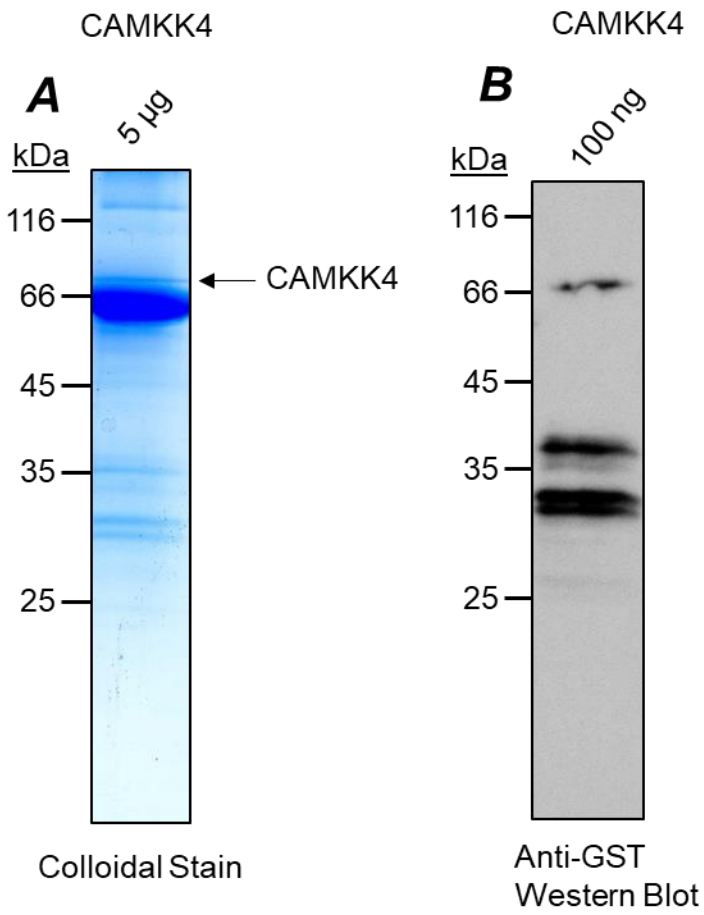

Figure 20. CAMKK-GST affinity purified protein. A) Colloidal stained 12% SDS-PAGE visualizing affinity purified AtCAMKK4-GST at 5 µg of total protein with an arrow indicating which of the major bands was determined to correspond with the AtCAMKK4-GST. **B)** Anti-GST western blot of 100 ng affinity purified AtCAMKK4-GST separated on a 12% SDS-PAGE for detection of the GST tag. Immunoblotting for anti-GST (Immunology Consultants Laboratory, RGST-45A-Z, 1 µg/mL) primary incubation was for 2 hr, followed by washing four times for 5 min in TBST 0.1%, before incubation with secondary anti-rabbit antibody (1:5000) for 1 hr. Anti-rabbit secondary antibody was washed off with TBST0.1% four times for 5 min before blot was incubated with ECL (GE Healthcare) for 3 min and developed. Low molecular weight ladder is shown to the left of the blot.

3.8 Phosphorylation of recombinant affinity purified MPK3 by CAMKK4

While MPK9 can be phosphorylated based on its autophosphorylation mechanism (Nagy *et al.*, 2015), the upstream MPK kinase (MKK) of MPK3 has been determined to be MKK4 (Kim *et al.*, 2011). Utilizing a constitutively active mutant of MKK4 (CAMKK4), MPK3 can be

phosphorylated and subsequently used to determine the substrate specificity of RLPH2 at a protein-protein interaction level.

After affinity purification of MPK3, immunoblotting with anti-pT antibodies showed no detection of phosphothreonine **(Figure 21)**. After incubation with 100 ng of CAMKK4, within one hour there is a noticeable increase in the detection of phosphothreonine. From the two hour to the four hour time points, there is no detectible increase in the phosphorylation status of MPK3, indicating maximum phosphorylation achievable via a phosphorylation assay with CAMKK4.

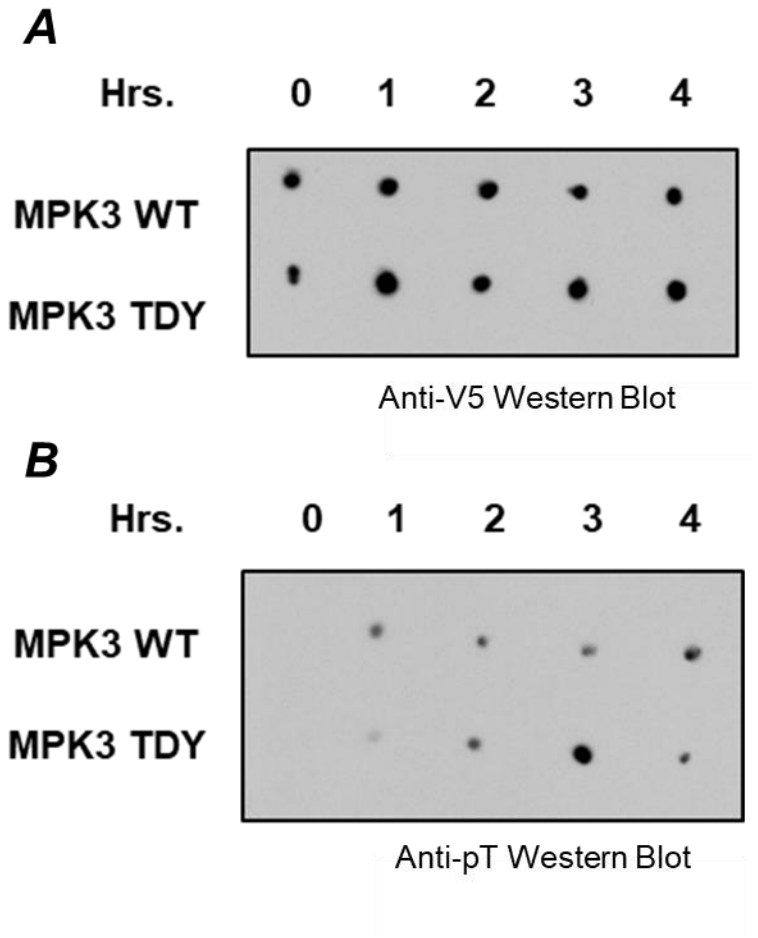

Figure 21. Phosphorylation of MPK3 WT and MPK3 TDY mutant by CAMKK4. A) Anti-V5 (Immunology Consultants Laboratory, RV5-45A-Z, 1 μg/mL) western blot detecting the V5 tag on 50 ng MPK3-V5-His6 and MPK3-V5-His6 TDY mutant proteins to observe presence of these proteins during the phosphorylation assay. **B)** Anti-pT western blot detecting the presence of phosphorylated threonine residues within 50 ng MPK3-V5-His6 and MPK3-V5-His6 TDY mutant proteins to determine phosphorylation by CAMKK4-GST. Proteins were incubated together with 100 ng of CAMKK4, and samples were taken at hourly time points to monitor the increase in phosphorylation status of these proteins. Immunoblotting for anti-V5 (Immunology Consultants Laboratory, RV5-45A-Z, 1 μg/mL) and anti-pT (Cell Signaling Technologies 42H4) primary incubation was for 2 hr, followed by washing four times for 5 min in TBST 0.1%, before incubation with either secondary anti-rabbit or anti-mouse antibody (1:5000) for 1 hr. Anti-rabbit secondary antibody was washed off with TBST0.1% four times for 5 min before blot was incubated with ECL (GE Healthcare) for 3 min and developed.

3.9 RLPH2 prefers dephosphorylation of MPK9 over MPK3 in a protein-protein dephosphorylation assay

The RLPH2 malachite green dephosphorylation assay result indicates a clear preference for RLPH2 substrate specificity towards D group MPKs over non-D group MPKs. To validate this evidence, a higher confidence experiment examining the interaction between RLPH2 and protein substrates, instead of peptide substrates, was conducted. Recombinant MPK9 and MPK3 were both affinity purified and phosphorylated via autophosphorylation and phosphorylation by CAMKK4, respectively.

The result of the RLPH2 protein dephosphorylation assay indicates a preference for dephosphorylation of D group MPKs over non-D group MPKs. This was determined through immunoblotting with an anti-pY antibody, which monitored the detection of phosphotyrosine on both MPK9 and MPK3. Individually MPK9 and MPK3 show phosphotyrosine detection, but in the presence of RLPH2 there is a loss of detection of phosphotyrosine in MPK9 **(Figure 22 A, B)**. This loss of phosphotyrosine detection was not observed in MPK3. This result indicates a clear dephosphorylation of phosphotyrosine in MPK9 by RLPH2 compared to no dephosphorylation of MPK3 in the presence of RLPH2, implying a preference by RLPH2 for the dephosphorylation of D group MPKs. To investigate whether the dephosphorylation between RLPH2 and the two phosphorylated protein substrates, MPK9 and MPK3, was phosphotyrosine specific as previous RLPH2 research has suggested (Labandera *et al.*, 2018), anti-pT immunoblotting was conducted to detect the presence of phosphothreonine. In both MPK9 and MPK3, with or without the presence of RLPH2, there was no loss in detection of phosphothreonine, indicating a clear phosphotyrosine dephosphorylation event between RLPH2 and its protein substrate MPK9 **(Figure 22 C)**.

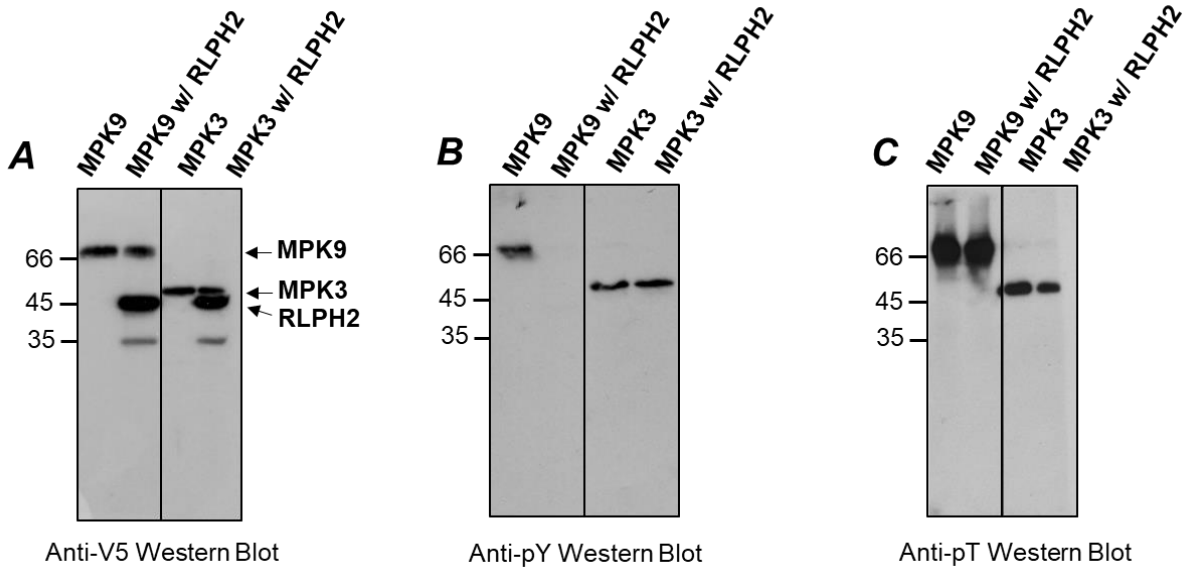

Figure 22. Dephosphorylation of MPK9-V5-His6 and MPK3-V5-His6 by RLPH2-V5-His6. A) Anti-V5 (Immunology Consultants Laboratory, RV5-45A-Z, 1 μg/mL) western blot detecting the presence of MPK9-V5-His6, MPK3-V5-His6, and RLPH2-V5-His6. **B)** Anti-pY (Cell Signalling Technologies p-Tyr-100) western blot detecting the presence of phosphorylated tyrosine residues found in MPK9-V5-His6 and MPK3-V5-His6 with or without the presence of RLPH2-V5-His6. **C)** Anti-pT (Cell Signaling Technologies 42H4 western blot detecting the presence of phosphorylated threonine residues found in MPK9-V5-His6 and MPK3-V5-His6 with or without the presence of RLPH2-V5-His6. Primary incubation was for 2 hr, followed by washing four times for 5 min in TBST 0.1%, before incubation with either secondary anti-rabbit or anti-mouse antibody (1:5000) for 1 hr. Anti-rabbit secondary antibody was washed off with TBST0.1% four times for 5 min before blot was incubated with ECL (GE Healthcare) for 3 min and developed. Low molecular weight ladder is shown to the left of the blot.

3.10 Microcystin Sepharose column chromatography of PP1 isoforms results in a single band pure protein sample.

The three isoforms of PP1 purified using the generated Microcystin Sepharose matrix resulted in a single band that through an anti-PP1 immunoblotting experiment was detected as PP1 **(Figure 23)**. The three bands that correspond to the three isoforms of PP1 purified are around the 35 kDa marker, which agrees with there theoretical protein sizes, all of which are around 35 kDa.

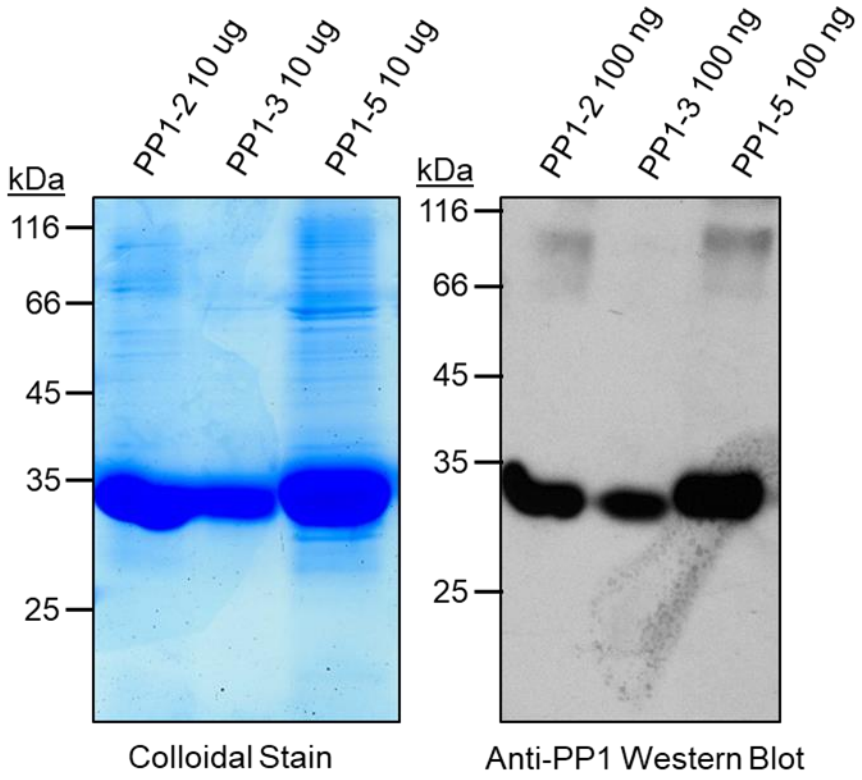

Figure 23. PP1 affinity purified protein (isoforms 2, 3, 5). A) Colloidal stained 12% SDS PAGE containing affinity purified isoforms of PP1 (2, 3, and 5). Proteins were purified using a microcystin affinity matrix. **B)** Anti-PP1 western blot containing affinity purified isoforms of PP1 (2, 3, and 5). Anti-PP1 primary antibody (3 µg/mL) was incubated with the membrane for 4 hr at RT, and secondary anti-rabbit antibody (1:5000) was incubated for 1 hr at RT before development. Blot was incubated with ECL (GE Healthcare) for 3 min and developed. Low molecular weight ladder is shown to the left of the blot.

3.11 Ni-NTA column chromatography of MPK9 RASA mutant results in a semi-pure protein.

The purified MPK9-V5-His6 RASA mutant via Ni-NTA column chromatography resulted in a semi-pure protein, present enough to be run in assays. Purified protein sample consists of three major bands, one just below, one on, and one just above the 66 kDa low molecular weight marker **(Figure 24)**. Examining the anti-V5 immunoblotting experiment of MPK9 RASA shows that the top band just above the 66 kDa marker is the band corresponding with purified MPK9 RASA

mutant. This slightly higher than the theoretical MPK9-V5-His6 RASA size of 63 kDa but could be the result of phosphorylation sites causing a decrease in MPK9 RASA migration through the gel.

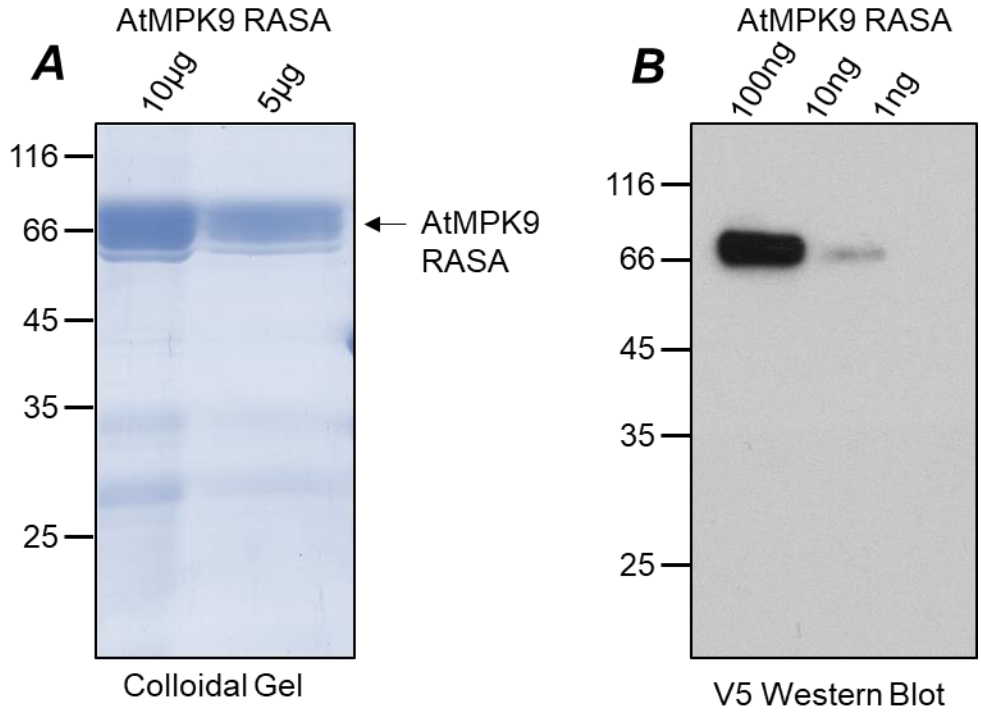

Figure 24. MPK9-V5-His6 RASA Mutant Affinity Purified Protein. A) Colloidal stained 12% SDS-PAGE visualizing affinity purified of the MPK9-V5-His6 RASA mutant at 10 µg and 5 µg of total protein with an arrow indicating which of the major bands was determined to correspond with the MPK9-V5-His6 RASA mutant. **B)** Anti-V5 western blot of 100 ng, 10 ng, and 1 ng of affinity purified RLPH2-V5-His6 RASA mutant separated on a 12% SDS-PAGE for detection of the MPK9-V5-His6 RASA mutant protein. Immunoblotting for anti-V5 (Immunology Consultants Laboratory, RV5-45A-Z, 1 µg/mL) primary incubation was for 2 hr, followed by washing four times for 5 min in TBST 0.1%, before incubation with either secondary anti-rabbit antibody (1:5000) for 1 hr. Anti-rabbit secondary antibody was washed off with TBST0.1% four times for 5 min before blot was incubated with ECL (GE Healthcare) for 3 min and developed. Low molecular weight ladder is shown to the left of the blot.

3.12 MPK9 interacts with PP1 via the hydrophobic amino acids in the PP1 interacting RVXF motif

RLPH2 is a strong candidate for the regulator of the D group MPKs through dephosphorylation of the TXY motifs phosphotyrosine, but this leaves the phosphothreonine untouched. A potential regulator for the phosphothreonine of the D group MPKs TXY motif is the well characterized serine/threonine phosphatase PP1. This is based on the presence of the putative PP1 interacting RVXF motif located nine amino acids upstream from the TXY motif. The RVXF motif is only found in the D group MPKs, and is not present in the A, B, or C group MPKs **(Figure 4)**.

To investigate into whether the D group MPKs RVXF motif could bind to the well characterized hydrophobic pocket on PP1, a protein binding assay was conducted between MPK9 and PP1 recombinant affinity purified proteins. PP1 either with or without the presence of MPK9-V5-His6 was incubated with an Ni-NTA matrix. After washing, the elution was immunoblotted against anti-PP1 antibodies to monitor the presence of PP1 and anti-V5 antibodies to monitor the presence of MPK9 in the elution. In the control lane where PP1 is incubated with Ni-NTA without the presence of MPK9, there is no detection of PP1 in the anti-PP1 immunoblotting experiment, indicating that PP1 did not strongly bind to the Ni-NTA matrix alone **(Figure 25)**. When the same experiment was conducted with the addition of MPK9, there was detection of both MPK9 and PP1 in the elution. This supports the binding interaction between MPK9 and PP1, as MPK9 is capable of binding to the Ni-NTA matrix via its His6 tag, and the presence of PP1 in the elution implies direct binding with MPK9.

The same experiment was repeated but instead of the MPK9 wild type recombinant protein, a MPK9 RASA mutant was used, where the two key hydrophobic amino acids of the RVXF motif

were switched out for alanine. The removal of the two key hydrophobic amino acids has been shown to negate the binding affinity between the RVXF motif and PP1 (O'Connell *et al.*, 2012; Choy *et al.*, 2014). The binding assay between PP1 and MPK9 RASA resulted in a lower detection of PP1 within the elution. This indicates that the RVXF motif plays a role in the binding interaction between PP1 and MPK9. Detection of PP1 within the MPK9 RASA mutant trial was slightly stronger than the control trial not containing MPK9, this could be because of extended RVXF motif factors present that are facilitating weak binding (Choy *et al.*, 2014).

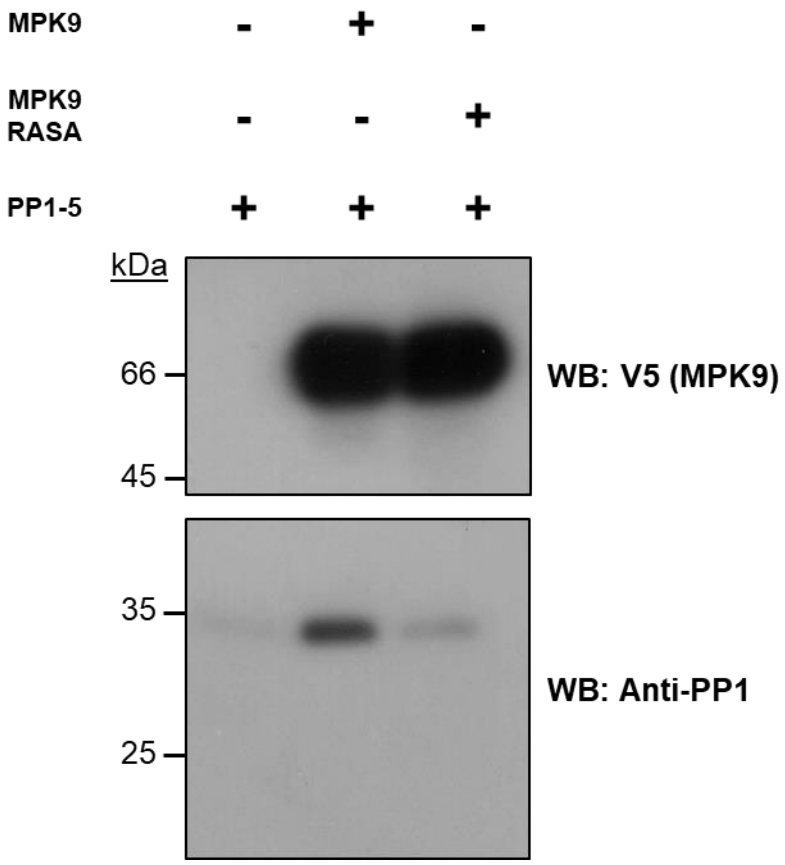

Figure 25. In vitro PP1/MPK9-V5-His6 Binding Assay. PP1 isoform 5 (1 µg) and MPK9 WT/RASA (5 µg) was incubated together for 1 hr at RT while simultaneously Ni-NTA was incubated with 5 mg/mL BSA to block non-specific interactions. Afterwards PP1 or PP1 with MPK9 WT/RASA was incubated together for 1 hr at RT, washed, then eluted in 2X SDS buffer to be analyzed by western blot. western blot detecting the presence of MPK9 WT and RASA using a V5 antibody and PP1 using a PP1 antibody generated in house. Immunoblotting for anti-V5

(Immunology Consultants Laboratory, RV5-45A-Z, 1 μg/mL) and anti-PP1 antibody primary incubation was for 2 hr, followed by washing four times for 5 min in TBST 0.1%, before incubation with either secondary anti-rabbit antibody (1:5000) for 1 hr. Anti-rabbit secondary antibody was washed off with TBST0.1% four times for 5 min before blot was incubated with ECL (GE Healthcare) for 3 min and developed. Low molecular weight ladder is shown to the left of the blot.

3.13 Anti-MPK9 antibody can detect the c-terminus derived MPK9 peptide, detecting recombinant protein, and binding to recombinant MPK9 during a trial immunoprecipitation.

Based on the dot blot experiments conducted to detect the generation of the anti-MPK9 antibody, there was a significant increase in the detection of the KLH, and the BSA/KLH with the coupled MPK9 peptide. While through the next two boosts and bleeds there was only a slight change in the anti-MPK9 immunoblotting, the slight change is an increase in the detection of KLH with the MPK9 peptide **(Figure 26)**. Finally, after using recombinant MPK9 to purify the anti-MPK9 antibodies, there is a complete loss in the detection of KLH, but also a slight loss in the detection of BSA/KLH coupled with the MPK9 peptide. This shows an affinity purified antibody that is specifically targeting the anti-MPK9 peptide.

When the anti-MPK9 antibody was used to detect the presence of recombinant MPK9, it was able to detect 100 ng of MPK9 but not 10 ng of MPK9. When the detection capabilities of the anti-MPK9 antibody were used to detect the presence of endogenous MPK9 in *Arabidopsis thaliana* rosette leaves, a band showed up at around 56 kDa which could potentially be the endogenous MPK9 with a theoretical size of 59 kDa. With MPK9 having a low expression across plant tissue, this could potentially be a non-specific signal at around the correct size.

One of the main goals with the anti-MPK9 antibody was its use in a co-immunoprecipitation of endogenous MPK9 and by association PP1. To test if the anti-MPK9 antibody was capable of binding to MPK9, a test immunoprecipitation was conducted using recombinant purified protein as the protein input **(Figure 27)**. The control experiment, which contained Protein A Sepharose without the anti-MPK9 antibody, was shown to have slight detection of recombinant MPK9 and two other minor bands in the anti-V5 immunoblotting experiment. The test immunoprecipitation using anti-MPK9 antibodies showed a significant increase in the detection of recombinant MPK9 in the anti-V5 immunoblotting experiment. This indicates the anti-MPK9 antibodies ability to bind to the recombinant MPK9 affinity purified protein.

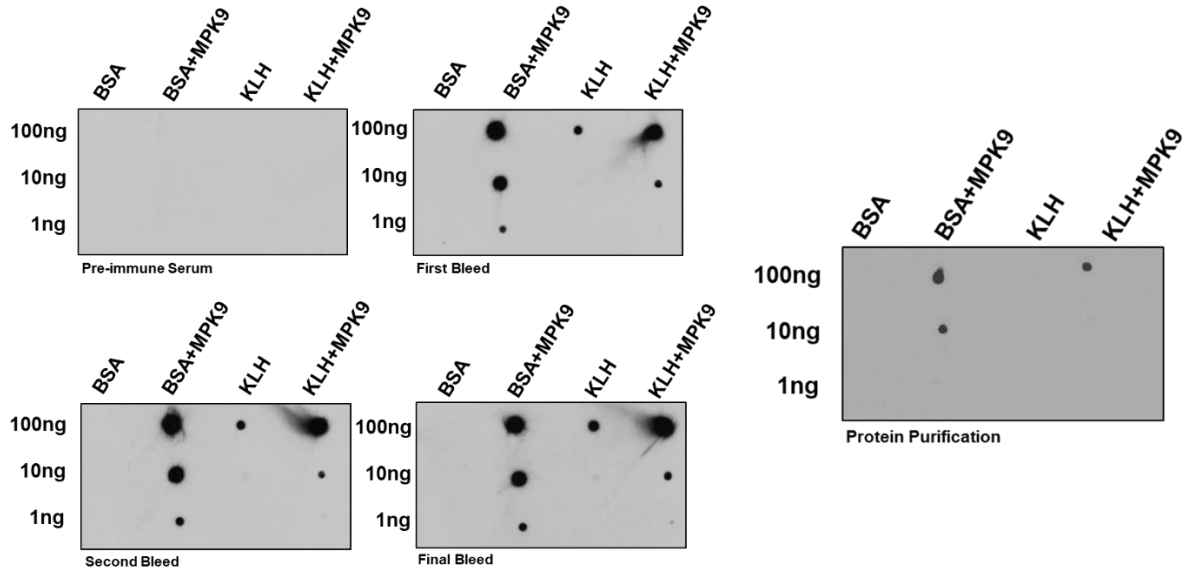

Figure 26. Anti-MPK9 antibody generation and affinity purification by protein column. Dot blot analysis of the anti-MPK9 antibodies detection capabilities against BSA, BSA coupled to the MPK9 peptide used to generate the antibody from rabbit (KPRNKSEYGE), KLH, and KLH coupled with the same peptide at 100 ng, 10 ng, and 1 ng. The primary antibodies were incubated for 2 hr each. After washing four times with TBST 0.1% (TBS + 0.1% Tween-20) the secondary anti-rabbit antibodies were incubated for 1 hour. Blot was incubated with ECL (GE Healthcare) for 3 min and developed.

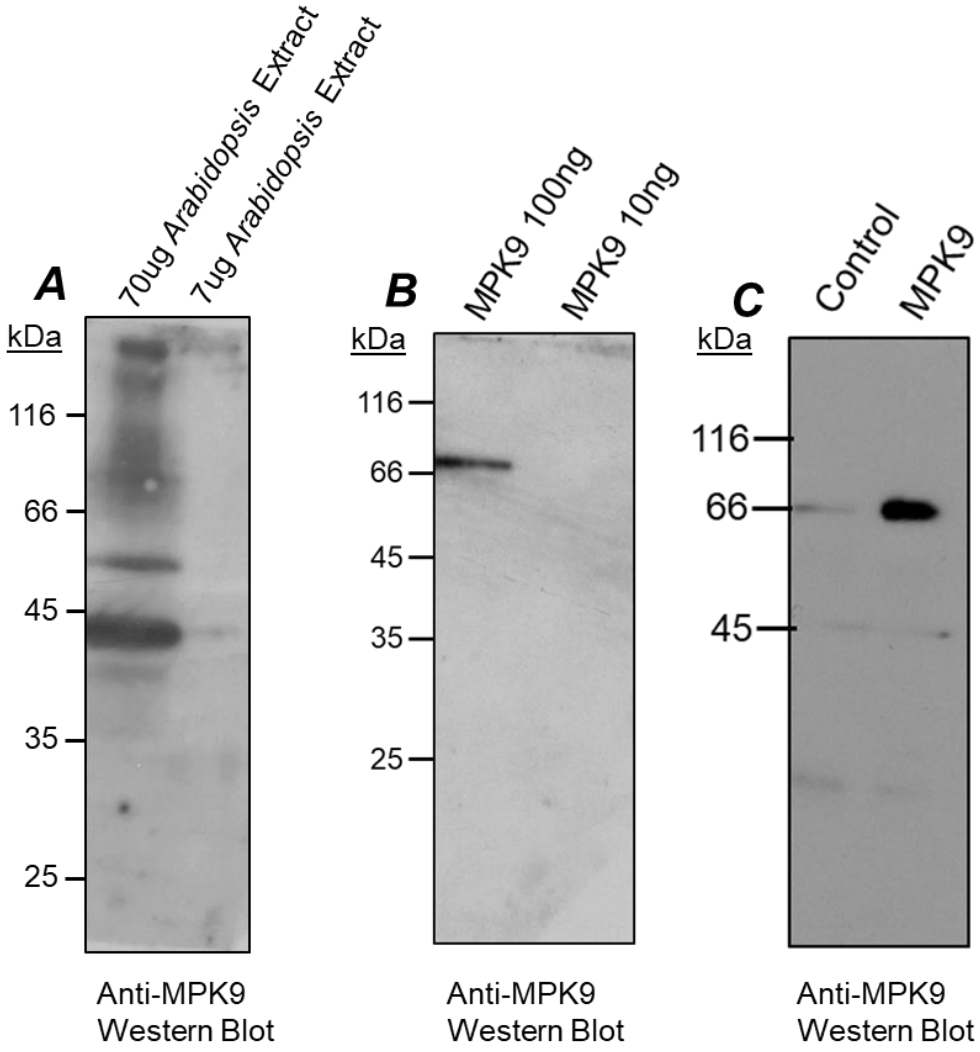

Figure 27. Characterizing Anti-MPK9 antibody capabilities to detect MPK9 in *Arabidopsis thaliana* extract, to detect recombinant affinity purified MPK9-V5-His6, and to immunoprecipitate MPK9. A) Anti-MPK9 western blot detecting the presence of MPK9 in 70 µg and 7 µg of *Arabidopsis thaliana* rosette extract after 12% SDS-PAGE. **B)** Anti-MPK9 western blot detecting the presence of affinity purified recombinant MPK9-V5-His6 at 100 ng and 10 ng on a 12% SDS-PAGE. **C)** Anti-MPK9 western blot analyzing the presence of MPK9-V5-His6 in a trial immunoprecipitation to determine the anti-MPK9 antibodies capabilities to bind with MPK9 and maintain binding through wash conditions. Immunoprecipitation was conducted following the methodology found in section 2.23, but instead of an *Arabidopsis* lysed cell, affinity purified MPK9-V5-His6 was used as the protein input. In all cases, anti-MPK9 primary antibody (1 µg/mL) was incubated with the membrane for 4 hr at RT, and secondary anti-rabbit antibody (1:5000) was incubated for 1 hr at RT before development. Blot was incubated with ECL (GE Healthcare) for 3 min and developed. Low molecular weight ladder is shown to the left of the blot.

3.14 MPK9 expression is too low for immunoprecipitation

In vitro evidence of the binding interaction between MPK9 and PP1 has been produced, but more confident *in vivo* evidence was pursued to support the binding interaction occurring within the cellular environment. Anti-MPK9 antibodies were generated from injecting a rabbit with a peptide sequence derived from a unique portion of MPK9s C-terminus (KPRNKSEYGE) coupled to BSA/KLH. The anti-MPK9 antibodies were utilized in a co-immunoprecipitation, attempting to pulldown endogenous MPK9 while simultaneously immunoprecipitating PP1 through the RVXF motif. Pre-immune serum, extracted from the rabbit prior to injection with the MPK9 peptide coupled to BSA/KLH antigen, was utilized as a control trail and was conducted simultaneously.

The results from the immunoprecipitation indicates no clear result, with no bands being detected in the anti-MPK9 immunoprecipitation elution that was not detected in the pre-immune serum elution in either the colloidal stain **(Figure 28 A)** or the anti-PP1 western blot **(Figure 28 B)**. The failure of the immunoprecipitation to capture MPK9 could be based on its low expression in plant tissue apart from the stomata (Khokon *et al.*, 2017). Immunoprecipitation was conducted by undergraduate researcher Kaitlin Chan.

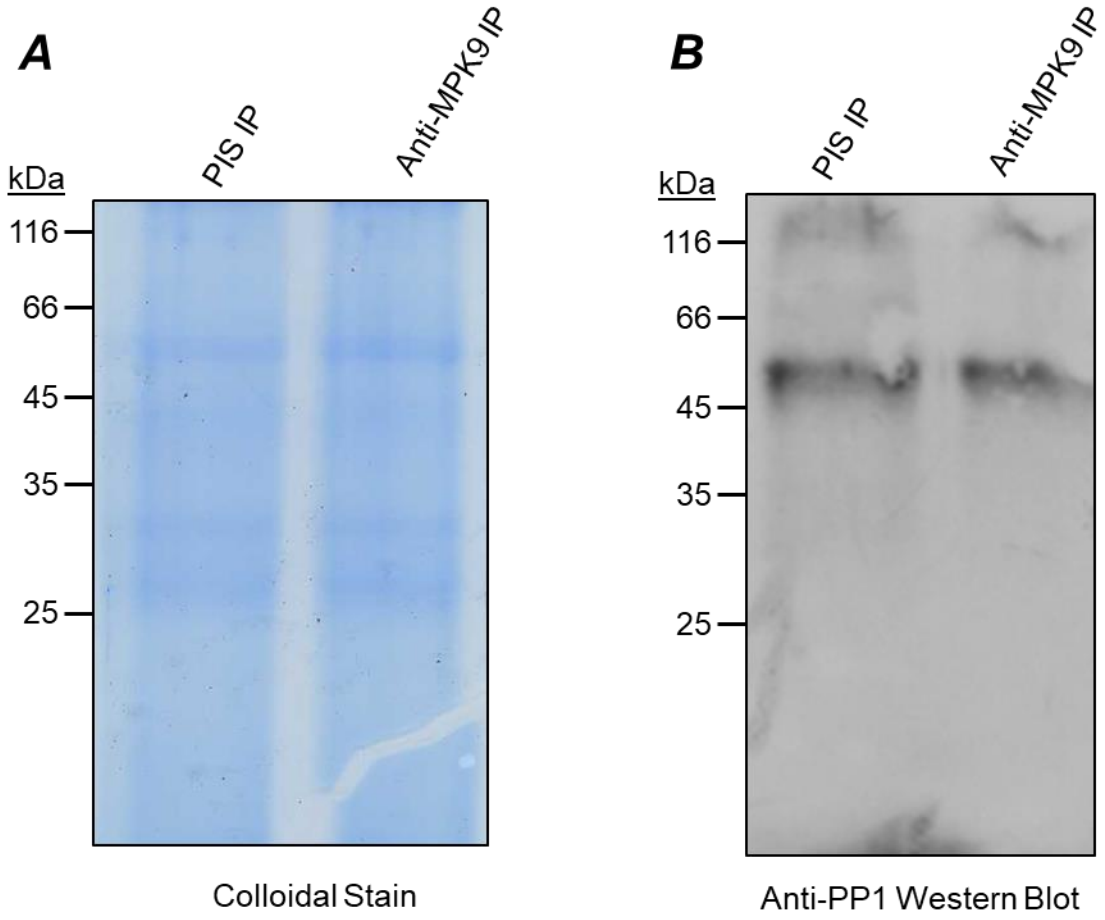

Figure 28. Immunoprecipitation of *Arabidopsis thaliana* rosette by MPK9 antibody and pre-immune serum. A) Colloidal stained 12% SDS-PAGE of MPK9 immunoprecipitation pre-immune serum (pIS IP) and Anti-MPK9 antibody elution. Total protein loaded is unknown, as both lanes were loaded with 25 µL of elution. **B)** Anti-PP1 western blot. Anti-PP1 primary antibody (3 µg/mL) was incubated with the membrane for 4 hr at RT, and secondary anti-rabbit antibody (1:5000) was incubated for 1 hr at RT before development. Blot was incubated with ECL (GE Healthcare) for 3 min and developed. Low molecular weight ladder is shown to the left of the blot.

3.15 PP1 peptide dephosphorylation assay shows a preference for dephosphorylating peptide substrates without the RVXF motif

While evidence of the binding interaction between the RVXF motif found on the activation loop of the D group MPKs and the hydrophobic pocket of PP1 has been shown, no

insight into the function or purpose of this interaction has been clarified. To examine the phosphatase activity of PP1 against MPK9 derived peptides **(Table 5)**, a malachite green dephosphorylation assay was conducted. Two peptides substrates were tested, an MPK9 peptide with an intact RVXF motif and one where the two key hydrophobic amino acids of the RVXF motif were switched out for alanine, which has been shown previously to negate binding. Both peptides were dual phosphorylated.

The PP1 malachite green dephosphorylation assay indicated PP1 had a 3-fold preference for the dephosphorylation of the substrate MPK9 peptide that did not contain a functional RVXF motif **(Figure 29)**. PP1 had a lower activity against a wild type derived MPK9 peptide where the RVXF motif was functional and able to bind to the hydrophobic pocket on PP1. This could indicate that the presence of the RVXF motif does not act in the capacity of recruiting MPK9 to PP1 as a substrate, since the removal of the RVXF motif did not decrease dephosphorylation by PP1 but instead slightly increased the activity, and could instead indicate a regulatory function behind the binding between PP1 and MPK9.

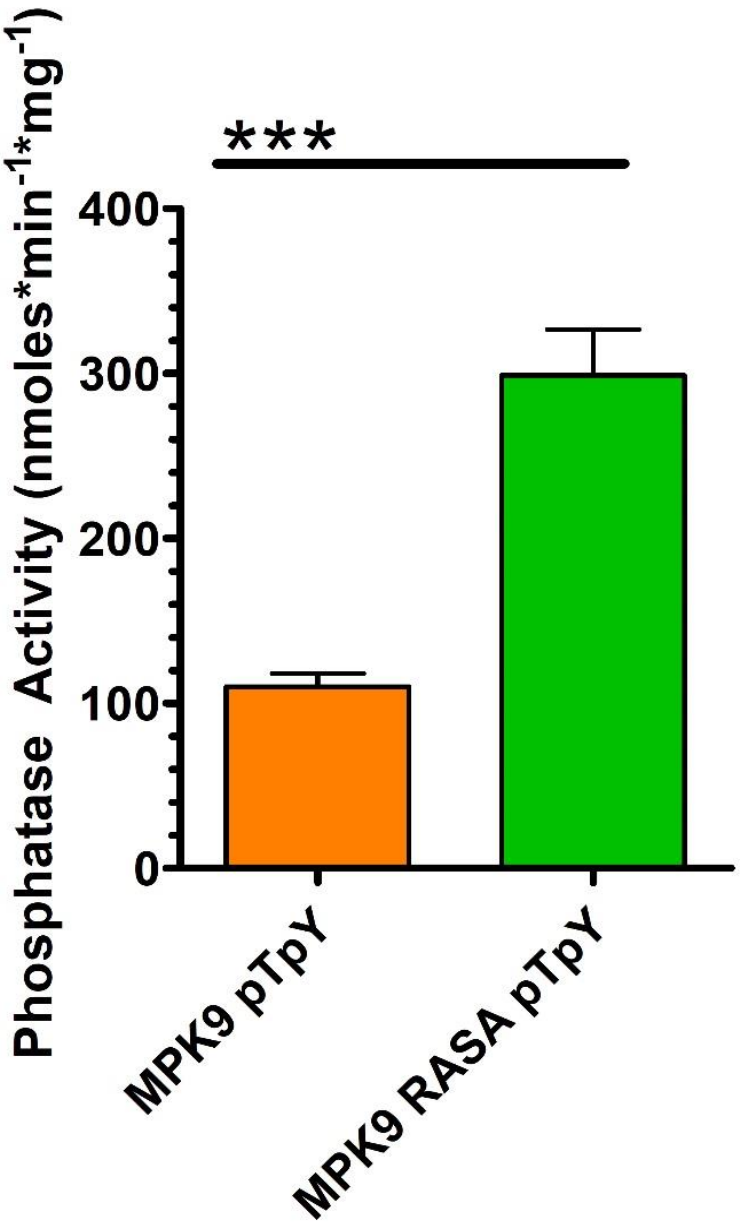

Figure 29. PP1 Malachite Green Dephosphorylation Assay. Observed result from the malachite green dephosphorylation assay of PP1 isoform 5 activity against peptide substrates MPK9 pTpY (GLA**RVSF**NDAPSAIFWpTDpYVATR) and MPK9 RASA pTpY (GLA**RASA**NDAPSAIFWpTDpYVATR). Peptide at an excess concentration (0.5 mM) was incubated with PP1-5 at 30 °C for 30 min in a shaker. Malachite green dye was added and absorbance at 630 nm was measured. Comparison of MPK9 pTpY and MPK9 RASA pTpY using a statistical t-test was conducted and showed a significant difference between these two points. *** represents that the P value for the difference was <0.0001. For MPK9 pTpY and MPK9 RASA pTpY n = 3. This data was gathered by technical replicates.

Table 5. Phosphorylated peptides derived from the activation loop of MPK9 used in PP1 malachite green dephosphorylation assay. Single letter amino acid code is shown, with "p" indicating a phosphorylated amino acid.

Peptide Name	Peptide Sequence
MPK9 pTpY	GLARVSFNDAPSAIFWpTDpYVATR
MPK9 RASA pTpY	GLARASANDAPSAIFWpTDpYVATR

3.16 PP1 dephosphorylation assay against MPK9 protein substrates

The PP1 malachite green dephosphorylation assay against peptides derived from the activation loop of MPK9 showed evidence of a dephosphorylation event occurring between PP1 and MPK9. To further investigate this interaction, a protein-protein dephosphorylation assay was conducted between PP1 and MPK9, examining their interaction by immunoblotting with anti-pT, pY, and pTpY antibodies. With these experiments the phospho-status of MPK9 could be monitored with and without the presence of PP1.

The results of the PP1 protein-protein dephosphorylation assay showed a noticeable loss in phosphothreonine detection when incubated in the presence of PP1 compared to without PP1 **(Figure 30 A)**. To examine if the loss of phospho-status was exclusive to phosphothreonine and not phosphotyrosine, since PP1 is a serine/threonine phosphatase, an immunoblotting experiment against anti-pY antibodies monitored the detection of phosphotyrosine in MPK9 with and without PP1. In both cases, there was no change in the detection of phosphotyrosine, indicating no dephosphorylation of the phosphotyrosine residues **(Figure 30 B)**. Finally, an immunoblotting experiment against anti-pTpY antibodies was conducted, monitoring the dual phosphorylation status of MPK9s TXY motif. Interestingly, there was no loss of detection with or without the presence of PP1 in the detection of the dual phosphorylated TXY motif **(Figure 30 D)**. Research into MPK9 has indicated the potential for autophosphorylation on three serine/threonine residues located on the D group MPK C-terminal extension (Nagy *et al.*, 2015). With no change in the

detection of the dual phosphorylated TXY motif, this could indicate that the loss of phosphothreonine signal was from dephosphorylation of these C-terminal phosphorylated residues. An additional observation is the noticeable decrease in MPK9 migration through the gel when incubated with PP1, indicating a loss in protein mass through dephosphorylation, clearly seen in the anti-pY and anti-pTpY western blots.

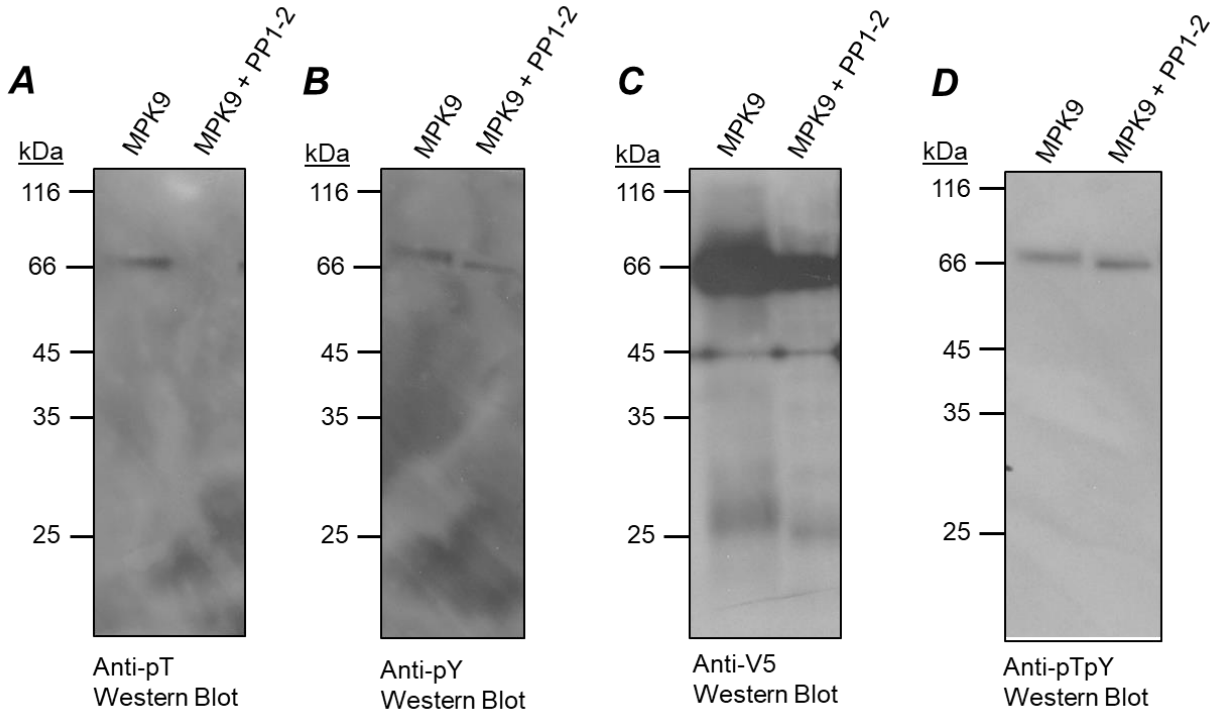

Figure 30. Dephosphorylation of MPK9-V5-His6 by PP1. A) Anti-pT (Cell Signaling Technologies 42H4) western blot detecting the presence of phosphorylated threonine residues within MPK9-V5-His6 with and without the presence of PP1 isoform 2. **B)** Anti-pY (Cell Signaling Technologies P-Tyr-100) western blot detecting the presence of phosphorylated tyrosine residues within MPK9-V5-His6 with and without the presence of PP1 isoform 2. **C)** Anti-V5 western blot detecting the presence of MPK9-V5-His6. **D)** Anti-pTpY (Cell Signaling Technologies Phospho-p44/42 MPK ERK1/2) western blot detecting the presence of phosphorylated threonine and phosphorylated tyrosine residues within MPK9-V5-His6's TXY motif with and without the presence of PP1 isoform 2. Primary incubation was for 2 hr, followed by washing four times for 5 min in TBST 0.1%, before incubation with either secondary anti-rabbit or anti-mouse antibody (1:5000) for 1 hr. Anti-rabbit secondary antibody was washed off with TBST0.1% four times for 5 min before blot was incubated with ECL (GE Healthcare) for 3 min and developed. Low molecular weight ladder is shown to the left of the blot.

DISCUSSION

The study of plant signaling mechanisms has clearly defined the important role that MPKs play in plant cellular mechanisms, such as plant development, plant immune responses, and responding to the external environment (Rodriguez, Petersen and Mundy, 2010; Xu and Zhang, 2015). While the targets of these signalling proteins has been a key research focus, equally important is the regulatory mechanisms that control the activity of these protein kinases. When traditionally seeking a MPK regulator, the dual specificity protein phosphatases, specifically the MPK phosphatases, become likely candidates with their ability to dephosphorylate both the phosphothreonine and phosphotyrosine of the TXY motif (Park *et al.*, 2011). Other candidates have been recently uncovered in plant research, such as PP2C/PPM and a tyrosine phosphatase, indicating the potential for protein phosphatases other than the dual specificity protein phosphatases to play a role in MPK regulation (Gupta *et al.*, 1998; Xu *et al.*, 1998; Schweighofer *et al.*, 2007; Ma *et al.*, 2009; Brock *et al.*, 2010; Umbrasaite *et al.*, 2010).

RLPH2, based on bioinformatic similarities, is a member of the PPP family of protein phosphatases (Uhrig and Moorhead, 2011b; Uhrig, Kerk and Moorhead, 2013). PPP family members are primarily responsible for dephosphorylating phosphoserine and phosphothreonine substrates. RLPH2 deviates from the other members of its family when a peptide dephosphorylation assay revealed RLPH2 prefers the dephosphorylation of phosphotyrosine, but more importantly, phosphotyrosine sites on the MPKs TXY motif when the threonine residue is also phosphorylated. This would be explained when the crystal structure of RLPH2 was obtained, and it was revealed that there is a basic binding pocket next to the active site of RLPH2 which would be ideal for interacting with phosphothreonine residues, explaining the increase in substrate binding when the TXY motif is dual phosphorylated **(Figure 31)**. Phosphoproteomic data

comparing the phosphostatus of two RLPH2 knockout lines (*atrlph2-1*, *atrlph2-2)* to a wild type *Arabidopsis thaliana* line revealed MPKs to be the potential substrates of RLPH2 (Labandera *et al.*, 2018; unpublished data).

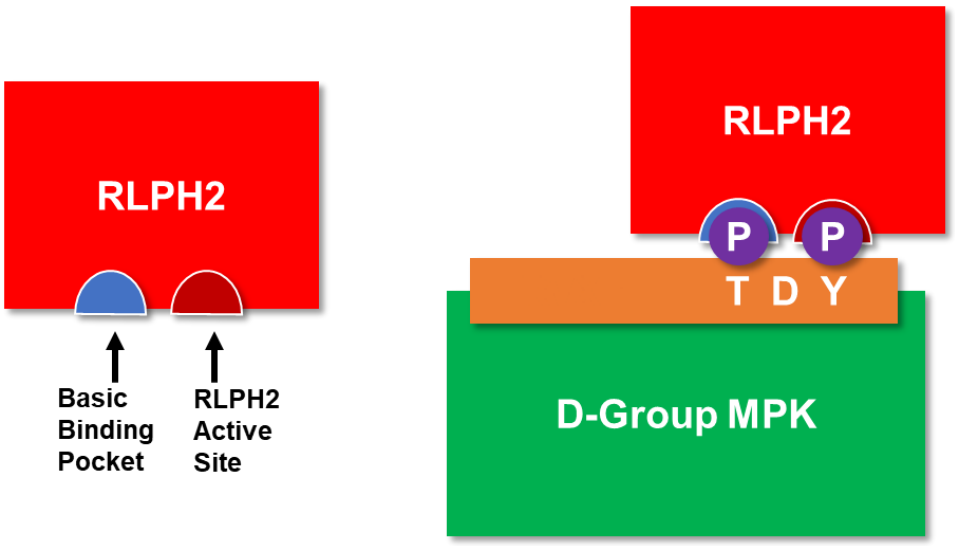

Figure 31. Model of RLPH2 binding towards a dual phosphorylated D group MPK substrate. A model of the interaction between the D group MPKs and RLPH2. RLPH2 (in red) binds to the D group MPKs (in green) TDY motif on its activation loop (in orange), utilizing its basic binding pocket to bind to the phosphorylated threonine residue, promoting dephosphorylation of the phosphotyrosine.

20 MPKs are found in *Arabidopsis*, separated into four groups (A, B, C, and D) based on their bioinformatic similarities (Ichimura *et al.*, 2002). The RLPH2 phosphoproteomic data would suggest that only members of the D group MPK family were potential substrates (Labandera, 2017). The D group MPKs are arguably the most unique group of the MPKs, with an extended C-terminus that has been shown to be phosphorylated through phosphoproteomic data, and their lack of a CD domain (Ichimura *et al.*, 2002). The CD domain is a key site on MPKs that allows for interaction with substrates, upstream kinases, and phosphatases making it important for the work discussed in this thesis, i.e., phosphatase regulators of the TXY motif (Ichimura *et al.*, 2002). The

fact that the D group MPKs lack the CD domain would indicate a novel mechanism being responsible for the recruitment of RLPH2 to the D group MPKs, as RLPH2 does not contain the [LH][LHY]Dxx[DE]xx[DE]EPxC sequence that is known to bind with the CD domain (Ichimura *et al.*, 2002). This could suggest the presence of an uncharacterized short linear motif present in the D group MPKs that is recruiting RLPH2.

MPK9 was chosen as the D group MPK representative based on its presence in the phosphoproteomic data and because MPK9 is one of the most studied D group MPKs (Khokon *et al.*, 2017; Frick and Strader, 2018). It has been shown that MPK9 is capable of autophosphorylation and that no upstream MKK in *Arabidopsis* is able to phosphorylate its TXY motif (Nagy *et al.*, 2015). The lack of the CD domain in the D group MPKs, which is responsible for the recruitment of MKKs, further suggests that activation of MPK9 is based on autophosphorylation. MPK9 has also shown the ability to autophosphorylate three serine sites on its extended C-terminus. In this thesis MPK3 was chosen to represent the non-D group MPKs, as MPK3 is a well characterized A group MPK (Rodriguez, Petersen and Mundy, 2010). It has also been shown that MPK3 is phosphorylated by an upstream MKK4 (Kim *et al.*, 2011). Utilizing a constitutively active mutant of MKK4 (CAMKK4), it is possible to phosphorylate MPK3 through a phosphorylation assay (Kim *et al.*, 2011).

For examining the interaction between RLPH2 and the MPK activation loops, a malachite green dephosphorylation assay was conducted monitoring RLPH2 activity against peptide substrates **(Figure 15)**. Initially, a dual phosphorylated peptide derived from the activation loop of MPK9 and one derived from the activation loop of MPK3 were tested. The RLPH2 peptide dephosphorylation data showed the specificity of RLPH2 was directed towards the D group MPK9 peptide over the non-D group MPK3 peptide with a 21-fold increase in activity against the D group

MPK peptide. The dephosphorylation assay with RLPH2 against recombinant MPK9 and MPK3 **(Figure 22)**, which were phosphorylated via autophosphorylation and phosphorylation by CAMKK4 respectively, showed a clear preference by RLPH2 for the dephosphorylation of MPK9 over MPK3 agreeing with the peptide data. There was a significant loss in the detection of phosphorylated tyrosine residues in the anti-pY immunoblotting experiment when MPK9 was incubated with RLPH2, compared to without the presence of RLPH2, while there was no change in the phospho-tyrosine status of MPK3 with or without the presence of RLPH2. This could be extended further to claim that RLPH2 prefers dephosphorylating the phosphotyrosine residues in D group MPKs over all non-D group MPKs. Additionally, there was no loss of phosphothreonine signal in any of the samples, showing again that RLPH2 preferably dephosphorylates phosphotyrosine residues. This indicates that RLPH2 is acting as an MPK phosphatase, regulating the activity of these D group MPKs.

Since the substrates in the peptide dephosphorylation experiment **(Figure 15)** were peptides based on MPK activation loop sequences, and there was a significant difference in the directed activity against these peptides, the regulatory mechanism that directs RLPH2s substrate specificity likely lies within this activation loop sequence. Two key differences are noticed when comparing an alignment of the 20 MPKs activation loops **(Figure 4).** One is the presence of an insert of amino acids in the D group MPKs that is not found in the non-D group MPKs. This insert was referred to as the APSAI insert. While the APSAI insert was potentially an unknown short linear motif that was promoting an interaction with RLPH2, the peptide MPK3 variant with the APSAI insert added did not result in any change in the substrate peptides dephosphorylation compared to the wild type MPK3 peptide. The second difference in the MPK activation loops is the conservation of the TXY motif within each of the MPK groups. While groups A, B, and C all

contain a TEY variant of the TXY motif, the D group contains a TDY motif. This change between aspartic acid and glutamic acid, while on a biochemical level might not be identified as a significant change in amino acid properties, it seems to have a significant role in the regulation of RLPH2 activity. When taking the MPK9 peptide and replacing its TDY motif for a TEY motif, there was a 14-fold drop in the dephosphorylation activity of RLPH2, bringing it down to a similar level to what was seen in the MPK3 peptide substrates dephosphorylation activity.

This would indicate that the aspartic acid within the TXY motif may allow for the accommodation of RLPH2, whereas the glutamic acid could structurally prevent the placement of the phosphorylated tyrosine residue into the RLPH2 active site. While this change from aspartic acid to glutamic acid does not seem like a significant change in amino acid characteristic, it is additionally worth noting that this is a completely conserved characteristic of the MPKs, with no non-D group MPK or D group MPK deviating from the TEY or TDY motif respectively. Bioinformatic searches into MPK members across *Nicotiana tabacum*, while its MPKs have not been bioinformatically grouped, show the same TDY/TEY ordering of MPKs. While this does indicate a substrate specificity mechanism for RLPH2, it would be worth transferring this peptide data into a protein dephosphorylation experiment to further confirm the potential role that the central residue within the TXY motif plays. Additionally, trying to direct RLPH2 activity towards an MPK3 peptide or protein substrate containing a D group-like TDY motif would solidify the aspartic acid within the TXY motif acting as the mechanism defining the substrate specificity of RLPH2.

To determine if the RVXF motif found in the D group MPKs was functional and capable of interacting with PP1, an *in vitro* protein binding assay was conducted **(Figure 25)**. The protein binding assay showed that there was an interaction between PP1 and the recombinant MPK9

protein, and when the MPK9 RASA mutant was utilized, it was further revealed that the RVXF motif is the site of interaction and necessary for the binding between these two proteins. An interesting observation in the protein binding assay is that there is still the detection of minor binding in the MPK9 RASA mutant sample. This could be based on the presence of an extended RVXF motif in MPK9 (Choy *et al.*, 2014). This motif utilizes two downstream hydrophobic residues and an additional further downstream arginine residue that promotes binding between PP1 and RVXF containing proteins.

While the *in vitro* protein binding assays showed evidence for the interaction between PP1 and MPK9 via the RVXF motif, stronger *in vivo* evidence would show that this interaction is occurring in the cellular environment, and further support that PP1 and the D group MPKs interact in some capacity. To show *in vivo* binding between MPK9 and PP1, a co-immunoprecipitation was conducted. For this, anti-MPK9 antibodies were generated against KLH coupled with a peptide derived from a unique portion of the C-terminus of MPK9 (KPRNKSEYGE).

To test the capabilities of the in-house generated anti-MPK9 antibody, an immunoblotting experiment was conducted against both recombinant purified MPK9 protein and *Arabidopsis* rosette leaves extract **(Figure 27)**. The anti-MPK9 antibody was able to detect MPK9 at 100 ng, and at 70 µg of *Arabidopsis* extract, there was detection of a band around 56 kDa which could be the endogenous MPK9 which is 59 kDa. To test if the anti-MPK9 antibody was capable of binding MPK9 and maintain this interaction through wash conditions, a test immunoprecipitation was conducted, following the same immunoprecipitation protocol but instead of *Arabidopsis* extract as the protein input, recombinant purified MPK9 was utilized. There was detection of the MPK9 recombinant protein after the test immunoprecipitation, indicating the anti-MPK antibodies ability to bind and maintain binding through immunoprecipitation wash conditions.

The co-immunoprecipitation experiment unfortunately showed no detection of either MPK9 in the elution, as no bands appeared in the anti-MPK9 trial that were not detected in the pre-immune serum control **(Figure 28)**. The anti-PP1 western blot also showed no detection of PP1 in the eluted samples. This could be because MPK9 has a low expression across plant tissue with the exception of the stomata guard cells (Khokon *et al.*, 2017). This would also indicate that the immunoblotting experiment with the anti-MPK9 antibody **(Figure 27)** against *Arabidopsis* tissue was not detecting the endogenous MPK9 and the band around 59 kDa is most likely a non-specific interaction.

To solve the problem of the low expression of MPK9 not being enough to detect by immunoprecipitation, a co-immunoprecipitation that utilizes the TMM (Too Many Mouth) mutant line, a mutation in a leucine-rich repeat containing receptor-like protein, as a protein input could have a higher chance of success because of this mutant lines phenotype showing an increase in stomata development, and by association, a theoretical increase in the quantity of MPK9 per tissue sample (Guseman *et al.*, 2010). If immunoprecipitation of MPK9 is impossible because of low expression, utilizing an over expression mutant of MPK9 with a GFP tag for a GFP trap experiment could potential a co-purification of PP1.

To determine if there is a dephosphorylation activity occurring in the interaction between MPK9 and PP1, a malachite green dephosphorylation assay of PP1 against dual phosphorylated peptides derived from the activation loop of MPK9 was conducted **(Figure 29)**. The results of the PP1 malachite green dephosphorylation assay show a 3-fold increase in dephosphorylation of the peptide containing a non-functional RASA motif compared to the wild type peptide with a functional RVSF motif. The PP1 malachite green peptide dephosphorylation assay could indicate the interaction between MPK9 and PP1 does not involve dephosphorylation of the TXY motif,

since the removal of the RVXF motif results in a higher dephosphorylation activity against the activation loop peptide substrate, which questions if the RVXF motif is recruiting MPK9 to PP1 as a substrate. Since it has been observed that the D group MPKs have an extended RVXF motif **(Figure 13)** and it is known that the additional factor in this motif bind away from the PP1 active site, this could also indicate that the binding interaction between MPK9 and PP1 does not result in PP1 activity against the TXY motif of MPK9. While additional RVXF motifs have been characterized such as the MyPhone and the SILK motif, neither has been bioinformatically found in the D group MPKs (Hendrickx *et al.*, 2009; Choy *et al.*, 2014). Unfortunately, this change in activity based on the presence of the RVXF motif could be the fault of peptide dephosphorylation assays, with potentially little or no protein structure, these RVXF peptides could be binding to the hydrophobic pocket and blocking interactions for further peptide substrates with PP1.

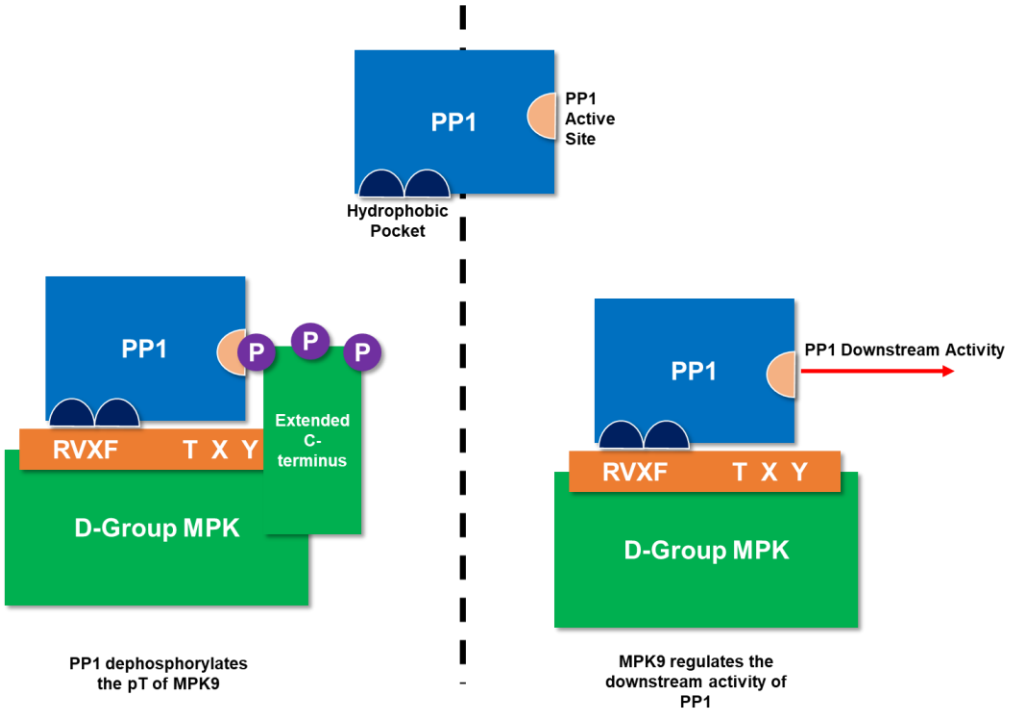

Figure 32. Model of the two potential interactions occurring between D group MPKs and PP1. A model depicting the two potential interactions that could be occurring between the D group MPKs (in green) and PP1 (in blue). PP1 utilizes its hydrophobic pocket to bind to the RVXF motif

in the D group MPKs, specifically the hydrophobic valine and phenylalanine residues. (Left) shows an interaction in which PP1 dephosphorylates the D group MPKs either on their heavily phosphorylated extended C-terminus. (Right) shows an interaction in which the D group MPK is acting as a regulatory subunit and directing the downstream substrate specificity of PP1.

To examine the interaction on a deeper level, a PP1 protein dephosphorylation assay with protein substrates was conducted monitoring PP1 activity against recombinant purified MPK9 substrates **(Figure 30)**. After the assay, phospho-status was monitored utilizing anti-pT, anti-pY, and anti-pTpY immunoblotting experiments. The PP1 protein-protein dephosphorylation assay shows that PP1 dephosphorylates the phosphothreonine residue in MPK9, as there is a complete loss of phosphothreonine detection in MPK9 when incubated with PP1, compared to without the presence of PP1. The result also indicates that there was no loss in the detection of phosphotyrosine, an expected result as PP1 is a phosphothreonine/serine phosphatase. Finally, the dual phosphorylation immunoblotting experiment showed that there was no change in the phosphorylation status of MPK9s TXY motif. Since there was still a loss in the detection of phosphothreonine, this could indicate that PP1 is dephosphorylating residues found on the C-terminus extension of MPK9 **(Figure 32)**. A limitation to this experiment is the non-specific detection of the immunoblots which could be a result of the dephosphorylation of any phosphorylated residue of MPK9. To determine exactly which sites are being dephosphorylated, a more specific method of detection such as mass spectrometry would be required.

One of the greatest roadblocks in researching the interaction between MPK9 and PP1 is determining the function behind this interaction. A potential purpose behind the interaction between PP1 and MPK9, is MPK9 as a regulatory protein for PP1, implying that when MPK9 is binding to PP1 it directs the PP1 downstream substrate specificity **(Figure 32)**, a common function of RVXF containing proteins (Uhrig, Labandera and Moorhead, 2013). The difficulty with this

interpretation is forming evidence to support this hypothesis would not be easily achievable, made more difficult by the already unclear interactions of both MPK9 and PP1 in plants. To examine this further, knowing what substrate MPK9 phosphorylates and interacts with could further be examined to see how PP1 plays a role in this interaction, and unravel the purpose of the interaction between MPK9 and PP1.

Finally, there is the potential for crosstalk to occur between RLPH2 and PP1 on MPK9. Hypothetically, the binding interaction of PP1 with MPK9s RVXF motif could block RLPH2 from dephosphorylating MPK9s TXY motif. The function of the three phosphorylated sites on the C-terminus in the D group MPKs have still not been determined, which could be interacting with RLPH2 or MPK9s downstream substrate and are potentially being dephosphorylated by PP1 **(Figure 30)**. There are many unanswered questions with no real evidence to clarify if RLPH2 and PP1 do play a role in each other signalling pathway, but with them both binding to the same D group MPKs on the same activation loop, there is likely to be some relationship between RLPH2 and PP1 in regards to MPK9.

CONCLUSION

RLPH2 is a tyrosine specific protein phosphatase that was shown in this thesis by *in vitro* peptide dephosphorylation and *in vitro* protein substrate dephosphorylation assays to be a regulator of the D group MPK TXY motif. The D group of the MPKs are unique compared to the other MPK groups with their extended C-terminus, lack of a CD domain, presence of the RVXF PP1 interacting motif, and conserved TDY version of the more classic TEY motif. Peptide dephosphorylation assays demonstrated that the aspartic acid within the TXY motif of D group MPKs likely plays a significant role in the substrate specificity of RLPH2. *In vitro* protein binding assays confirmed a binding interaction between the RVXF motif of MPK9 and PP1. While binding has been shown between PP1 and MPK9, it is unclear why they associate, with PP1 potentially dephosphorylating phosphothreonine residues of MPK9.

FUTURE DIRECTIONS

5.1 Further characterizing the interaction between RLPH2 and the D group MPKs

RLPH2 malachite green peptide dephosphorylation data have indicated that the glutamic acid and aspartic acid within the 20 *Arabidopsis* MPKs could be directing the substrate specificity of RLPH2. Peptide substrates have caveats, such has having little to no structure, and therefore the results obtained from the peptide assay are not as confident as results obtained from a RLPH2 dephosphorylation assay utilizing full-length protein substrates.

To further examine this interaction that RLPH2 has with the TXY motif of the D and non-D group MPKs (A, B, C), a mutant of MPK9 and MPK3 were generated that switches out their respective TXY motif version for their opposite (MPK9 TDY to TEY, MPK3 TEY to TDY). An experiment, similar to the RLPH2 dephosphorylation assay against protein substrates, but with the addition of these two TXY mutants, would support with higher confidence the role that the TXY motif plays in the regulation of RLPH2. Due to time limitations these experiments have not been performed.

Additionally, an ADY and TDF mutant of MPK9 have been generated. These two mutations within the TXY motif would result in proteins that are unable to be phosphorylated their threonine or tyrosine motif, respectively. Monitoring a RLPH2 dephosphorylation assay against the ADY mutant of MPK9 could potentially show the role of the phosphothreonine residue in binding to the RLPH2 basic binding pocket that previous peptide assays have shown impacts substrate binding. In a RLPH2 dephosphorylation assay the TDF mutant of MPK9 could provide insight about the activity of RLPH2 being directed towards the phosphotyrosine residue of the TXY motif, and not another phosphotyrosine residue. These interactions between RLPH2 and the

mutant versions of MPK9 would clearly show the specificity and mechanisms of RLPH2 against the D group MPKs.

Another step forward in the determination of RLPH2 function is to move from *in vitro* to *in vivo* experiments to show more evidence of the interaction occurring in the plant cell. An issue with RLPH2 pulldown and binding experiments is hypothetically that after dephosphorylating substrates, RLPH2 loses binding affinity for that substrate since one of the key binding sites is the phosphotyrosine residue. To circumvent this, a substrate trap could be generated. Recently, a mutation in one of the *Homo sapiens* PP1 metal binding residues was determined to generate a hypoactive mutant of PP1 (Wu *et al.*, 2018). This hypoactive PP1 mutant was able to bind onto its substrate phosphorylated sites but was unable to dephosphorylate them with an almost complete loss in activity. RLPH2 is another member of the PPP family and utilizes the same catalytic mechanism. By generating the same hypoactive mutant, a substrate trap of RLPH2 could be formed which would be able to bind and interact with substrates but prevent their dephosphorylation. This could open a new series of experiments such as overlays and pulldowns from an *Arabidopsis* extract that could lead to strong *in vivo* evidence for the role RLPH2 plays in the regulation of the D group MPKs.

5.2 Further examining the interaction between PP1 and the D group MPKs

Through a protein binding assay, the interaction between MPK9 and PP1 via the RVXF motif has been shown. Unfortunately, this interaction has only been shown with the fifth isoform of PP1. Expanding this interaction to all nine isoforms could show if this is interaction is specific to certain isoforms or consistent within all isoforms of PP1.

Additionally, while MPK9 immunoprecipitations did not show a detection of MPK9 or PP1 in the elution, further steps can be taken to increase the chance of a successful

immunoprecipitation, such as using a protein input that contains a higher quantity of MPK9. The Too Many Mouths (TMM) mutant has been shown to increase the presence of stomata, where MPK9 is highly expressed, and could be used as an alternative protein input (Guseman *et al.*, 2010). A GFP trap in a MPK9-GFP over expression mutant line could also be utilized, which would remove the issue that comes with the low expression of MPK9, and also have a higher certainty that the GFP trap would immunoprecipitate GFP tagged MPK9 compared to the in-house generated anti-MPK9 antibody. Using the generated Microcystin Sepharose matrix to pulldown PP1 isoforms from *Arabidopsis* extract and use immunoblotting with the anti-MPK9 antibody could also show *in vivo* binding between MPK9 and PP1.

These steps could be taken to further support this interaction between MPK9 and PP1 *in vivo* but would still leave unanswered the purpose behind these two proteins interacting. The PP1 malachite green dephosphorylation assay against peptides derived from MPK9's activation loop with and without the RVXF motif showed a preference for dephosphorylation against the RASA mutant peptide of MPK9. Examining PP1s activity against MPK9 WT and RASA phosphorylated protein substrates could further be used to examine the affect that the RVXF motif has on the activity of PP1.

This thesis has shown key features in the interaction between MPK9 and RLPH2 or PP1. In order to move forward and unravel the role that RLPH2 and PP1 play in the functionality of MPK9, the biological role that MPK9 plays must be determined. Using quantitative phosphoproteomics between a wild type and an MPK9 knockout line of *Arabidopsis* would reveal potential substrates based on the phospho-status of proteins within these two lines. This would indicate a downstream pathway from MPK9 and then combined with our understanding of RLPH2 and PP1 could lead to clarifying the role that they play in plants.

REFERENCES

Alemany, S. *et al.* (1986) 'The protein phosphatases involved in cellular regulation', *European Journal of Biochemistry*, 156(1), pp. 101–110.

Andreeva, A. and Kutuzov, M. (2004) 'Widespread presence of "bacterial-like" PPP phosphatases in eukaryotes', *BMC evolutionary biology*. BioMed Central, 4, p. 47.

Brock, A. *et al.* (2010) 'The Arabidopsis Mitogen-Activated Protein Kinase Phosphatase PP2C5 Affects Seed Germination, Stomatal Aperture, and Abscisic Acid-Inducible Gene Expression', *Plant Physiology*, 153(3), pp. 1098–1111.

Burnett, G. and Kennedy, E. (1954) 'The Enzymatic Phosphorylation of Proteins', *Journal of biochemistry*, pp. 969–980.

Cardinale, F. *et al.* (2002) 'Convergence and divergence of stress-induced mitogen-activated protein kinase signaling pathways at the level of two distinct mitogen-activated protein kinase kinases', *Plant Cell*, 14(3), pp. 703–711.

Cargnello, M. and Roux, P. (2011) 'Activation and Function of the MAPKs and Their Substrates, the MAPK-Activated Protein Kinases', *Microbiology and Molecular Biology Reviews*, 75(1), pp. 50–83.

Choy, M. *et al.* (2014) 'Understanding the antagonism of retinoblastoma protein dephosphorylation by PNUTS provides insights into the PP1 regulatory code', *Proceedings of the National Academy of Sciences*, 111(11), pp. 4097–4102.

Cohen, P. (2002a) 'Protein kinases - the major drug targets of the twenty-first century?', *Nature Reviews Drug Discovery*, 1(April), p. 309.

Cohen, P. (2002b) ‘The origins of protein phosphorylation’, *Nature Cell Biology*, 4(5).

Cristina, M., Petersen, M. and Mundy, J. (2010) ‘Mitogen-Activated Protein Kinase Signaling in Plants’, *Annual Review of Plant Biology*, 61(1), pp. 621–649.

Frick, E. and Strader, L. C. (2018) ‘Kinase MPK17 and the peroxisome division factor PMD1 influence salt-induced peroxisome proliferation’, *Plant Physiology*, 176(1), pp. 340–351.

Fuchs, S. *et al.* (2013) ‘Type 2C protein phosphatases in plants’, *FEBS Journal*, 280(2), pp. 681–693.

Ghelis, T. (2011) ‘Signal processing by protein tyrosine phosphorylation in plants’, *Plant Signaling and Behavior*, 6(7), pp. 942–951.

Gribskov, M. (2001) ‘PlantsP: a functional genomics database for plant phosphorylation’, *Nucleic Acids Research*, 29(1), pp. 111–113.

Gupta, R. *et al.* (1998) ‘Identification of a dual-specificity protein phosphatase that inactivates a MAP kinase from Arabidopsis’, *The Plant Journal*, 16(5), pp. 581–589.

Guseman, J. *et al.* (2010) ‘Dysregulation of cell-to-cell connectivity and stomatal patterning by loss-of-function mutation in Arabidopsis chorus (Glucan Synthase-Like 8)’, *Development*, 137(10), pp. 1731–1741.

Hanks, S. (2003) ‘Genomic analysis of the eukaryotic protein kinase superfamily: A perspective’, *Genome biology*, 4, p. 111.

Hemmer, W. *et al.* (1997) ‘Role of the glycine triad in the ATP-binding site of cAMP-dependent protein kinase’, *Journal of Biological Chemistry*, 272(27), pp. 16946–16954.

Hendrickx, A. *et al.* (2009) ‘Docking Motif-Guided Mapping of the Interactome of Protein

Phosphatase-1', *Chemistry & Biology*, 16(4), pp. 365–371.

Hunter, T. and Pawson, T. (2012) 'The evolution of protein phosphorylation. Preface. Philosophical transactions of the Royal Society of London', *Philosophical Transactions of the Royal Society B: Biological Sciences*, 367(1602), p. 2512.

Ichimura, K. *et al.* (2002) 'Mitogen-activated protein kinase cascades in plants: a new nomenclature', *Trends in Plant Science*, 7(7), pp. 301–308.

Ito, J. *et al.* (2009) 'A survey of the Arabidopsis thaliana mitochondrial phosphoproteome', *Proteomics*, 9, pp. 4229–4240.

Jia, Z. *et al.* (1995) 'Structural basis for phosphotyrosine peptide recognition by protein tyrosine phosphatase 1B', *Science*, 268(5218), pp. 1754–1758.

Kataya, A., Muench, D. and Moorhead, G. (2019) 'A Framework to Investigate Peroxisomal Protein Phosphorylation in Arabidopsis', *Trends in Plant Science*. Elsevier Ltd, 24(4), pp. 366–381.

Kerk, D., Templeton, G. and Moorhead, G. (2008) 'Evolutionary radiation pattern of novel protein phosphatases revealed by analysis of protein data from the completely sequenced genomes of humans, green algae, and higher plants', *Plant Physiology*, 146(2), pp. 351–367.

Khokon, M. *et al.* (2017) 'MPK9 and MPK12 function in SA-induced stomatal closure in Arabidopsis thaliana.', *Bioscience, biotechnology, and biochemistry*, 81(7), pp. 1394–1400.

Kim, S. *et al.* (2011) 'Arabidopsis MKK4 mediates osmotic-stress response via its regulation of MPK3 activity.', *Biochemical and biophysical research communications*, 412(1), pp. 150–154.

Kornev, A., Taylor, S. and Ten Eyck, L. (2008) 'A helix scaffold for the assembly of active

protein kinases', *Proceedings of the National Academy of Science*, 105(38), pp. 14377–14382.

Kyosseva, S. (2003) 'Mitogen-activated protein kinase signaling', *International Review of Neurobiology*, 59, pp. 201–220.

Labandera, A. (2017) *Identification and Characterization of a Novel Tyrosine Phosphatase in Plants*. University of Calgary.

Labandera, A. *et al.* (2018) 'Structural basis for the preference of the Arabidopsis thaliana phosphatase RLPH2 for tyrosine-phosphorylated substrates.', *Science signaling*, 11(524).

Leung, J. *et al.* (2006) 'Antagonistic interaction between MAP kinase and protein phosphatase 2C in stress recovery', *Plant Science*, 171(5), pp. 596–606.

Ma, Y. *et al.* (2009) 'Regulators of PP2C phosphatase activity function as abscisic acid sensors.', *Science*, 324(5930), pp. 1064–1068.

Manning, G. *et al.* (2002) 'The protein kinase complement of the human genome', *Science*, 298, pp. 1912–1934.

Meskiene, I. *et al.* (2003) 'Stress-induced protein phosphatase 2C is a negative regulator of a mitogen-activated protein kinase.', *The Journal of biological chemistry*, 278(21), pp. 18945–18952.

Moorhead, G. *et al.* (1994) 'Purification of type 1 protein (serine/threonine) phosphatases by microcystin-Sepharose affinity chromatography', *FEBS Letters*, 356(1), pp. 46–50.

Moorhead, G. *et al.* (2009) 'Evolution of protein phosphatases in plants and animals', *Biochemical Journal*, 417(2), pp. 401–409.

Nagy, S. *et al.* (2015) 'Activation of AtMPK9 through autophosphorylation that makes it

independent of the canonical MAPK cascades', *Biochemical Journal*, 467(1), pp. 167–175.

Nakagami, H. *et al.* (2010) 'Large-Scale Comparative Phosphoproteomics Identifies Conserved Phosphorylation Sites in Plants 1', 153(July), pp. 1161–1174.

Nasa, I. (2016) *Regulation of Protein Phosphatase One During Cell Cycle*. University of Calgary.

Nigg, E. *et al.* (2010) 'Quantitative Phosphoproteomics Reveals Widespread Full Phosphorylation Site Occupancy During Mitosis', *Science Signaling*, 3(104).

O'Connell, N. *et al.* (2012) 'The molecular basis for substrate specificity of the nuclear NIPP1:PP1 holoenzyme', *Structure*, 20(10), pp. 1746–1756.

Olsen, J. *et al.* (2006) 'Resource Global , In Vivo , and Site-Specific Phosphorylation Dynamics in Signaling Networks', 2, pp. 635–648.

Park, H. *et al.* (2011) 'Arabidopsis MAP kinase phosphatase 1 is phosphorylated and activated by its substrate AtMPK6.', *Plant cell reports*, 30(8), pp. 1523–1531.

Prabakaran, S. *et al.* (2012) 'Post-translational modification: Nature's escape from genetic imprisonment and the basis for dynamic information encoding', *Wiley Interdisciplinary Reviews: Systems Biology and Medicine*, 4(6), pp. 565–583.

Reiland, S. *et al.* (2009) 'Large-scale arabidopsis phosphoproteome profiling reveals novel chloroplast kinase substrates and phosphorylation networks', *Plant Physiology*, 150(2), pp. 889–903.

Robinson, D., Wu, Y. and Lin, S. (2000) 'The protein tyrosine kinase family of the human genome', *Oncogene*, 19(49), pp. 5548–5557.

Rodriguez, M., Petersen, M. and Mundy, J. (2010) ‘Mitogen-activated protein kinase signaling in plants.’, *Annual review of plant biology*, 61, pp. 621–649.

Schweighofer, A. *et al.* (2007) ‘The PP2C-type phosphatase AP2C1, which negatively regulates MPK4 and MPK6, modulates innate immunity, jasmonic acid, and ethylene levels in Arabidopsis’, *Plant Cell*, 19(7), pp. 2213–2224.

Schweighofer, A., Hirt, H. and Meskiene, I. (2004) ‘Plant PP2C phosphatases: emerging functions in stress signaling’, *Trends in Plant Science*, 9(5), pp. 236–243.

Seifried, A., Schultz, J. and Gohla, A. (2013) ‘Human HAD phosphatases: structure, mechanism, and roles in health and disease.’, *The FEBS journal*, 280(2), pp. 549–571.

Seo, J. and Lee, K. (2004) ‘Post-translational Modifications and Their Biological Functions: Proteomic Analysis and Systematic Approaches’, *BMB Reports*, 37(1), pp. 35–44.

Shi, Y. (2009) ‘Review Serine / Threonine Phosphatases : Mechanism through Structure’, 139(3), pp. 468–484.

Shiu, S. and Bleecker, A. (2001) ‘Receptor-like kinases from Arabidopsis form a monophyletic gene family related to animal receptor kinases’, *Proceedings of the National Academy of Sciences of the United States of America*, 98(19), pp. 10763–10768.

Stanford, S. and Bottini, N. (2017) ‘Targeting Tyrosine Phosphatases: Time to End the Stigma’, *Trends in Pharmacological Sciences*, 38(6), pp. 524–540.

Sugiyama, N. *et al.* (2008) ‘Large-scale phosphorylation mapping reveals the extent of tyrosine phosphorylation in Arabidopsis’, (193), pp. 1–5.

Szöör, B. (2010) ‘Trypanosomatid protein phosphatases.’, *Molecular and biochemical*

parasitology, 173(2), pp. 53–63.

Tagliabracci, V. *et al.* (2013) 'Secreted Kinase Phosphorylates Extracellular Proteins That Regulate Biomineralization', *Science*, 336(6085), pp. 1150–1153.

Takemiya, A., Ariyoshi, C. and Shimazaki, K. (2009) 'Identification and functional characterization of inhibitor-3, a regulatory subunit of protein phosphatase 1 in plants.', *Plant physiology*, 150(1), pp. 144–156.

Taylor, S. and Kornev, A. (2013) 'Protein Kinases: Evolution of Dynamic Regulatory Proteins', *Trends in biochemical sciences*, 36(2), pp. 65–77.

Templeton, G. (2010) *Bioinformatic analysis of the evolution of the plant phosphatome and the biochemical characterization of novel Arabidopsis thaliana Protein Phosphatase 1 complexes.* University of Calgary.

Templeton, G. *et al.* (2011) 'Identification and characterization of AtI-2, an Arabidopsis homologue of an ancient protein phosphatase 1 (PP1) regulatory subunit', *Biochemical Journal*, 435(1), pp. 73–83.

Trinkle-Mulcahy, L. *et al.* (2006) 'Repo-Man recruits PP1γ to chromatin and is essential for cell viability', *Journal of Cell Biology*, 172(5), pp. 679–692.

Ubersax, J. and Ferrell, J. (2007) 'Mechanisms of specificity in protein phosphorylation.', *Nature reviews. Molecular cell biology*, 8(7), pp. 530–541.

Uhrig, R. (2013) *Characterization of Novel Shewanella- and Rhizobiales-Like PPP-Family Protein Phosphatases from Arabidopsis thaliana*. University of Calgary.

Uhrig, R. *et al.* (2017) 'Activation of Mitochondrial Protein Phosphatase SLP2 by MIA40

Regulates Seed Germination.', *Plant physiology*, 173(2), pp. 956–969.

Uhrig, R., Kerk, D. and Moorhead, G. (2013) 'Evolution of Bacterial-Like Phosphoprotein Phosphatases in Photosynthetic Eukaryotes Features Ancestral Mitochondrial or Archaeal Origin and Possible Lateral Gene Transfer', *Plant Physiology*, 163(4), pp. 1829–1843.

Uhrig, R., Labandera, A. and Moorhead, G. (2013) 'Arabidopsis PPP family of serine/threonine protein phosphatases: Many targets but few engines', *Trends in Plant Science*, 18(9), pp. 505–513.

Uhrig, R. and Moorhead, G. (2011a) 'Okadaic acid and microcystin insensitive PPP-family phosphatases may represent novel biotechnology targets', *Plant Signaling and Behavior*, 6(12), pp. 2057–2059.

Uhrig, R. and Moorhead, G. (2011b) 'Two Ancient Bacterial-like PPP Family Phosphatases from Arabidopsis Are Highly Conserved Plant Proteins That Possess Unique Properties', *Plant Physiology*, 157(4), pp. 1778–1792.

Umbrasaite, J. *et al.* (2010) 'MAPK phosphatase AP2C3 induces ectopic proliferation of epidermal cells leading to stomata development in Arabidopsis.', *PloS one*, 5(12), p. e15357.

Wakula, P. *et al.* (2003) 'Degeneracy and Function of the Ubiquitous RVXF Motif That Mediates Binding to Protein Phosphatase-1', *Journal of Biological Chemistry*, 278(21), pp. 18817–18823.

Wu, D. *et al.* (2018) 'A substrate-trapping strategy for protein phosphatase PP1 holoenzymes using hypoactive subunit fusions', *Journal of Biological Chemistry*, 293(39), pp. 15152–15162.

Xu, J. and Zhang, S. (2015) 'Mitogen-activated protein kinase cascades in signaling plant growth

and development', *Trends in Plant Science*, 20(1), pp. 56–64.

Xu, Q. *et al.* (1998) 'Molecular characterization of a tyrosine-specific protein phosphatase encoded by a stress-responsive gene in Arabidopsis', *Plant Cell*, 10(5), pp. 849–857.

Zulawski, M. *et al.* (2014) 'The Arabidopsis Kinome: Phylogeny and evolutionary insights into functional diversification', *BMC Genomics*, 15(1).